TECHNICAL REPORT NO. LWL-CR-06P72

COBRA WINDOW DESIGN ANALYSIS AND NOEGLARE CANOPY DESIGN

by

Richard H. Daumit
James B. Kiesel
Westinghouse Defense and Electronic Systems Center
Systems Development Division
Baltimore, Maryland 21203

March 1974

Final Report

Contracts DAAD05-72-C-0284 and DAAD05-73-C-0305

APPROVED FOR PUBLIC RELEASE; DISTRIBUTION UNLIMITED

Prepared For

U. S. ARMY LAND WARFARE LABORATORY
Aberdeen Proving Ground, Maryland 21005

The findings in this report are not to be construed as an official Department of the Army position unless so designated by other authorized documents.

UNCLASSIFIED

SECURITY CLASSIFICATION OF THIS PAGE *(When Data Entered)*

REPORT DOCUMENTATION PAGE

READ INSTRUCTIONS BEFORE COMPLETING FORM

1. REPORT NUMBER: LWL-CR-06P72
2. GOVT ACCESSION NO.:
3. RECIPIENT'S CATALOG NUMBER:

4. TITLE *(and Subtitle)*: Cobra Window Design Analysis and Noeglare Canopy Design

5. TYPE OF REPORT & PERIOD COVERED: Final

6. PERFORMING ORG. REPORT NUMBER:

7. AUTHOR(s): Richard H. Daumit, James B. Kiesel

8. CONTRACT OR GRANT NUMBER(s): DAAD05-72-C-0284, DAAD05-73-C-0305

9. PERFORMING ORGANIZATION NAME AND ADDRESS: Westinghouse Defense & Electronic Systems Center, Systems Development Division, Baltimore, MD 21203

10. PROGRAM ELEMENT, PROJECT, TASK AREA & WORK UNIT NUMBERS: LWL Task 06-P-72, Work Assignments No. 3 & 6

11. CONTROLLING OFFICE NAME AND ADDRESS: US Army Land Warfare Laboratory, ATTN: AMXLW-ADP, Aberdeen Proving Ground, MD 21005

12. REPORT DATE:

13. NUMBER OF PAGES: 74

14. MONITORING AGENCY NAME & ADDRESS *(if different from Controlling Office)*:

15. SECURITY CLASS. *(of this report)*: UNCLASSIFIED

15a. DECLASSIFICATION/DOWNGRADING SCHEDULE:

16. DISTRIBUTION STATEMENT *(of this Report)*

Approved for Public Release; Distribution Unlimited.

17. DISTRIBUTION STATEMENT *(of the abstract entered in Block 20, if different from Report)*

18. SUPPLEMENTARY NOTES

None

19. KEY WORDS *(Continue on reverse side if necessary and identify by block number)*

Helicopter Canopy Glare
Sun Reflections
Attack Helicopter
Helicopter Canopy Glint
Visible Signature
Helicopter Survivability
Mid-Intensity Warfare
Simulation Model
Low Altitude Flight
Detection
Glare Reduction
AH-LG Cobra
Reflectivity Analyses
Reflective Mapping

20. ABSTRACT *(Continue on reverse side if necessary and identify by block number)*

This report details the work related to the redesign and modification of the canopy of the Attack Helicopter (AH-1G) to minimize sun reflections and thereby reduce the probability of detection through visual observation. There were two objectives in this effort, namely: Canopy redesign through analysis of directional components of reflections and computer analysis of the design in a modified version of a special program developed in earlier work entitled "Cobra Glint Model, AH-1G."

Continued on Reverse

DD FORM 1 JAN 73 1473 EDITION OF 1 NOV 65 IS OBSOLETE

UNCLASSIFIED

SECURITY CLASSIFICATION OF THIS PAGE *(When Data Entered)*

BLOCK 20. ABSTRACT CON'T

In this effort emphasis was placed on the role of the attack helicopter against enemy armor in a mid-intensity scenario. Altitude stipulated as nap-of-the-earth was defined as being less than 100 feet above ground level. There were ground maps produced that portrayed the intersection of reflected sun rays with the ground from various canopy configurations. By this ground map/area coverage technique a figure of merit for various canopy configuration was developed. These included the existing canopy, a porthole canopy (side sections partly obscured) and the LWL35 canopy (a four flat-plate version used for a feasibility demonstration) as well as version employing baffles or sun-shades.

The results of this work produced a design nearly free of sun reflections that can be seen by a ground observer located at or below the altitude of the helicopter. In comparison the existing canopy on the attack helicopter has numerous reflections, detectable by a ground observer at each sun elevation, due to its curved characteristics.

AD-778165

FOREWORD

This effort was sponsored by the US Army Land Warfare Laboratory, Aberdeen Proving Ground, MD. It was carried out under the Technical Supervision of Mr. Gerald E. Cook of the Applied Physics Branch, Advanced Development Division. The work was conducted to refine and further develop the capabilities required by LWL Task 06-P-72, entitled "Glare Reduction" and LWL Task 21-P-73 entitled "Glare Reduction-AAVSCOM". The first task concerned itself with various approaches to reduction of the visible sun reflections from the attack helicopter canopy whereas the second task specifically addressed the design, fabrication installation and test of a flat-surfaced canopy. This was the LWL-35, referred to within the report, which was modelled along with other experimental configurations. To aid in the side-by-side comparison of the flat canopy with a standard canopy, work reported upon herein was carried out to predict the occurrences and locations of reflections from the flat canopy. Assisted by these predictions motion picture views of the comparison tests were taken, edited and compiled into a narrated, 16 mm film entitled "Reduction of Helicopter Canopy Sun Reflections". This film was submitted as the visual record/report of the second task (21-P-73) by the USALWL to the sponsoring office, the AMC Product Manager For Aircraft Survivability Equipment.

THIS PAGE INTENTIONALLY LEFT BLANK

TABLE OF CONTENTS

TABLE OF CONTENTS (Cont.)

LIST OF FIGURES

LIST OF FIGURES (Cont.)

LIST OF FIGURES (Cont.)

LIST OF FIGURES (Cont.)

LIST OF FIGURES (Cont.)

LIST OF FIGURES (Cont.)

LIST OF FIGURES (Cont.)

LIST OF TABLES

THIS PAGE INTENTIONALLY LEFT BLANK

1.0 INTRODUCTION AND SUMMARY

This report covers the work performed on Work Assignment #6 of contract number DAAD05-72-C-0284 and on Work Assignment #3 of contract number DAAD05-73-C-0305. The latter work assignment was an extension of the first such that the work covered by this report was performed as if it had been one task.

The two work assignments are concerned with the redesign or modification of the canopy in the Cobra helicopter so as to minimize the probability of detection of the canopy, and thus the helicopter, by a ground observer aided by sun glint.

The objectives of the tasks were to perform the redesign of the Cobra canopy and to analyze the design in a modified version of a digital computer program (COBWIN) developed under Work Assignment #2 of contract number DAAD05-72-C-0284.

Both objectives were successfully met. A canopy design involving five flat plate windows and nine baffles was developed after analyzing the directional components of reflections from a single flat plate rotated in space and the baffles required to block either the incoming rays or their reflections.

The digital computer program developed in the earlier task was modified so that its output was an x-y map of the reflected rays' intersection with the ground. The model was verified by comparing its output with data from tests at MASSTER. This version of the digital computer program, called SEEHC2, was used to analyze all windows which did not have baffles. These windows included the 'Existing' Cobra canopy, the 'Porthole' canopy

(a modified version with the side windows blocked out except for two portholes on each side) and the 'LWL-35' canopy (a four flat-plate window canopy designed by LWL and used to demonstrate the feasibility of flat plate windows for reduction of glint).

The SEEHC2 program was further modified to accept baffles. This version, called SEEHC3, was used to analyze the redesigned canopy configuration, called '40° Baffled' and its non-baffled counterpart, the '40°'.

Additional work was performed under the work statement to assist LWL in preparing for the flat plate window demonstration and to analyze the probability of various sun elevations during the year.

The output of the work on the two tasks is the design for a Cobra canopy configuration which allows no glints which can be seen on the ground over almost all sun elevations below 65° and single detectable glints at sun elevations near 2° and 20° while having a minimal effect on the aerodynamics of the helicopter and on the pilot's and gunner's vision blockage. In comparison, the existing Cobra canopy has a numerous ground detectable sun glints at each sun elevation due to its curved canopy and the non-baffled flat plate canopies have several ground detectable glints over some sun elevations including those near 0° while having none over others.

We would like to express our thanks to the LWL staff in general and Gerald Cook in particular for their assistance in performing these tasks. We would also like to thank Dick Higby, John Goodell, and Warren Kendig of Westinghouse for their inputs to our effort.

2.0 FLAT SURFACE CANOPY ANALYSIS

2.1 Introduction

Results obtained in earlier studies as well as experiments performed at Aberdeen Proving Ground indicate that a curved surface canopy is very undesirable from a glint standpoint. However, flat surface canopies have been found to be much more desirable than curved surface canopies in reducing glint characteristics. This result led to a concentrated effort to examine the glint properties of flat surfaces in hopes that it would lead to a physically feasible design which would reduce the glint pattern to as low a level as is possible.

2.2 Ground Scenario

The helicopter scenario is illustrated in figure 2-1. The helicopter is 100 feet above a horizontal plane region and maintains an aspect of 0^{o} yaw,

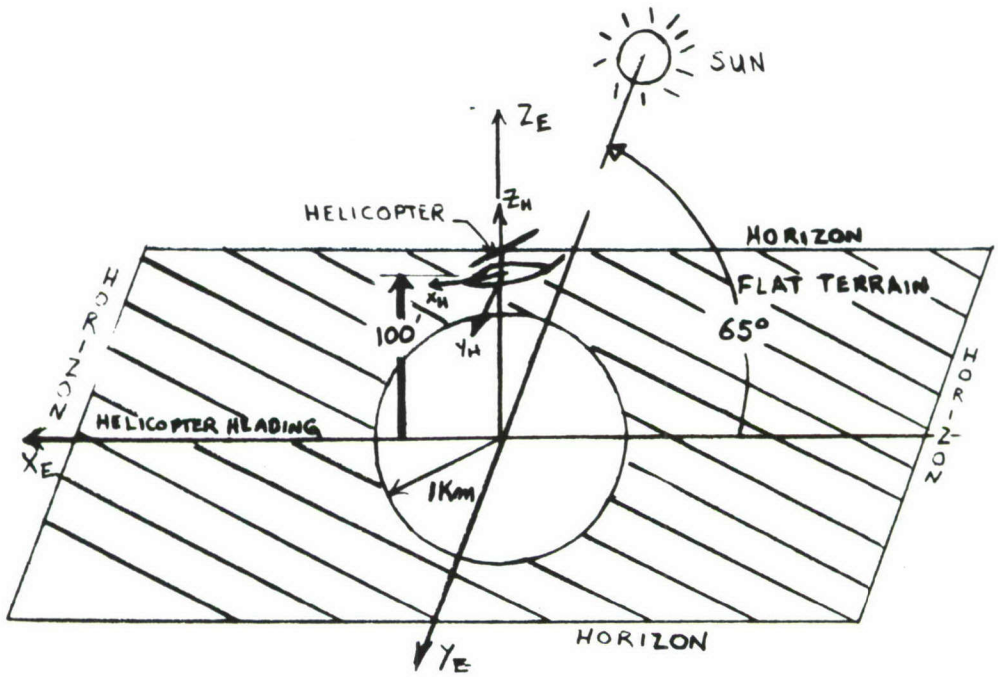

Figure 2-1. Helicopter Scenario

5° pitch and 0° roll. A helicopter motion of $\pm 2^{\circ}$ in yaw, pitch and roll about the basic aspect is assumed. The ground region in which glints are of interest is shaded and includes all areas beyond a 1 km semicircle. The reason for this region is due to the fact that glints are of interest primarily beyond a ground range of 1 km since within the 1 km range the helicopter is generally visible to the naked eye without the aid of glints.

The sun positions of interest are sun elevations from 0° to 65° and sun azimuth from 0° to 360°. The sun elevation extremes were set by LWL to cover combat zones of interest.

2.3 Variables in the Design of Flat Plate Canopy

The basic design structure considered in this study is shown in figure 2-2. The variables to be studies are the slope and the physical

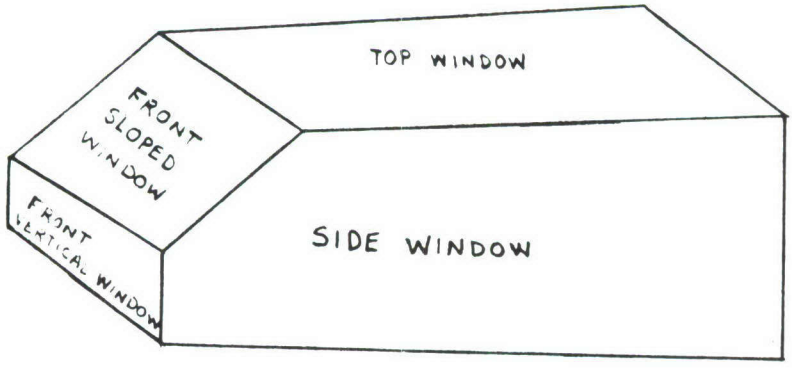

Figure 2-2. Basic Canopy Structure

dimensions (i.e. length and height) of each window. As will be seen later, the initial consideration was the slope of each window and it will become clear in section 2.4 why this variable received early attention. It was

decided early in the analysis that for physical reasons the slope of each window should lie within certain ranges as is shown in table 2-1.

Table 2-1	Window Slopes
Front Window	$30^\circ \leq \text{QE} \leq 90^\circ$
Top Window	$0^\circ \leq \text{QE} \leq 12^\circ$
Side Window	$90^\circ \leq \text{QE} \leq 96^\circ$
Front Vertical Window	$\text{QE} = 90^\circ$

The upper boundary on the elevation angle (QE) for the front window was due to aerodynamic considerations as well as the fact that angles larger than 90° would cause the top and side windows to have larger surface areas. The lower limit on the QE for the front window is necessary to allow enough room for the gunner to fit comfortably in the cockpit. The initial limits on the slope of the top window were set arbitrarily with the idea of reducing the surface area of the front and side windows by possibly sloping it at 12°. The limits on the side window were set for optical reasons which will become clear in a later section. The purpose of the following analysis is to determine the best slopes for the windows within these ranges in order to minimize glints from the canopy surfaces. A factor which greatly influences the final slope of the window is baffling effectiveness which will not become clear until a later section.

The other variables which must be considered are the physical sizes of the windows. These variables are constrained primarily by geometrical considerations which will be discussed later in the report.

2.4 Analysis of Direction of Reflected Vector From a General Flat Surface In Space

The following development leads to one of the key algorithms for the analysis of specular reflections (glints) from a flat surface (window surface) due to a point source (the sun). The development will be done with the aid of figure 2-3.

The object of this development is to determine an expression for the unit reflected vector in terms of the unit normal to the surface and the unit incident ray. From figure 2-3:

(1) $\hat{I} = -\sin \Theta_I \cos \phi_I \hat{i} - \sin \phi_I \sin \Theta \hat{j} - \cos \Theta_I \hat{k}$

(2) $\hat{N} = \sin \Theta_N \cos \phi_N \hat{i} + \sin \phi_N \sin \Theta_N \hat{j} + \cos \Theta_N \hat{k}$

From optics theory the reflected vector can be described by:

(3) $\hat{R} = \hat{I} - 2 (N \cdot I) \hat{N}$ where $\hat{R}$ = unit reflected vector

This equation is arrived at by applying Snell's Law and some vector analysis. In order to use equation (3), N·I must be calculated:

$$\hat{I} \cdot \hat{N} = \hat{N} \cdot \hat{I} = -\sin \Theta_I \cos \phi_I \sin \Theta_N \cos \phi_N - \sin \phi_I \sin \Theta_I \sin \phi_N \sin \Theta_N - \cos \Theta_I \cos \Theta_N$$

This expression can be simplified to:

$$\hat{N} \cdot \hat{I} = -\sin \Theta_I \sin \Theta_N \cos (\phi_I - \phi_N) - \cos \Theta_I \cos \Theta_N$$

Denoting the X, Y, Z components by $(\hat{R})X$, $(\hat{R})Y$, $(\hat{R})Z$:

(4) $(\hat{R})X = -\sin \Theta_I \cos \phi_I + 2 (\sin \Theta_I \sin \Theta_N \cos (\phi_I - \phi_N) + \cos \Theta_I \cos \Theta_N) \sin \Theta_N \cos \Theta_N$

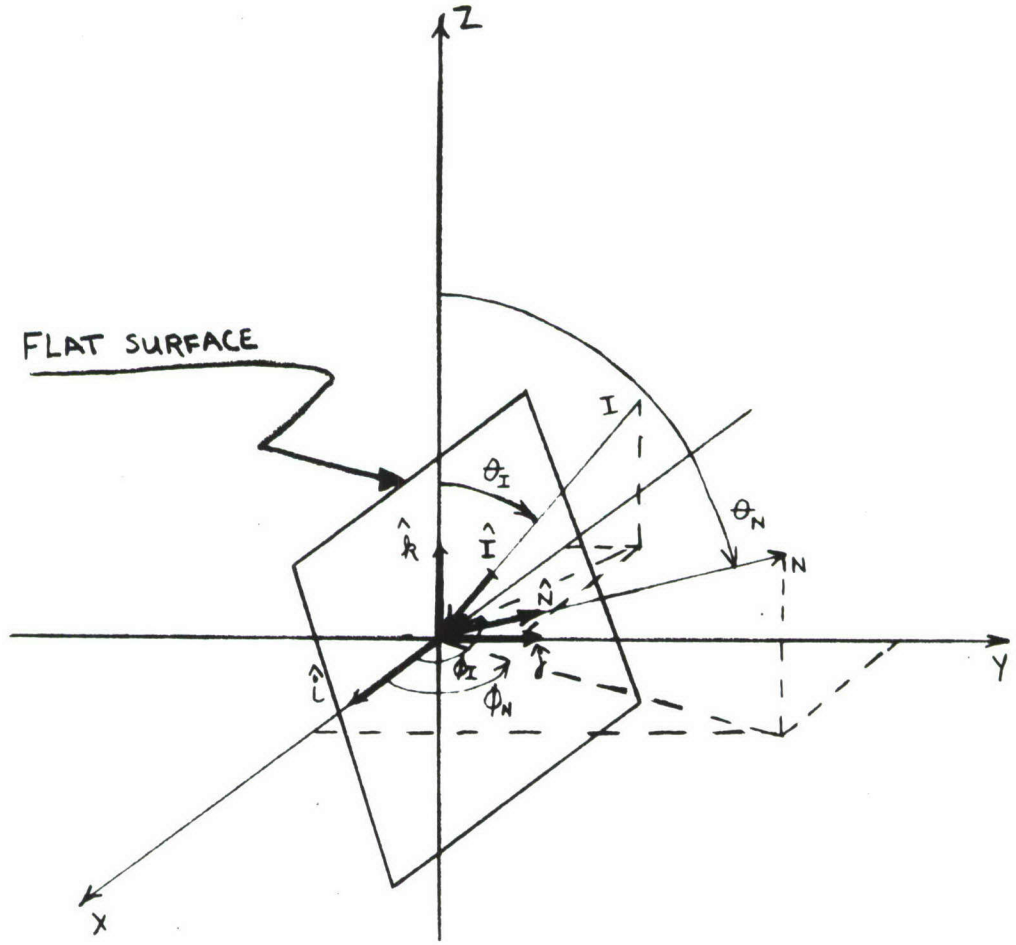

θ_I = Zenith Angle of Incident Ray
θ_N = Zenith Angle of Surface Normal
$\hat{I}$ = Unit Vector in the Direction of Incident Ray
$\hat{N}$ = Unit Vector In The Direction of Surface Normal
ϕ_N = Azimuth Angle of Surface Normal
ϕ_I = Azimuth Angle of Incident Ray

Figure 2-3. Reflected Vector From a Flat Surface in Space

(5) $(\hat{R})Y = -\text{Sin}\theta_I \text{Sin}\phi_I + 2 (\text{Sin}\theta_I \text{Sin}\theta_N \text{Cos} (\phi_I - \phi_N) + \text{Cos}\theta_I \text{Cos}\theta_N) \text{Sin}\theta_N \text{Sin}\phi_N$

(6) $(\hat{R})Z = -\text{Cos}\theta_I + 2 (\text{Sin}\theta_I \text{Sin}\theta_N \text{Cos} (\phi_I - \phi_N) + \text{Cos}\theta_I \text{Cos}\theta_N) \text{Cos}\theta_N$

2.5 Determination of Sun Positions Which Cause Glints In The Region of Interest for a Given Window Elevation.

The region of interest is shown in figure 2-4. (Note that only reflected vectors in this region give glints on the ground outside of the 1 km semicircle.)

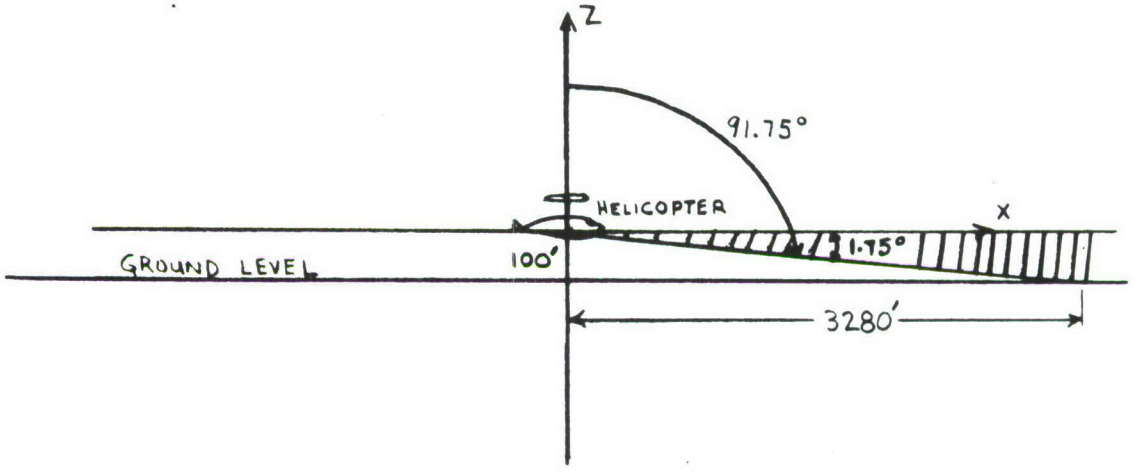

Figure 2-4. Glint Region of Interest

This region results from the fact that glints from the canopy are of interest only if they strike the ground at a distance of 1 km or greater from the helicopter. Hence the region of interest can be described by the following angular region:

$$90^\circ \leq \text{Zenith Angle} \leq 91.75^\circ$$

$$-90^\circ \leq \text{Azimuth Angle} \leq 90^\circ$$

The reflected vector calculated in section 2.4 is only of interest if it emanates from the surface within the above angular region. In equations (4), (5), (6), ϕ_N is the azimuth angle of the normal to the surface. This angle can be set to zero in the following development without loss of generality since glint directions are referenced to the x-axis of the helicopter. Setting $\theta_N = \phi$, equations (4), (5), (6) become:

(7) $(\hat{R})X = -\sin\theta_I \cos\phi_I + 2\,(\sin\theta_I \sin\theta_N \cos\phi_I + \cos\theta_I \cos\theta_N)\sin\theta_N$

(8) $(\hat{R})Y = -\sin\theta_I \sin\phi_I$

(9) $(\hat{R})Z = -\cos\theta_I + 2\,(\sin\theta_I \sin\theta_N \cos\phi_I + \cos\theta_I \cos\theta_N)\cos\theta_N$

Now if approximately the middle of the region of interest is considered, then the zenith angle of the reflected vector is 91°. Since the reflected vector $\hat{R}$ is a unit vector, then the Z component must be -.01745 ft. Hence from equation (9):

$$(\hat{R})Z = -.01745 = -\cos\theta_I + 2\,(\sin\theta_I \sin\theta_N \cos\phi_I + \cos\theta_I \cos\theta_N)\cos\theta_N$$

or

$$(10)\quad \cos\phi_I = \frac{\cos\theta_I - 2\cos\theta_I \cos^2\theta_N - .01745}{2\sin\theta_N \cos\theta_N \sin\theta_I}$$

The above equation expresses the conditions that must be satisfied in order for the reflected vector to be in the region of interest. In other words, for a given window elevation, and a given sun vector elevation, equation (10) gives the reflected vector azimuth at which the reflected vector zenith is 91°. To gain a better physical feeling for the meaning of equation 10, consider the following.

Suppose that the window is positioned as follows:

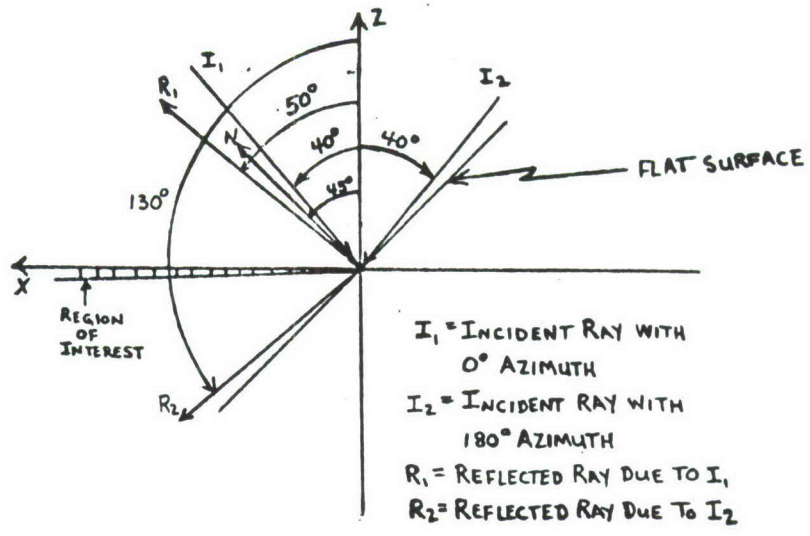

Figure 2-5. Illustration of Window Reflections

Suppose also that the incident sun ray elevation is 50°. Consider figure 2-5. Note that when the sun ray azimuth is zero degrees, the reflected ray eminates above the region of interest. When the sun ray azimuth is at 180° the reflected ray is below the region of interest. Hence for some sun ray azimuth between 0° and 180°, the reflected vector must sweep through the region of interest. Equation (10) can be used to calculate this sun ray azimuth.

The results from equation (10) are shown in graphical form in figures 2-6 through 2-11. All angles are with respect to earth coordinates and the window yaw and roll angles are zero. Note that the earth coordinates are the basic inertial frame for this problem as shown in figure 2-1 (denoted by X_H, Y_H, Z_H). The window aspect can be referenced directly in earth coordinates since the helicopter yaw, pitch, and roll are assumed to be zero.

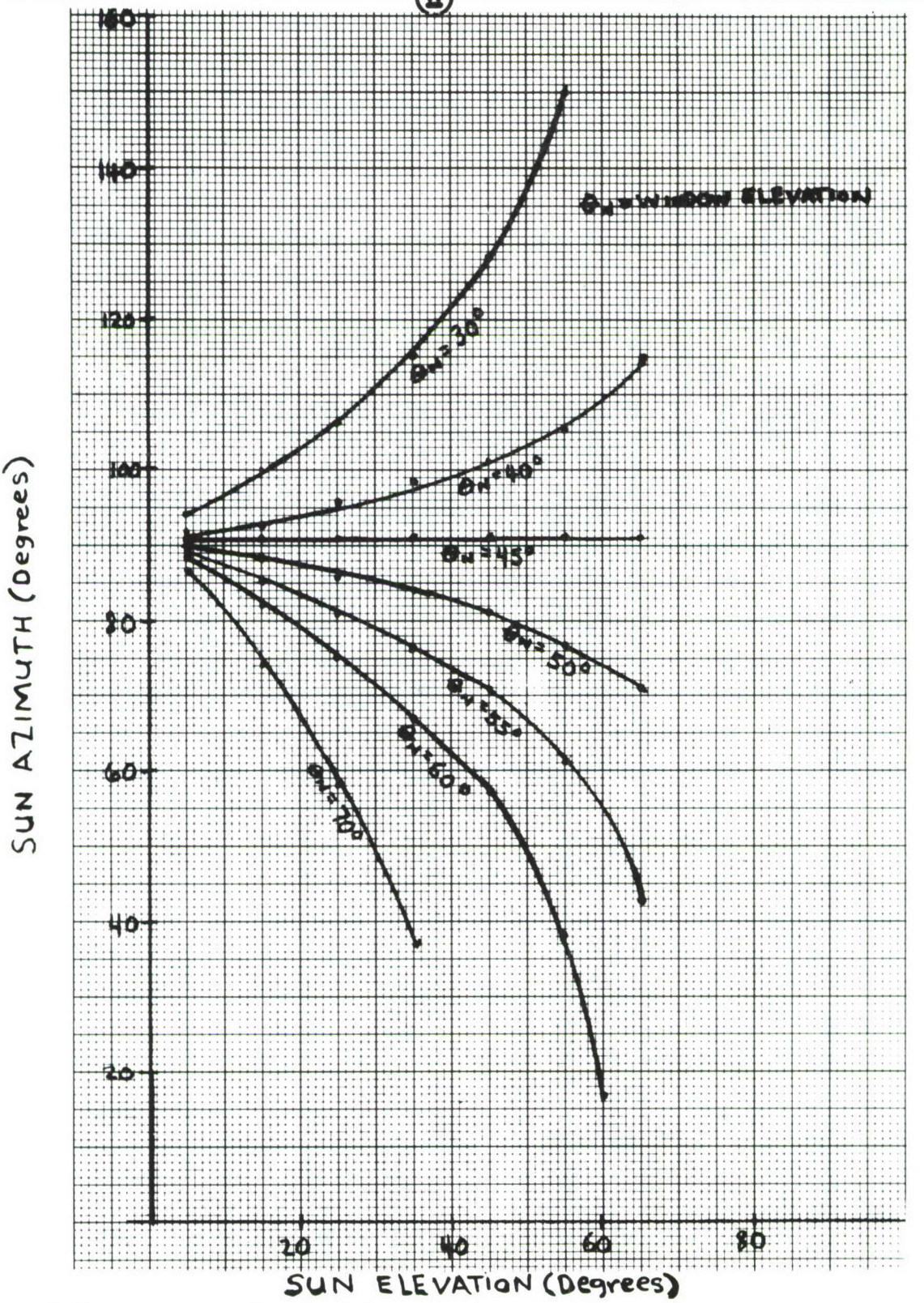

Figure 2-6. Offending Sun Positions for Various Elevations of Front Sloped Window

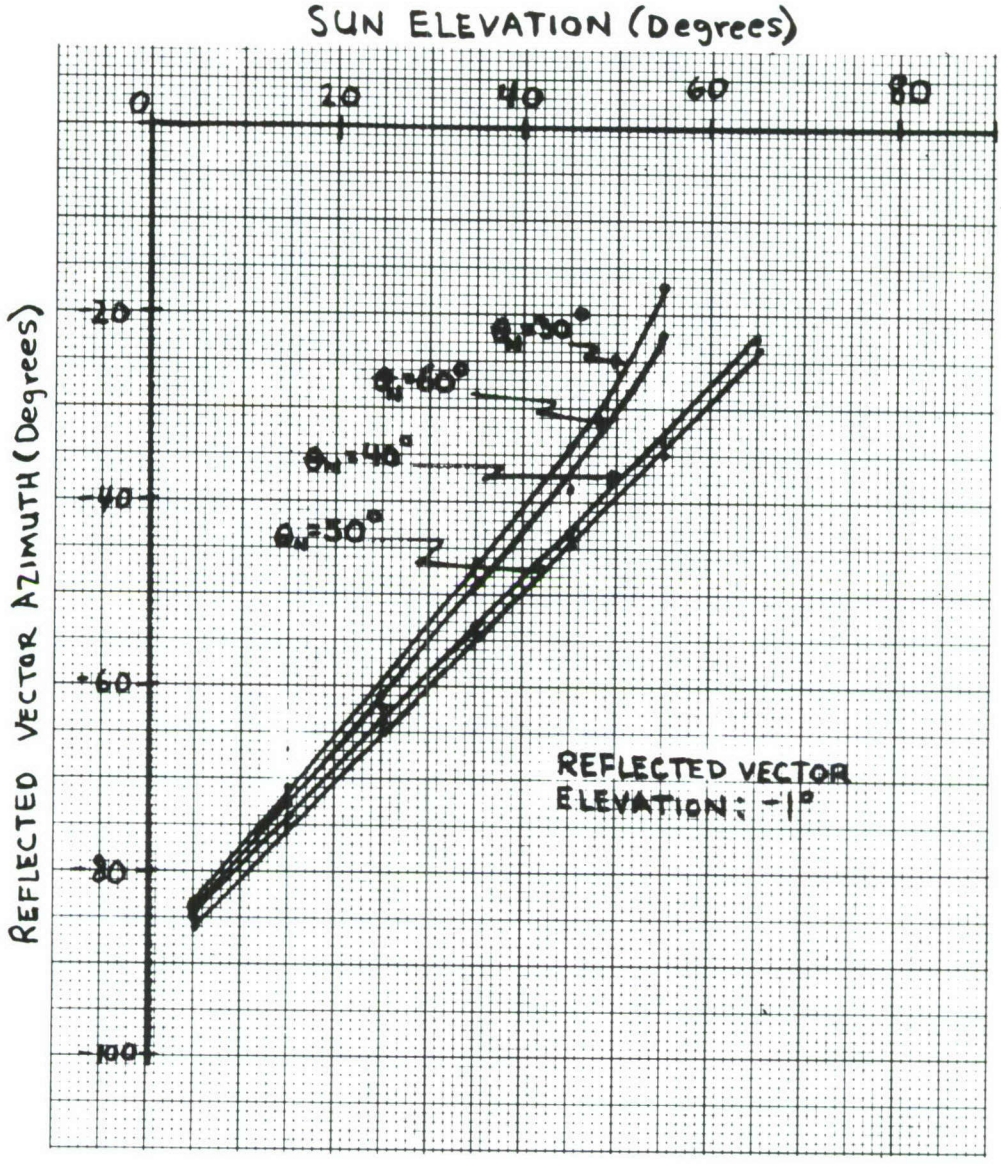

Figure 2-7. Reflected Vectors Which Correspond to the Offending Sun Positions in Figure 2-6

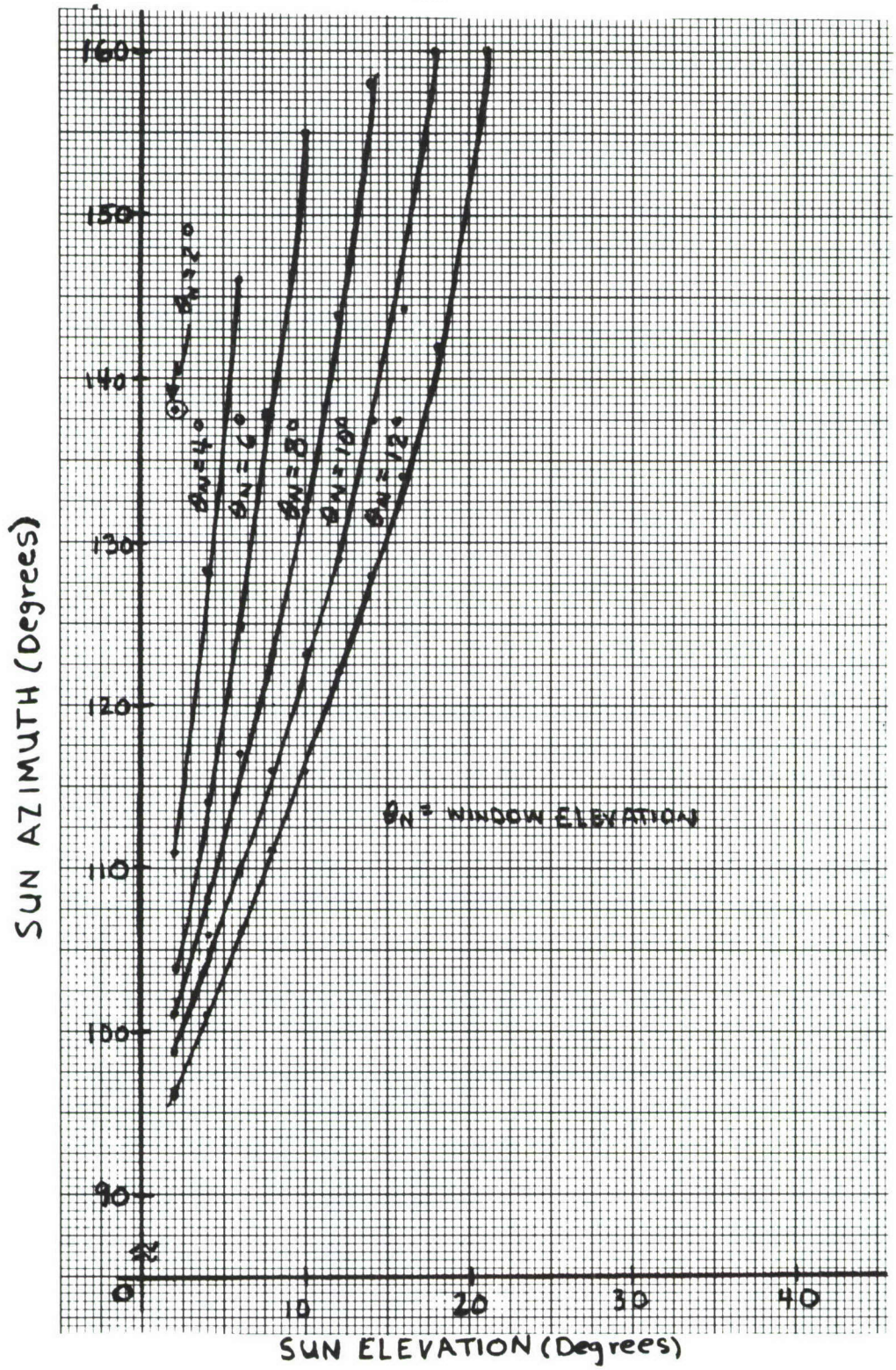

Figure 2-8. Offending Sun Postions for Various Elevations of Top Window

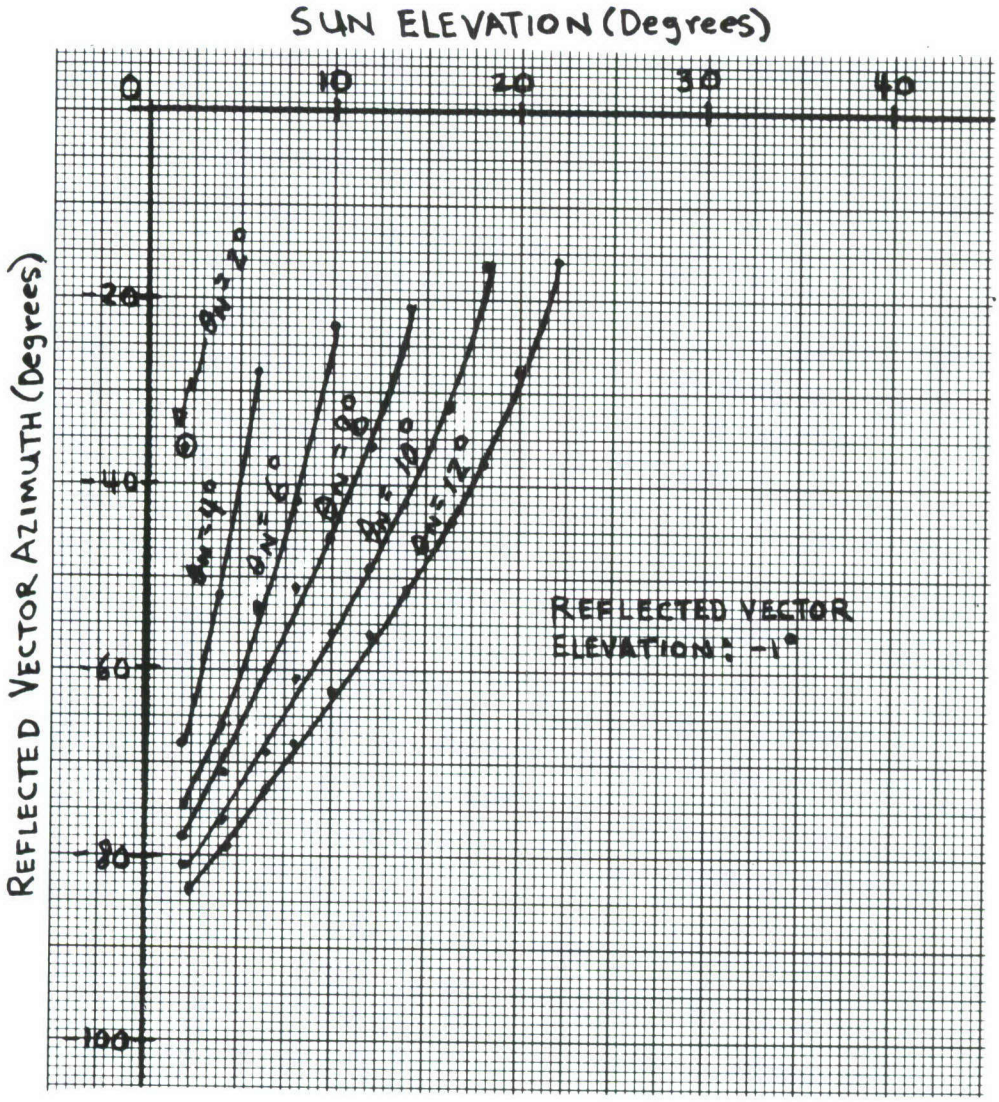

Figure 2-9. Reflected Vectors Which Correspond to the Offending Sun Positions in Figure 2-8

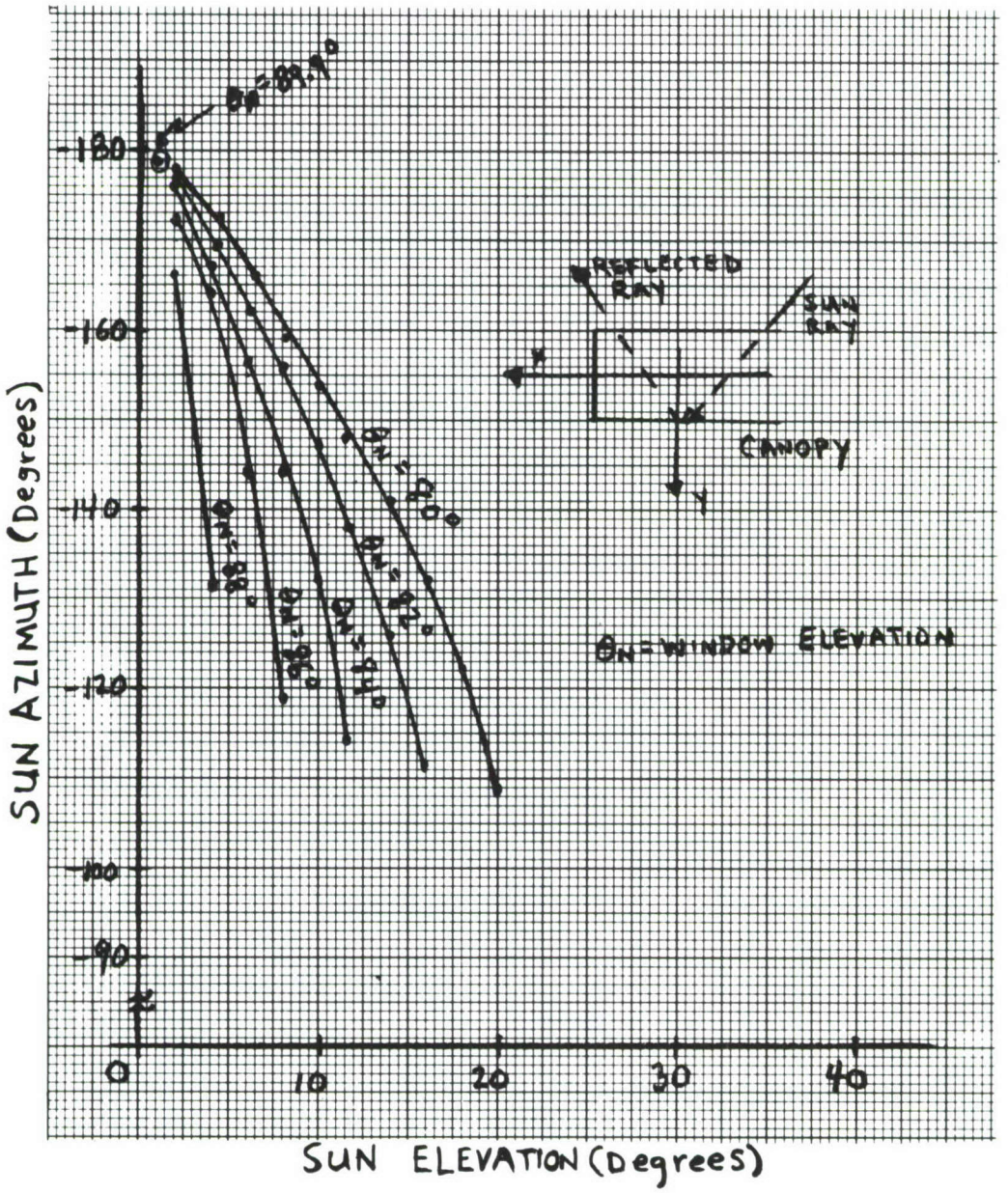

Figure 2-10. Offending Sun Positions for Various Elevations of the Side Windows

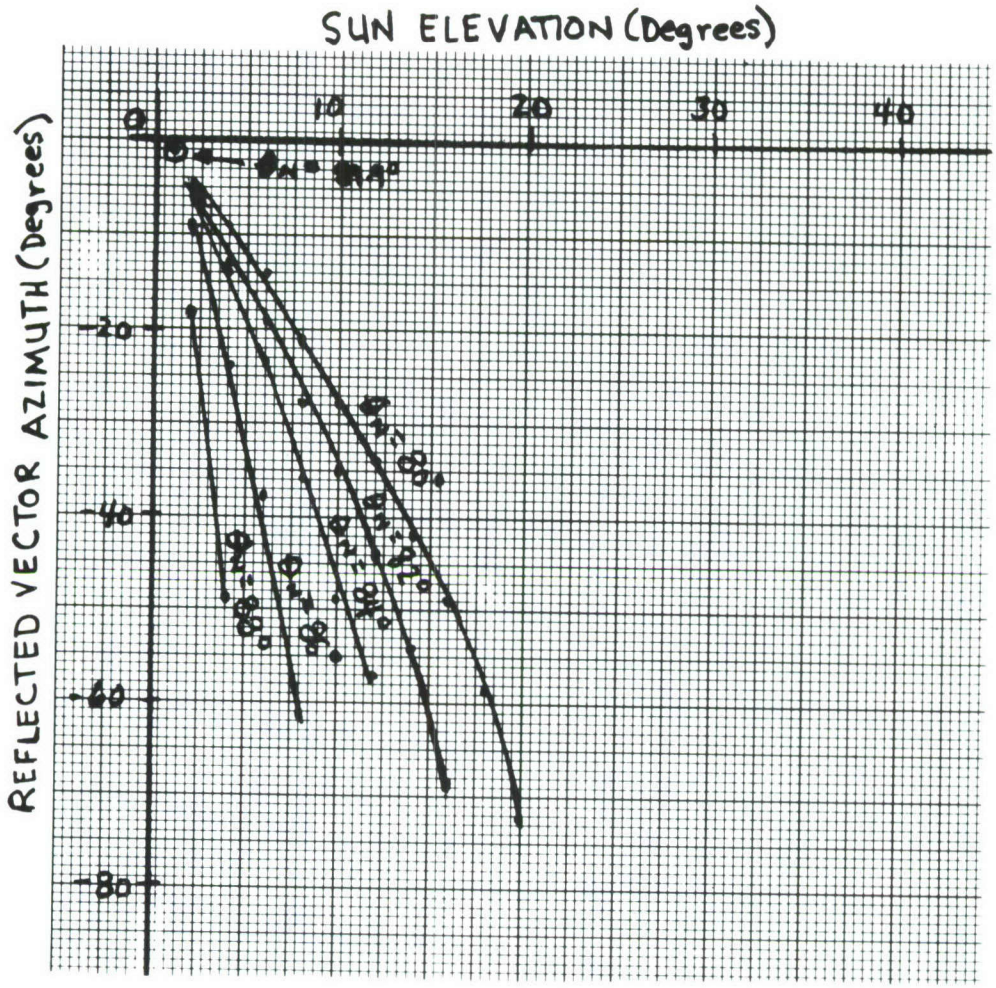

Figure 2-11. Reflected Vectors Which Correspond to the Offending Sun Positions in Figure 2-10

in the region of interest for a given window elevation and a given sun elevation. For example, consider the curve labeled $\theta_N = 45^\circ$ which corresponds to a window elevation of 45°. The curve indicates that the sun vector azimuth which causes specular reflections in the region of interest is approximately 91° for all sun elevations from 0° to 65°. Note that the data is plotted for window elevations from 30° to 70°. Also note that as the window elevation is decreased below 45°, the offending sun azimuths tend toward the rear of the aircraft, and as the window elevation is increased, the offending sun azimuths tend toward the front of the aircraft. Whereas the 45° window elevation has offending sun rays coming from the side of the craft. As will be seen shortly, this information yields considerable insight into the design of baffles for the front windows.

Figure 2-7 corresponds to figure 2-6 and illustrates the azimuth of the reflected vector when the reflected vector is in the region of interest for a given window elevation and a given sun elevation. Note that for all the cases considered, the reflected vector emanates toward the front of the aircraft beginning with small azimuths for high suns and increasing in azimuth as the sun gets lower in the sky. For example, when the window elevation is 45° and the sun vector elevation is 40°, the reflected vector has an azimuth of -44° and a zenith of 91°.

It is important to note that figure 2-6 could have been plotted for sun ray azimuths from 360° to 180° and the curves would have the same form. For example, when the window elevation is 45° and the sun elevation is 65°, a sun azimuth of 270° would cause a reflected vector with 91° zenith and an azimuth of 22.5°. In other words, the sun azimuths which cause glints in the region of interest are symmetric with respect to the X-axis of the helicopter.

The same comment can be made of the curves for the top window.

Figures 2-8 and 2-9 represent the same type of data for the top window as figures 2-6 and 2-7 do for the front sloped window. Figures 2-10 and 2-11 illustrate this data for the inside of the side windows. In this case, the sun ray would go through the cockpit and reflect off the opposite window back through the cockpit and toward the ground. For the outside of the side windows, there were no sun positions which cause glints in the region of interest for window elevations of 92° through 100°. Note that figures 2-6 through 2-11 can be used to predict the positions of glints on the ground for a variety of canopy designs which have the basic form shown in figure 2-2. Also, a very important point is that for any glint on the ground, the sun position which caused that glint can be located for a given window elevation.

2-6. Canopy and Baffle Design

It is clear from the curves in figures 2-6 through 2-11 that adjusting the slopes of the window surfaces for the basic canopy will not eliminate glints in the region of interest. The best that can be done is to adjust the window slopes such that sun positions which cause glints in the region of interest are located so as to result in the most efficient baffling system in terms of number and sizes of baffles.

This leads to the next question: How can the data in figures 2-6 through 2-11 be used in order to aid in the design of baffles for each of the surfaces? The first step, however, will be to define the basic baffle configurations to be considered in this study. The next step will then be to use the data in figures 2-6 through 2-11 in order to evaluate the basic configurations.

The basic baffle configurations are shown in figure 2-12.

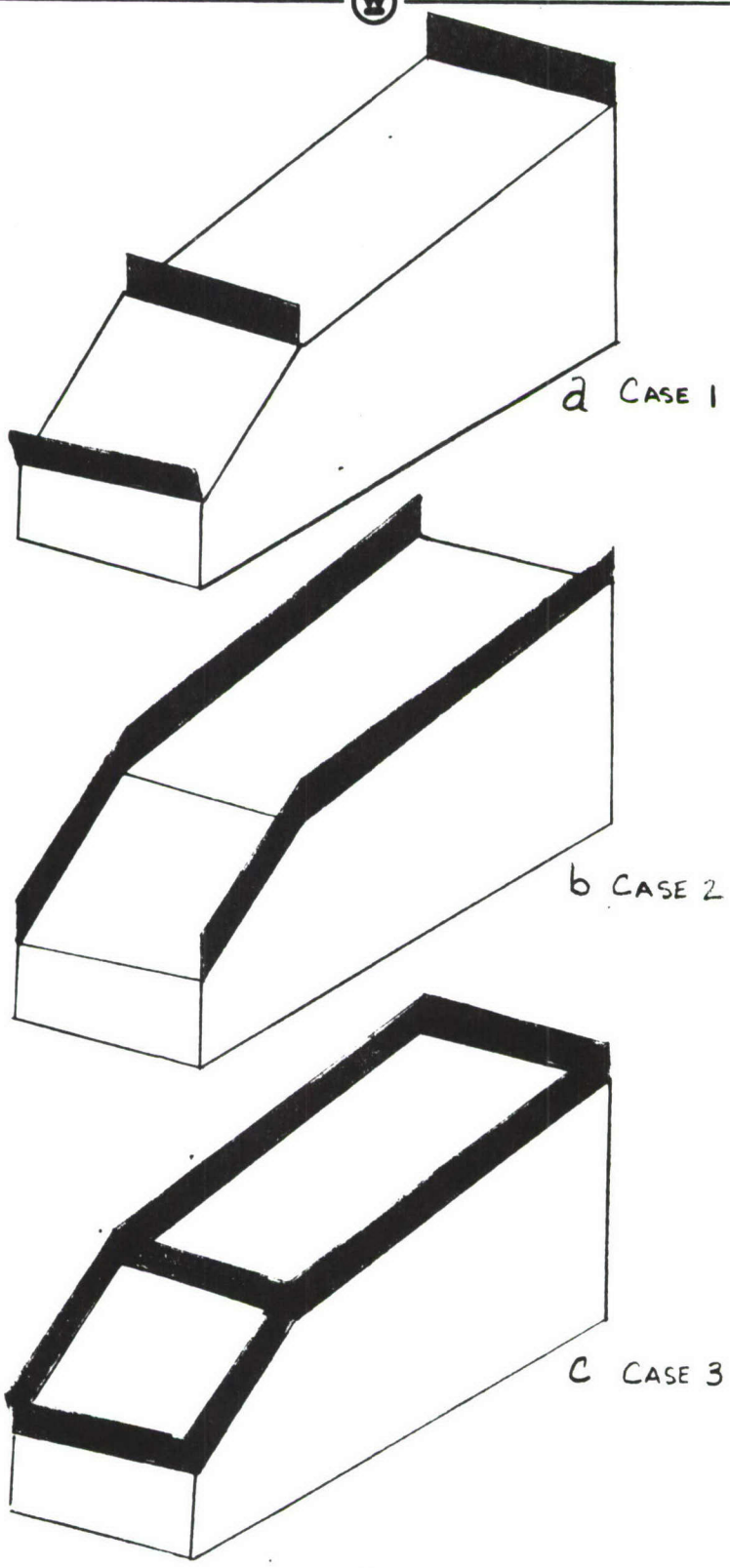

Figure 2-12. Basic Baffle Configurations

2.6.1 Front Sloped Window and Baffle Design

The offending sun position data can now be used to adjust the slopes of the basic canopy structure in order to minimize the sizes of baffles and gain insight into the most efficient placement of baffles.

The approach used to analyze the required baffle height for a given window elevation will be discussed in the next few paragraphs. The basic philosophy of the analysis is illustrated in figure 2-13.

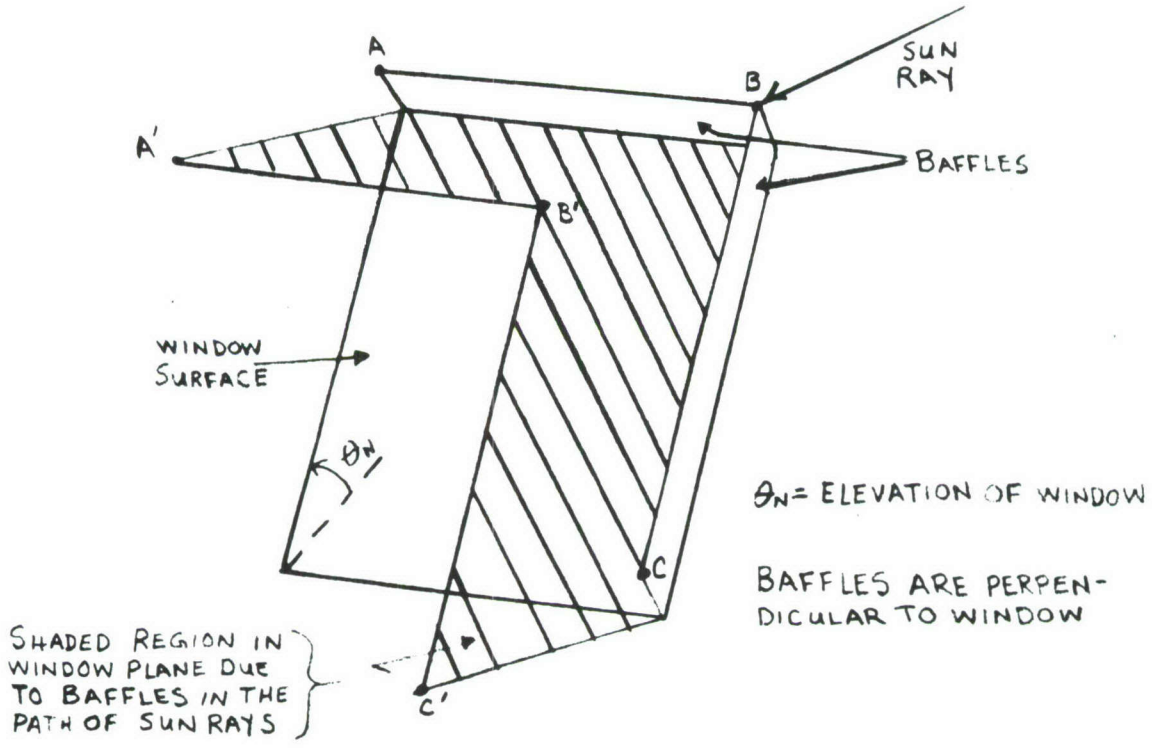

Figure 2-13. Shade Map of Baffles in the Window Plane

Notice that corners A, B, C in figure 2-13 are contained in all three basic baffle configurations in figure 2-12. The approach is to map corners A, B, C

into the plane of the window in order to assess how large the baffles must be in order to shade the entire window. This is the point at which the curves in figures 2-6 through 2-11 are very useful. These curves indicate, for a given window elevation, the positions of the sun which must be baffled. In order to illustrate the approach, the analysis will be done thoroughly for a specific case and then the results will be presented for all the cases considered.

Suppose that the window elevation is set at 40° and suppose that the window is 2.67 ft. by 3.25 ft. (size of front window in the LWL Flat Canopy design). Then from figure 2-6, the offending sun positions can be found and are shown in Table 2-2 along with the zenith and azimuth angles of the corresponding reflected vectors.

Table 2-2

Offending Sun Positions and Corresponding Reflected Vectors For a Window Elevation of 40 Degrees

Sun Position	Sun Elevations	Sun Azimuth	Reflected Vector Zenith	Vector Azimuth
1	65°	115°	91°	-22.5°
2	55°	105°	91°	-34°
3	45°	101°	91°	-44°
4	35°	98°	91°	-54°
5	25°	94°	91°	-64°
6	15°	92°	91°	-74°
7	5°	91°	91°	-84°

The algorithm is to pass a sun vector with the given angles through corners A, B, C and find the intercept of the ray with the window plane. This procedure generates a baffle shadow map in the plane of the window. The first

step is to fix the baffle height to determine the change in the shape of the shadow as the sun moves through the positions shown in table 2-2. The results of this analysis are shown in figures 2-14 through 2-20. As can be seen, the basic shape of the shadow does not change as the sun moves through the positions in table 2-2.

The basic baffle configuration in figure 2-12C can now be examined in light of the maps generated. The major question for this baffle system is how large must the baffles be in order to cause the line A'-B' to be outside line C-D or in other words shade the entire window. The approach here was to vary the baffle height until the corner B' remained outside the line for all sun positions in table 2-2. This map is illustrated in figure 2-21 and as can be seen, a baffle height of 2.3 ft was required to shade a window 2.67 ft x 3.25 ft.

The same approach was used to map corner A, C, D into window plane along the reflected vectors in table 2-2. It was found that a baffle height of 2.3 ft was required to shade the entire window. Observe, as shown in figure 2-22, that it is only necessary to shade one-half of the window along the reflected vector and one half along the sun vector.

This same analysis was done for window elevations of 43°, 45°, 50°, 55°, and 60°. The results are shown in figures 2-23 and 2-24. Note that the baffle heights shown are those which would be required to shade one-half the window in the sun direction and in the reflected vector direction. Note also that the figures given are only approximate and only show the trends in the size of baffle required vs. the elevation angle of the window. The range of elevations shown correspond to the range being considered for the front sloped window. There is one major trend to notice in the curves. As the elevation

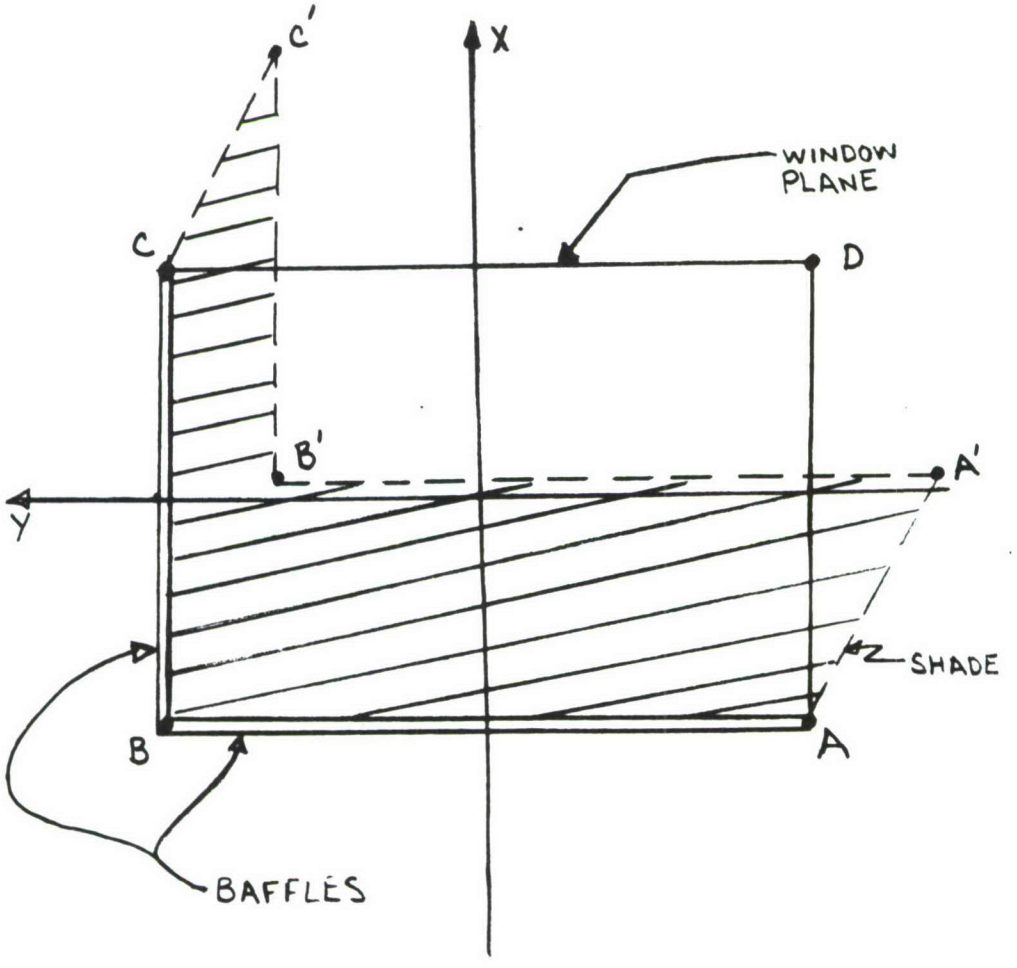

Window Elevation: 40°
Sun Azimuth: 115°

Figure 2-14. Baffle Shade Map in Window Plane for Baffle in Figure 2-12C With Sun Elevation of 65°

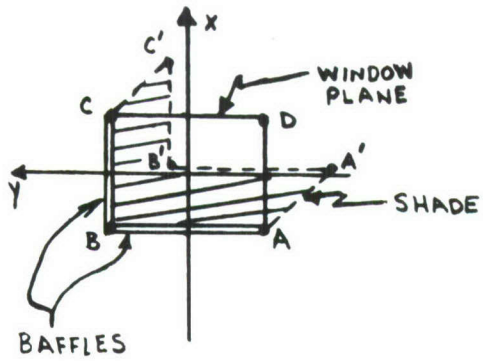

Window Elevation: 40°
Sun Azimuth: 105°

Figure 2-15. Baffle Shade Map in Window Plane for Baffle in Figure 2-12C With Sun Elevation of 55°

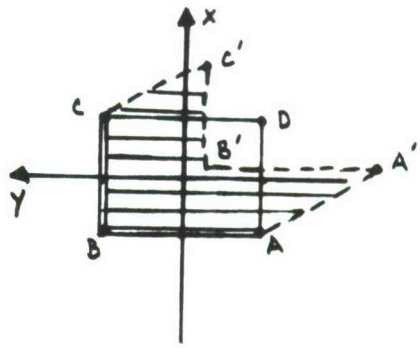

Window Elevation: 40°
Sun Azimuth: 101°

Figure 2-16. Baffle Shade Map in Window Plane for Baffle in Figure 2-12C With Sun Elevation of 45°

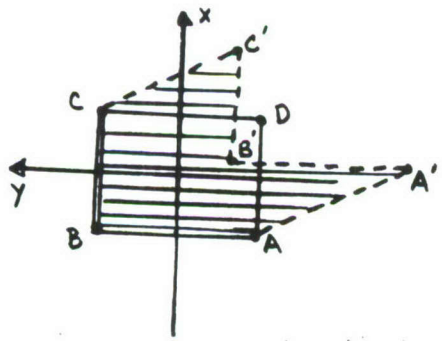

Window Elevation: 40°
Sun Azimuth: 98°

Figure 2-17. Baffle Shade Map in Window Plane for Baffle in Figure 2-12C With Sun Elevation of 35°

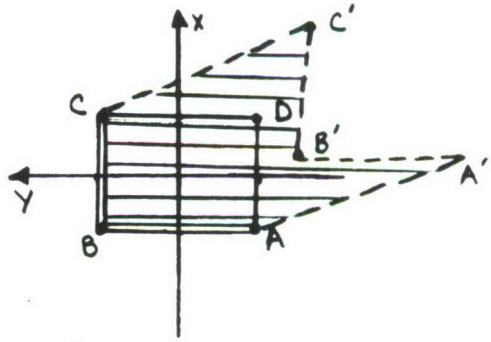

Window Elevation: 40°
Sun Azimuth: 94°

Figure 2-18. Baffle Shade Map in Window Plane for Baffle in Figure 2-12C With Sun Elevation of 25°

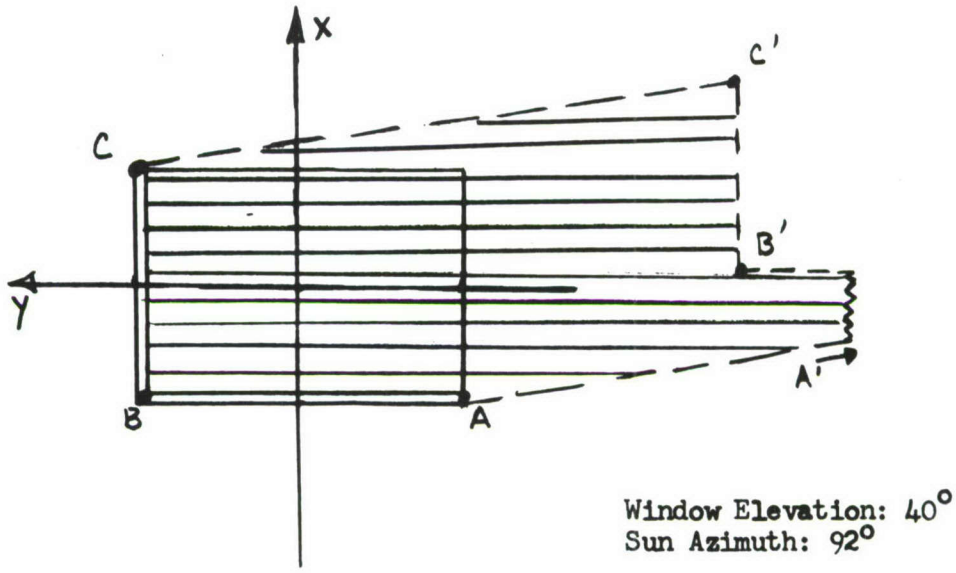

Figure 2-19. Baffle Shade Map in Window Plane for Baffle in Figure 2-12C With Sun Elevation of 15°

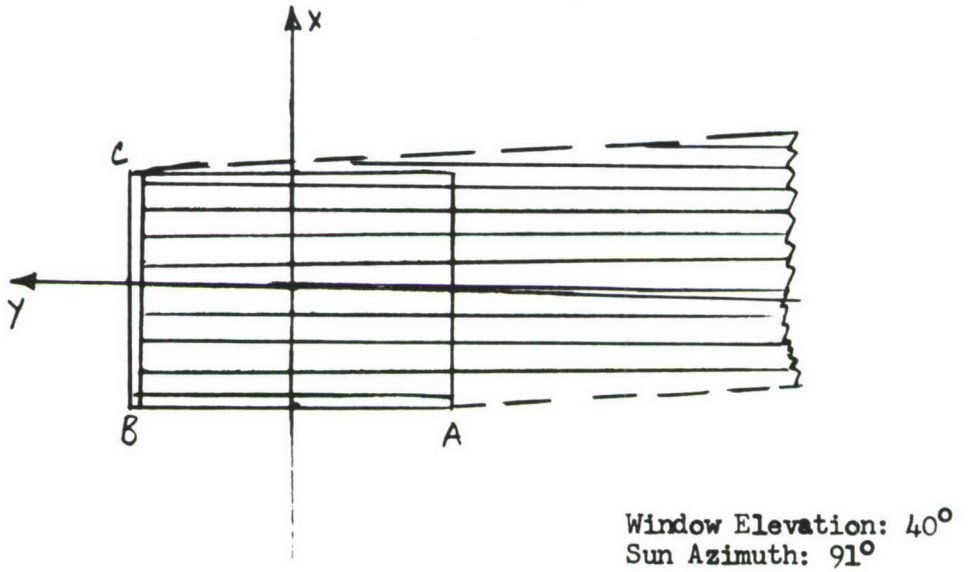

Figure 2-20. Baffle Shade Map in Window Plane for Baffle in Figure 2-12C With Sun Elevation of 5°

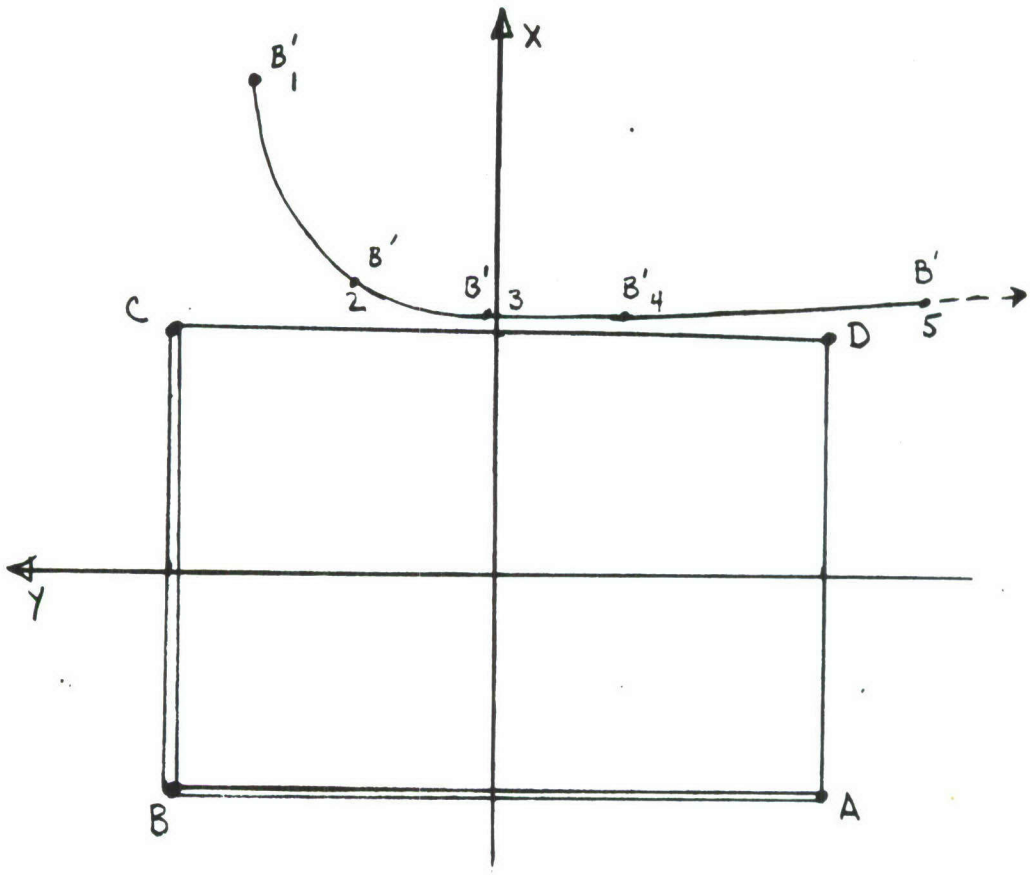

THIS DRAWING ILLUSTRATES THE BAFFLE SIZE REQUIRED FOR FULL SHADING USING THE BAFFLE CONFIGURATION IN FIGURE 2-12C AND THE SUN POSITIONS IN TABLE 2-2 THE NUMBERS ASSOCIATED WITH EACH POINT DENOTE CORRESPONDING SUN POSITIONS AS SHOWN IN TABLE 2-2.

Figure 2-21. Map of Corner B in Window Plane for a Baffle Height of 2.3 Feet and Baffle Configuration in Figure 2-12C

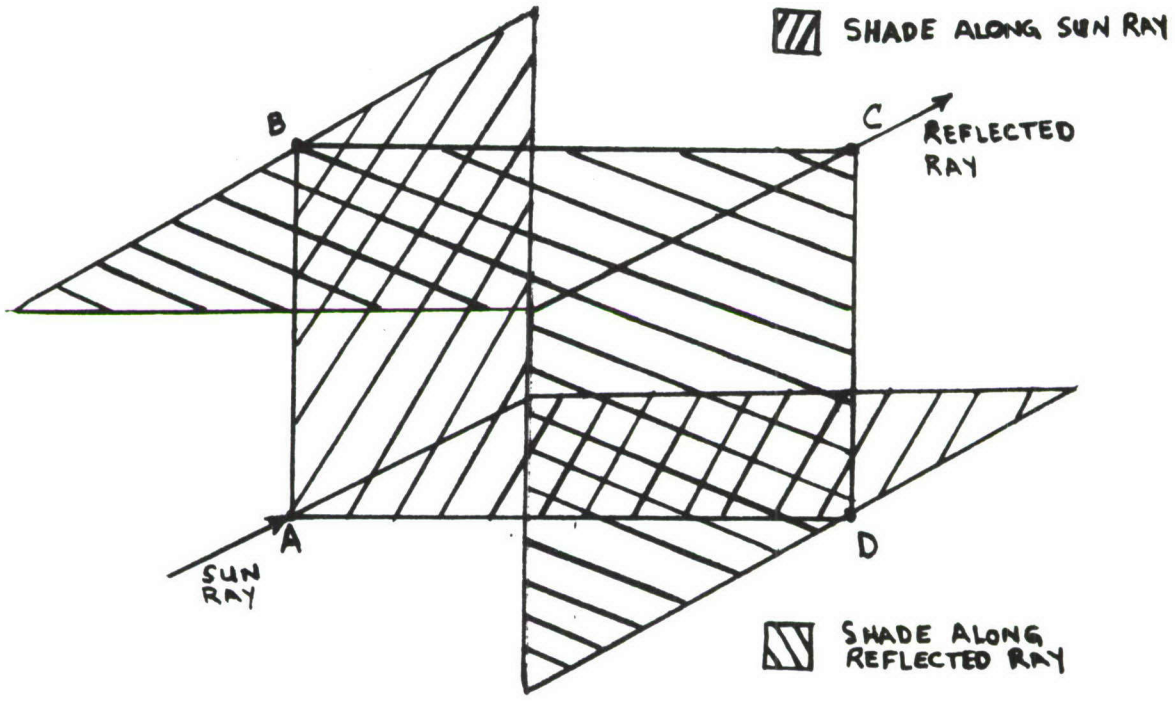

Figure 2-22. Illustration of Shadows of Baffle System in Figure 12C Under the Condition That the Entire Window is Shaded

of the window is increased, the size of baffle required gets larger. This can be explained by using figure 2-6. Notice that as the elevation angle of the window is increased from 45°, the offending sun positions move to the front of the craft and hence the baffles must increase in size to shade the same area in the window plane. To see this, imagine the limiting case that the sun is directly in front of the helicopter with a vertical window and it is easy to see that infinitely long baffles would be required.

The first major observation can now be made in regard to the adjustment of the slope of the front window. It is clear from the results shown in figures 2-23 and 2-24 that the elevation of the front window should be no greater than 45°. The lower limit on the elevation of the front window is

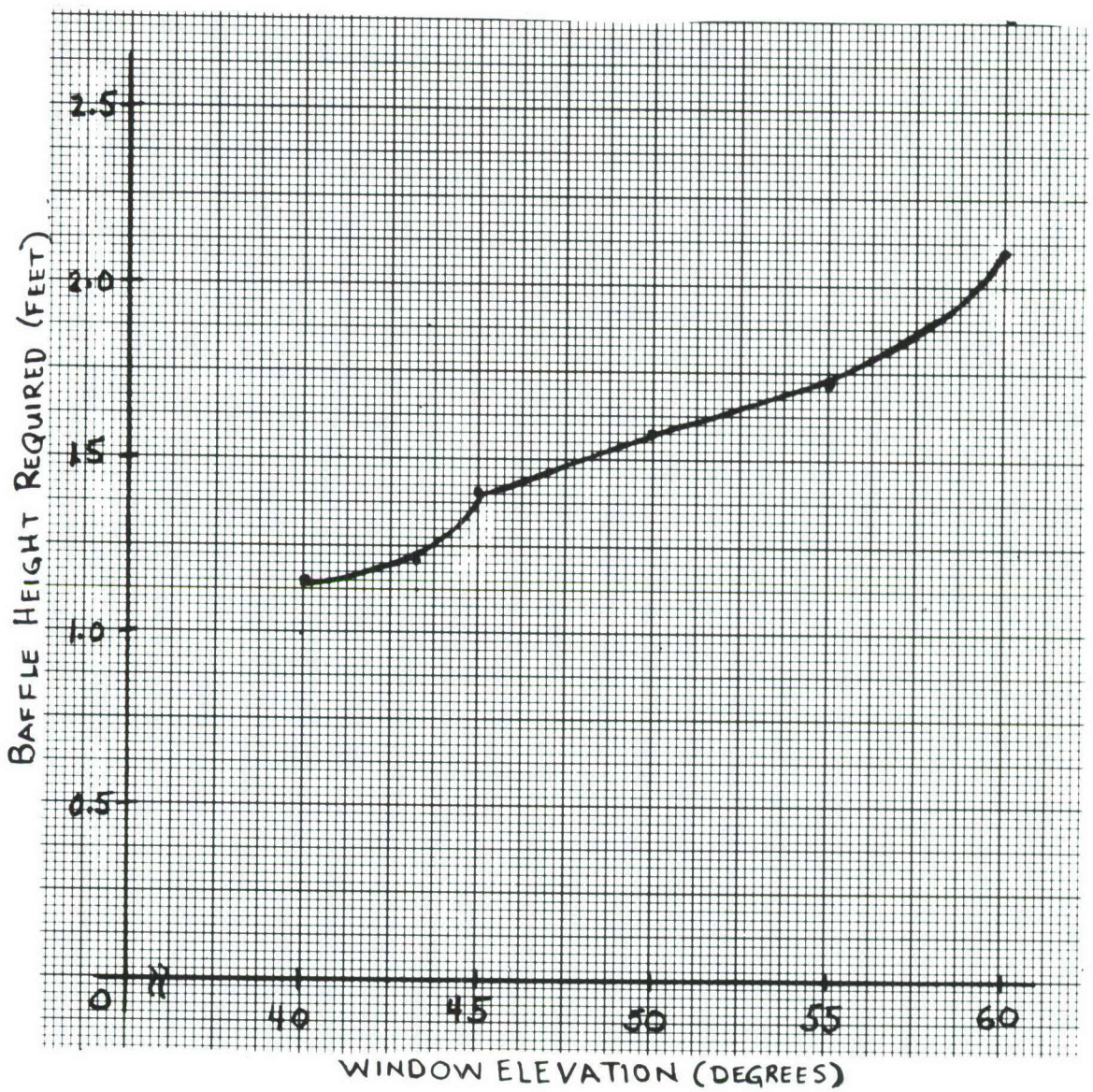

Figure 2-23. Illustration of the Relation Between Required Baffle Height and Front Window Elevation for Full Shading Along the Sun Vector (see Figure 2-22)

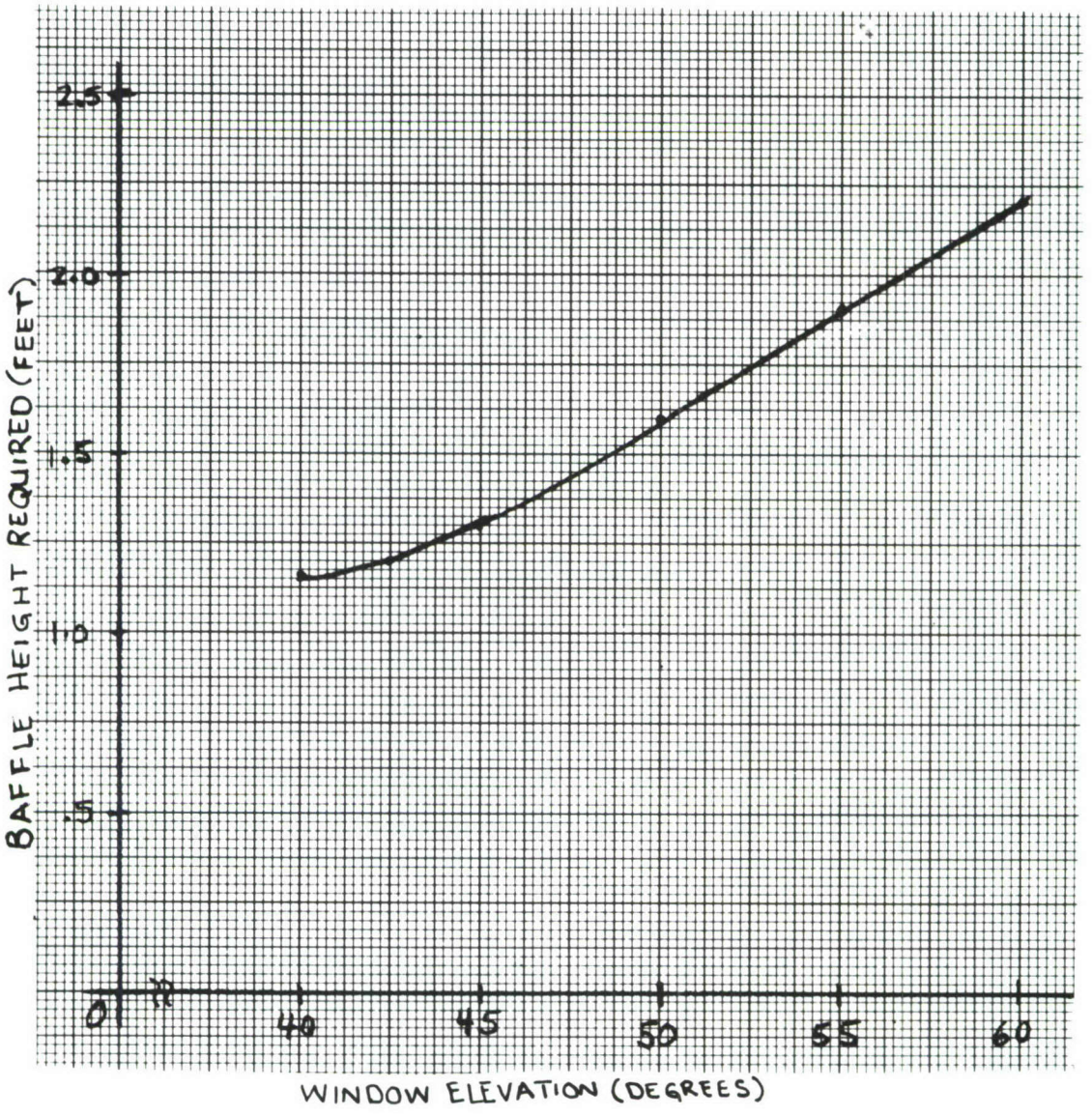

Figure 2-24. Illustration of the Relation Between Required Baffle Height and Front Window Elevation for Full Shading Along the Reflected Vector (see Figure 2-22)

due to physical considerations which will be discussed later.

After a meeting with Mr. G. Cook, it was determined that the baffle configuration in Figure 2-12C was unacceptable with the size of baffles required. The reason for this is due to obscuration of gunner and pilot vision particularly by the lower baffle. A venitian blind affect was also discarded as being unreasonable from a sight obscuration point of view.

The results of the above mentioned meeting led to the consideration of the basic baffle configuration illustrated in figure 2-12(b). The purpose of the analysis was to evaluate the placement and sizes of the baffles in order to reduce glints from the canopy. (Note that the baffle configuration in figure 2-12(a) can be discarded immediately since the offending sun positions for any of the window elevations are at azimuths which would require side baffles as shown in figure 2-6.)

The first aspect of this final design of the front sloped window was the placement of the baffles in such a manner as to create minimum obscuration of pilot and gunner vision but allow reasonable baffle sizes to be utilized. The existing curved surface canopy provided some insight into the placement of the baffles. Consider the drawing of the existing Cobra canopy in figure 2-25. The 16" flat portion in the center of the canopy suggested the placement of four baffles on the front window as shown in figure 2-26. With the baffles positioned as shown, the remaining variables to be determined were the heights of the baffles above the window surface.

In order to determine the required height of the baffles, it was necessary to use the results of the shadow mapping study discussed earlier in this report. The method for doing this was a straight forward application of

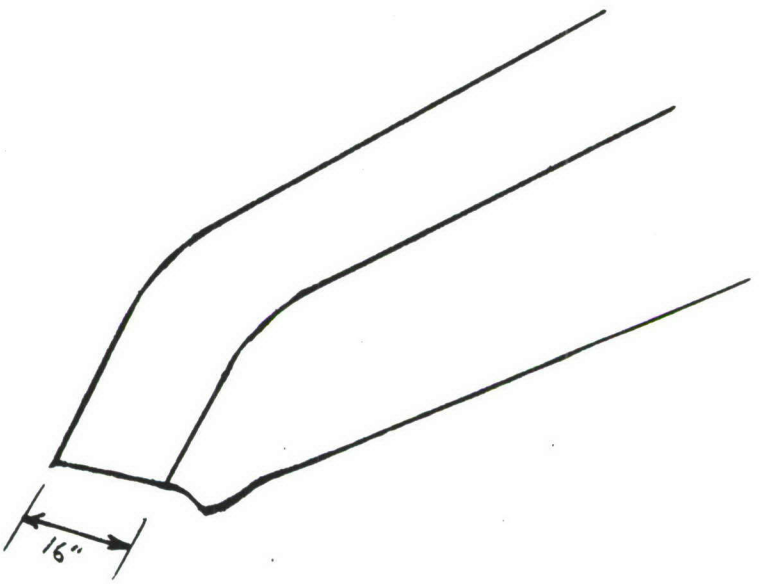

Figure 2-25. Sketch of Existing Curved Surface Cobra Canopy

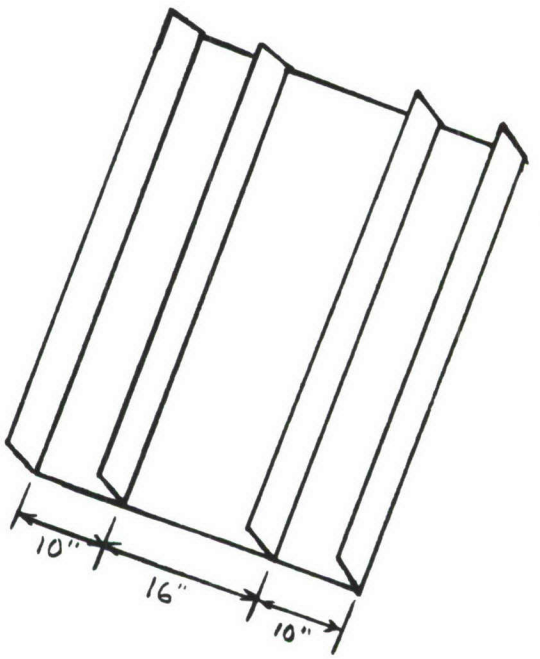

Figure 2-26. Baffle Configuration Analyzed for Front Window

the mapping results. Consider figure 2-27. The idea was to vary the height of baffle AB until the shadow of baffle AB along the sun vector overlapped with the shadow of baffle CD along the reflected vector as shown in figure 2-27. The same analysis was done for baffles CD and EF, and baffles EF and GH. It was found that the minimum size baffles required were for window elevations (with respect to earth coordinates) of from 40° to 45°. The reason for this can be seen by considering figure 2-6. Notice that for window elevations in this range, that offending sun rays approach the aircraft from the side. In other words, the offending sun rays have azimuths (with respect to helicopter coordinates) of from 91° to 115° (or from 245° to 269° by symmetry) for the case when the window elevation is 40°. When the window elevation is 45°, the offending sun rays approach the helicopter from an azimuth of 91° (or from 269°) for all sun elevations from 0° to 65°. The fact that the baffle system under consideration should be smallest for these azimuths is intuitively obvious since they would be expected to be most effective in baffling sun rays approaching from the side.

The results of the above analysis showed the following size requirements for the baffles in figure 2-27.

Baffle	Height
AB	6"
CD	12"
EF	12"
GH	6"

A further decision for the front window resulted in a window elevation of 40°. This was chosen because the helicopter is normally pitched by approximately

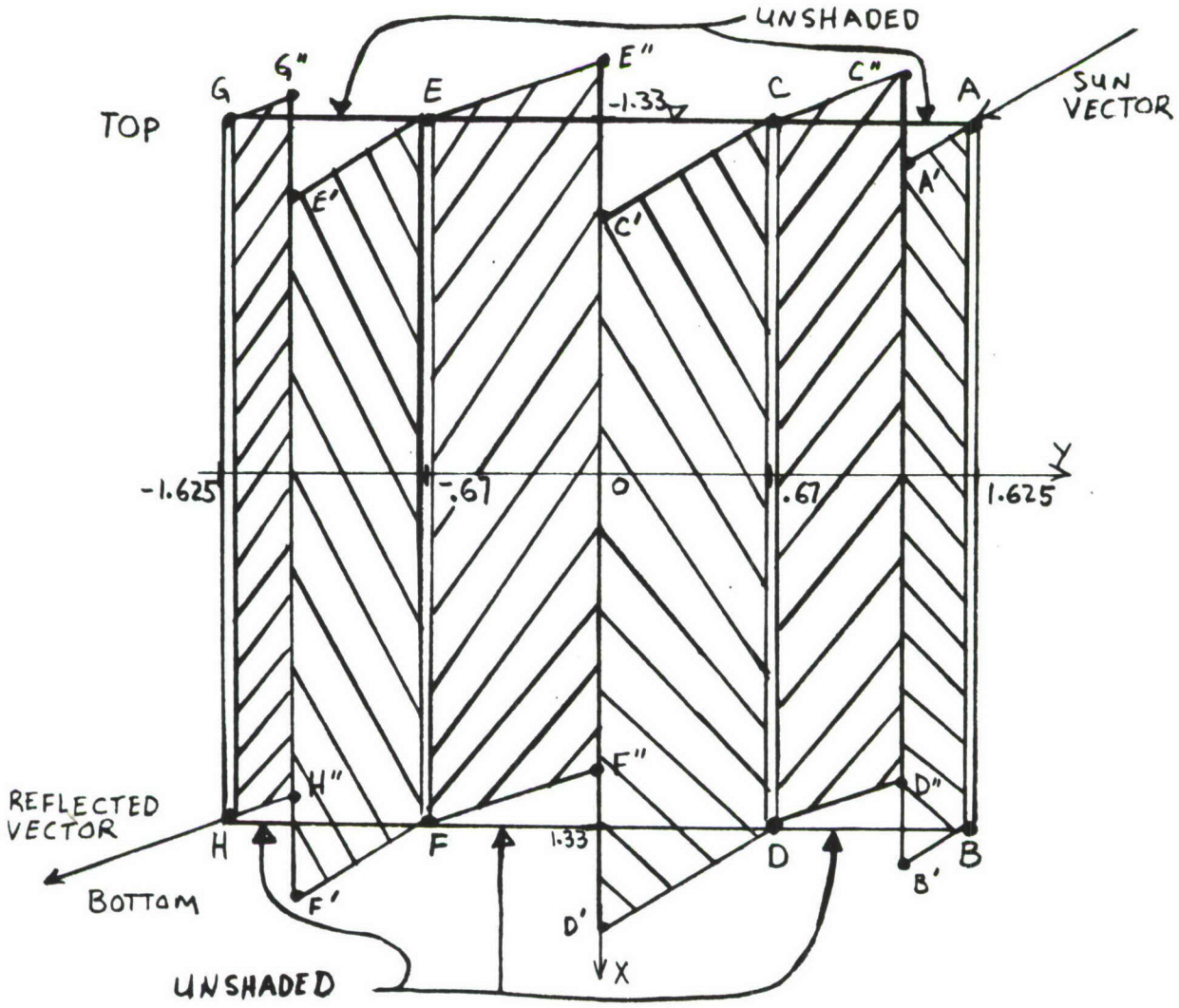

Figure 2-27. Illustration of Technique Used to Analyze the Baffle

5° while flying. This would cause a total front window pitch of 45° to take advantage of the baffle system's effectiveness against side suns. While hovering at 0° pitch, the window would be at an elevation of 40° which is a less restrictive case. The high sun position at a zenith of 25° places the strongest requirement on the size of the baffle since, as the sun position gets lower in the sky, the width of the shadows gets wider in the Y direction. Notice the unshaded portions of the window in figure 2-27.

These unshaded areas created a need to lengthen the baffles in the X-direction. The amount that the baffles have to be lengthened depends on their height. The mapping analysis showed that the 12" baffles had to be lengthened beyond the window surface by 12" in order to eliminate these unshaded regions. The 6" baffles had to be extended by 9". Note that the length of the window in the X-direction does not affect the baffle design so that this dimension can be varied to meet other constraints. The final front sloped window and baffle design is shown in figure 2-28. Note that if it is allowable to have high sun positions which give glints in the region of interest, both height and the extension of the baffles can be reduced in size.

2.6.2 Top Window and Baffle Design

The analysis of the top window follows the same procedure as the analysis of the front window. That is, the first step was to determine the offending sun positions for the range of window elevations considered. Then, those results were used to map baffle shadows into the window plane in order to cause total shading of the top window for all offending sun positions.

Figures 2-8 and 2-9 show the offending sun positions for top window elevations from 2° to 12°, along with reflected vector azimuths due to these offending sun positions. The elevation of the top window was set at

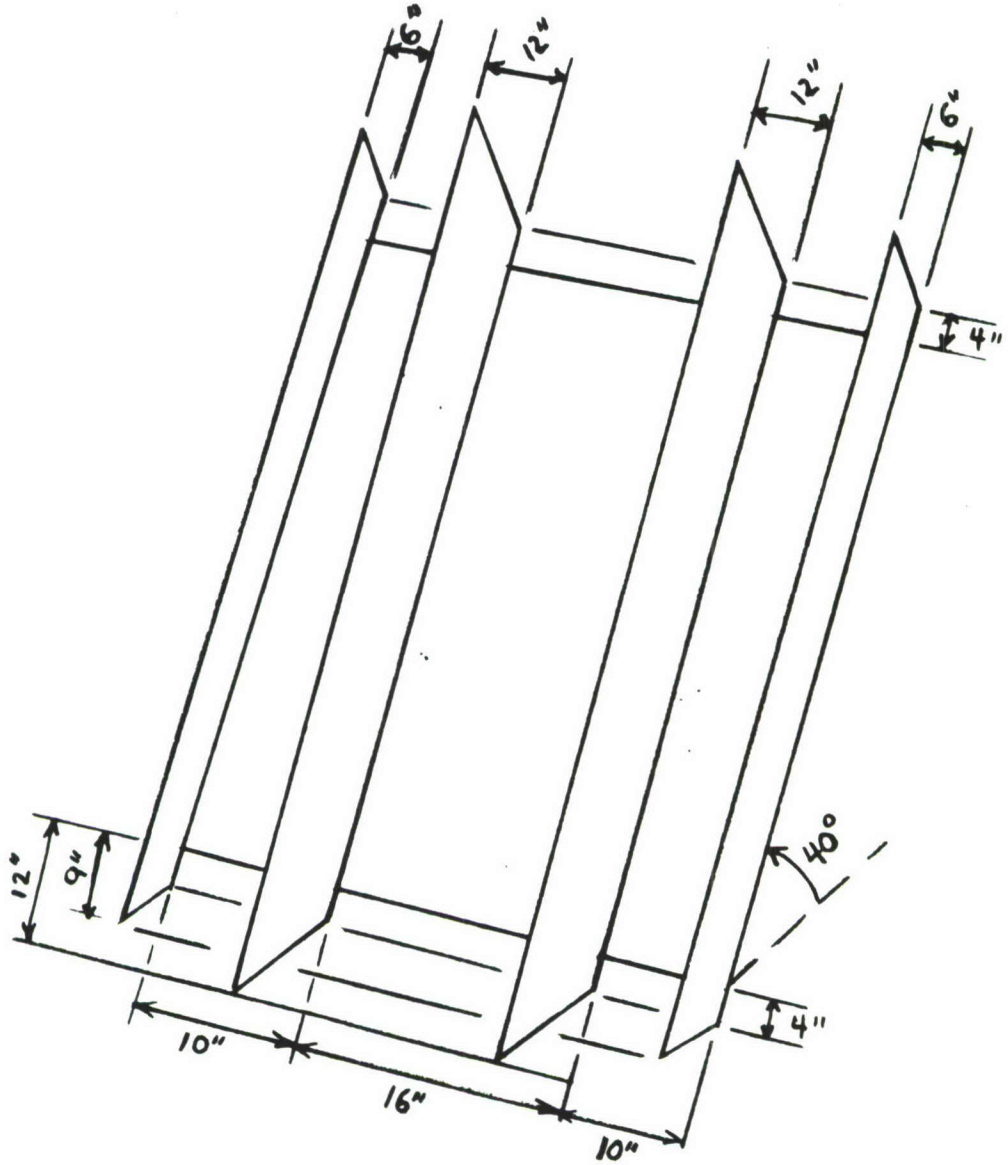

Figure 2-28. Final Baffle Design for the Front Shaped Window

5° to match the slope of the existing Cobra overhead window and as a compromise between glint characteristics and reduction in surface area for the front and side windows. Since the helicopter is assumed to have a 5° pitch with a dither of ±2°, the total elevation of the top window must be considered to be 12°. Using the offending sun positions and reflected vector data for the 12° case from figures 2-8 and 2-9, it was determined that 6" baffles placed as shown in figure 2-29, were sufficient to shade the top window as illustrated in figure 2-30.

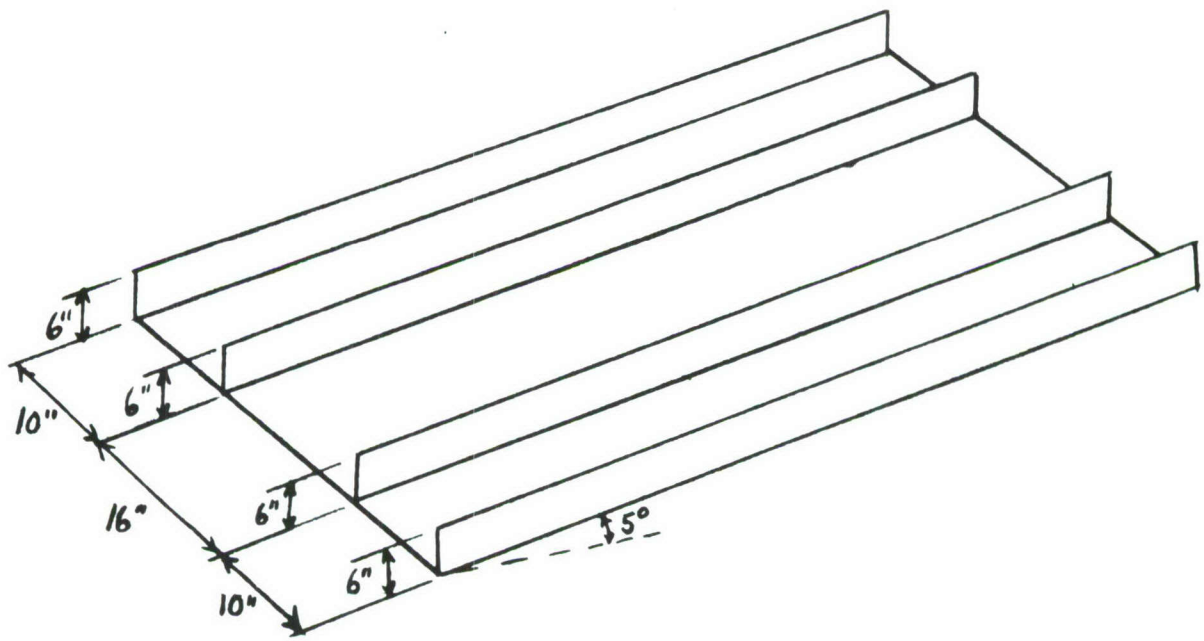

Figure 2-29. Top Window Baffle Configuration

Notice again that there are triangular regions which are unshaded by the top window baffles. It was expected that the extended baffles from the front windows would shade the triangular regions in the front of the top window,

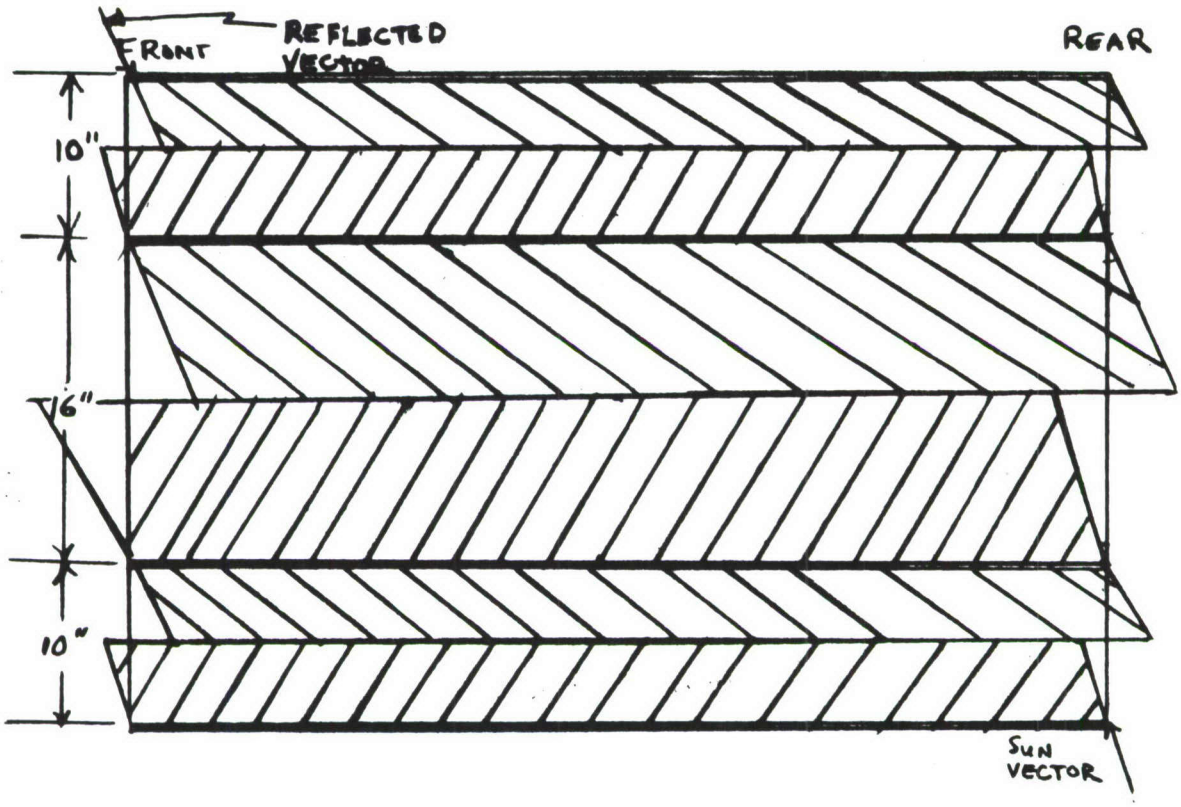

Figure 2-30. Shadows of Baffles in the Top Window Plane

except for sun azimuths near 180°. However, it was necessary to provide another baffle at the rear of the top window in order to shade the triangular regions in the rear of the top window. This back baffle is actually an extended fairing on the sail to increase its width to 36" and retain its height at 15" above the existing overhead window. The final configuration of the top window baffle system is shown in figure 2-31.

2.6.3 Side Window Design

The side window elevations under consideration were from 90° to 100°. For window elevations from 92° to 100°, there are no sun positions above the horizon that can cause glints in the region of interest from the outside of the window. However, figures 2-10 and 2-11 show the results of

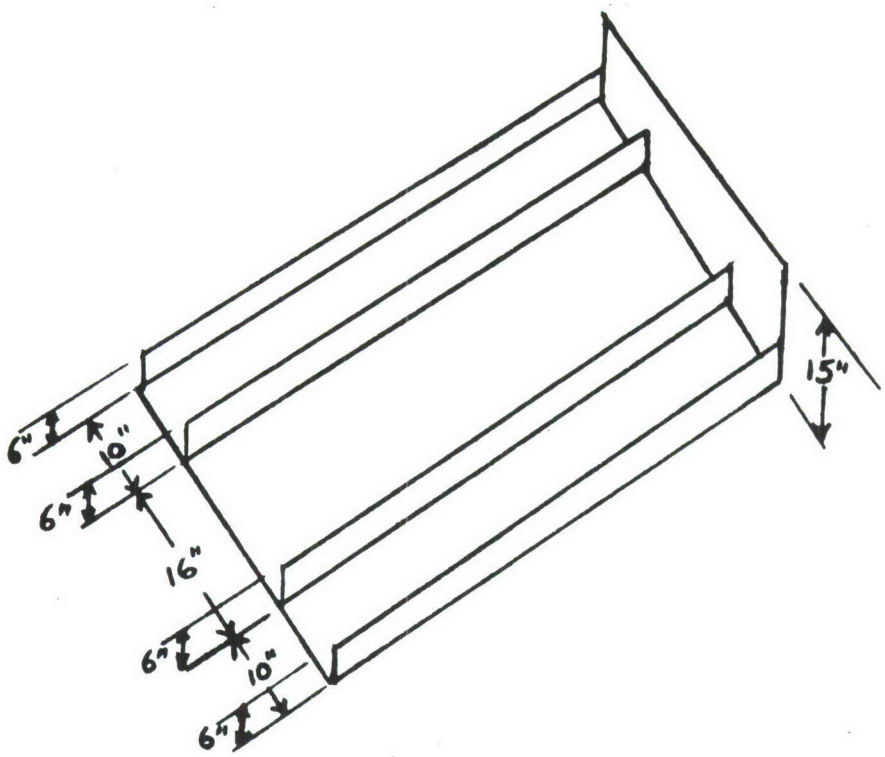

Figure 2-31. Final Baffle Configuration for the Top Window

the above window elevations on the inside of the window. Note that outside window elevations of 92° to 100° correspond to inside window elevations of 88° to 80° respectively. These curves show that by "tilting" the side windows inward, glints can be eliminated from the outside surface but the inside surface becomes a source of glints. Hence, it was decided that the side windows should be vertical. A secondary reason for this decision was the fact that "tilting" the windows inward as shown in figure 2-32 causes the top and front windows to have larger surface areas. For a vertical side window, it is only possible for glints to enter the regions of interest for very low suns. This region of sun zeniths was estimated to be in the range of from 80° to 90°. As will be seen later, the results verify this estimation.

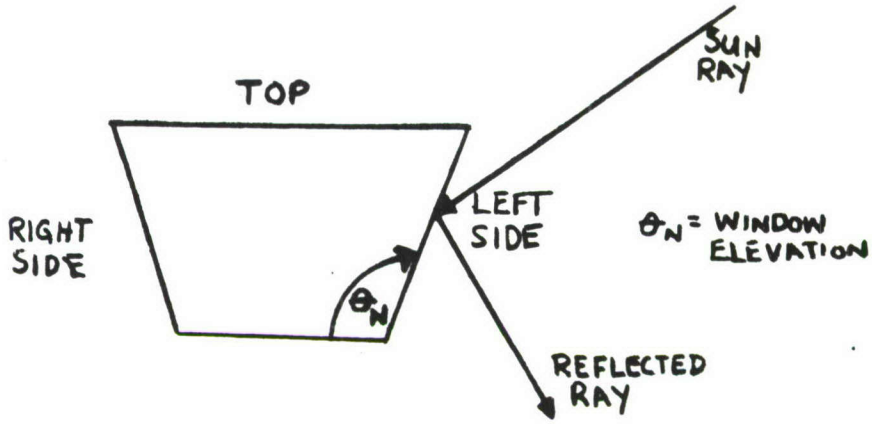

Figure 2-32. Illustration of Tilted Side Windows

2.6.4 Front Vertical Window

The front vertical window requires no baffling because the reflected ray will always be into the ground at less than 1 km when the helicopter is flying with a 5° down pitch. Even at a level attitude, a sun elevation of greater than 1.75° will put the reflected ray into the ground at a range of less than 1 km.

2.7 Physical Considerations in the Design of the Canopy

There are three main considerations in the physical design of the canopy:

(a) The canopy must be geometrically compatible with the existing body design of the Cobra,

(b) The design must allow adequate space for comfort and performance of the gunner and pilot,

(c) Along with minimizing unaided vision obscuration, the design must take into account the forward optical sighting device used by the gunner in tracking ground targets.

In order for the canopy to fit into the existing body design, the base of the canopy must be 36 inches wide and the height of the rear section of the canopy must be 35.67 inches. Also, the length of the canopy must be 114 inches long. These dimensions are illustrated in figure 2-33.

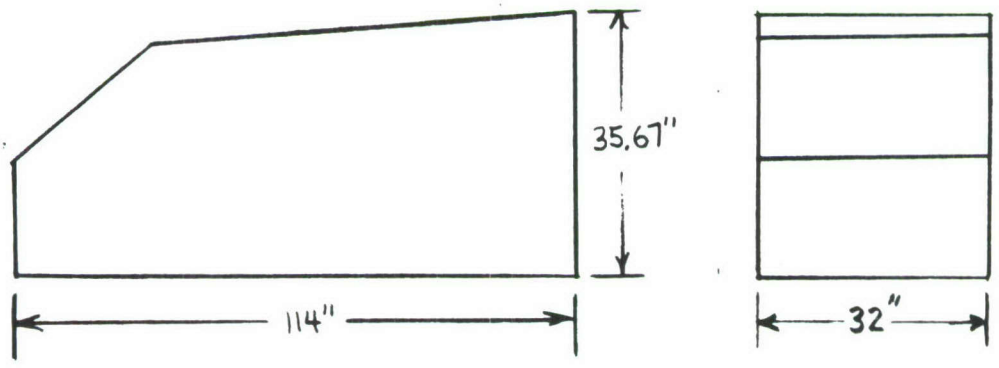

Figure 2-33. Geometrical Requirements on the Canopy Design

The limiting factor in the design of the canopy for the comfort and performance of the gunner and pilot is the position of the gunner. Figure 2-34 shows the location of the gunner's eyes along the x-axis with respect to

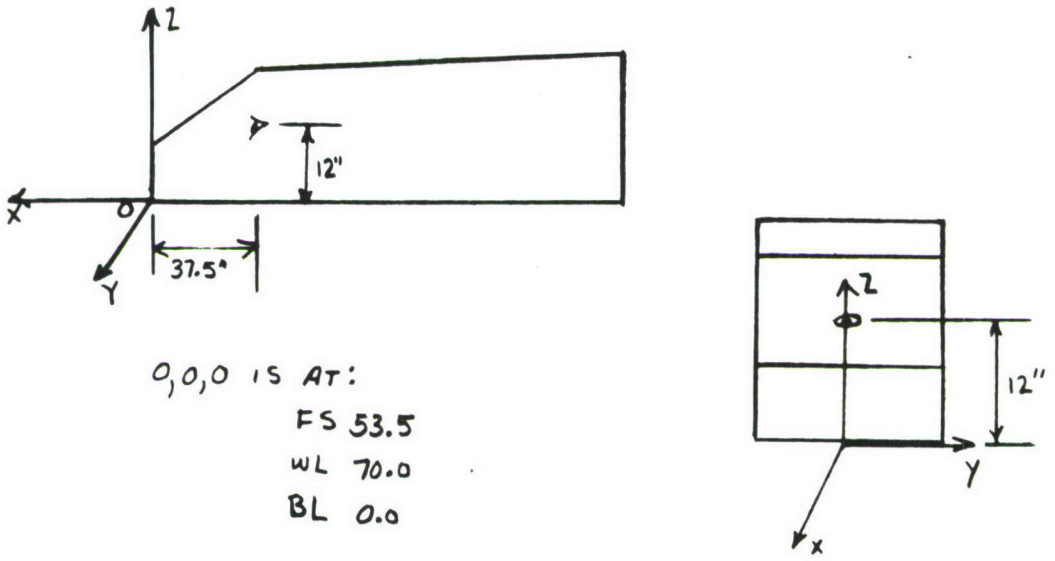

Figure 2-34. Position of Gunner's Eye

a coordinate system placed as shown (with the center at FS 53.5, WL 70, BL 0). The coordinates of the gunners eyes are:

$$x = -37.5" \qquad y = 0 \qquad z = 12"$$

The final design will have to be consistent with these coordinates.

The final physical consideration is the optical sighting device used by the gunner. Since no information has been provided as to the exact location of the device, this aspect will not be considered. However, it will be seen later that this is not an important consideration to the final basic design. It is important to consider the optical path of the device. In a meeting with G. Cook, it was deemed undesirable to place baffles in the direction of the optical path. On the basis of this meeting, a decision was

made to place a vertical front window below the sloped front window which would provide a path for the sighting device. Since the helicopter is normally pitched at 5° in a hovering position, the front vertical window cannot act as a source of glints in the region of interest. The reason for this is that the vertical window will be pitched downward by 5° and any glints caused by suns above the horizon would project inside the 1 km region about the helicopter.

2.8 Final Recommended Canopy Design

The canopy design is illustrated in figures 2-35 and 2-36.

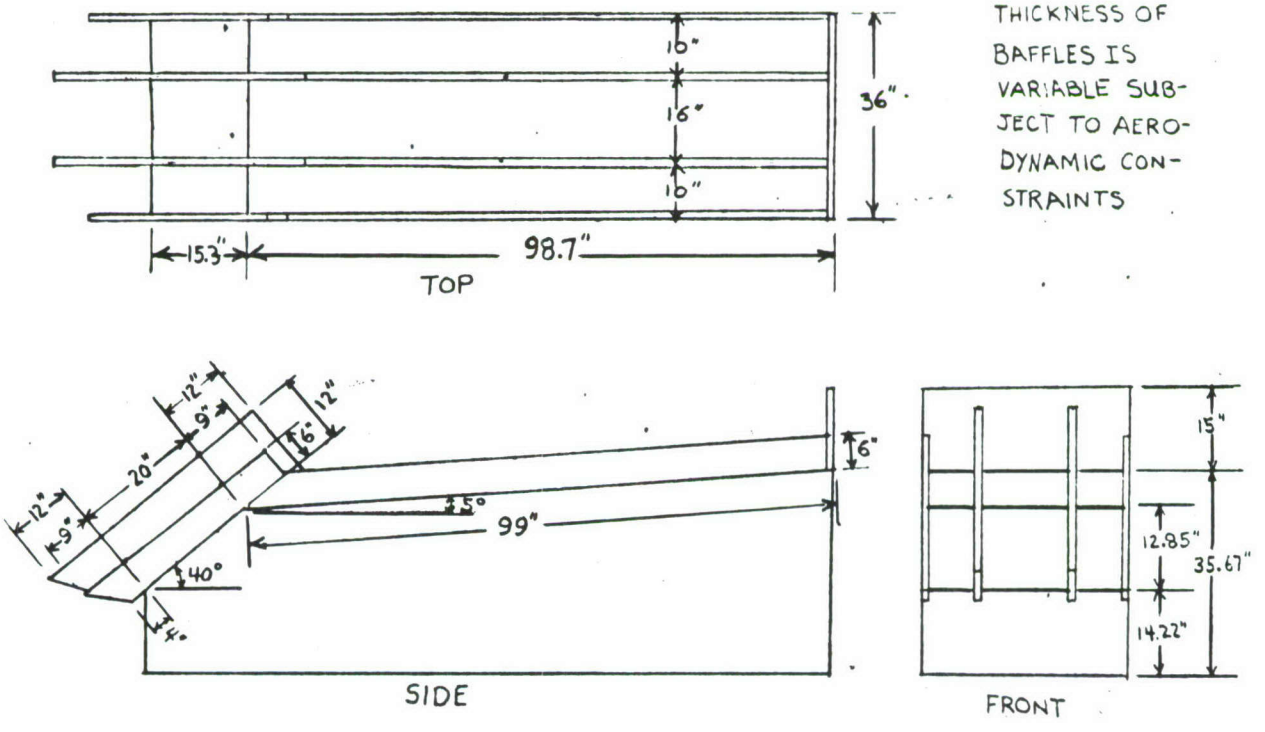

Figure 2-35. Final Canopy Design

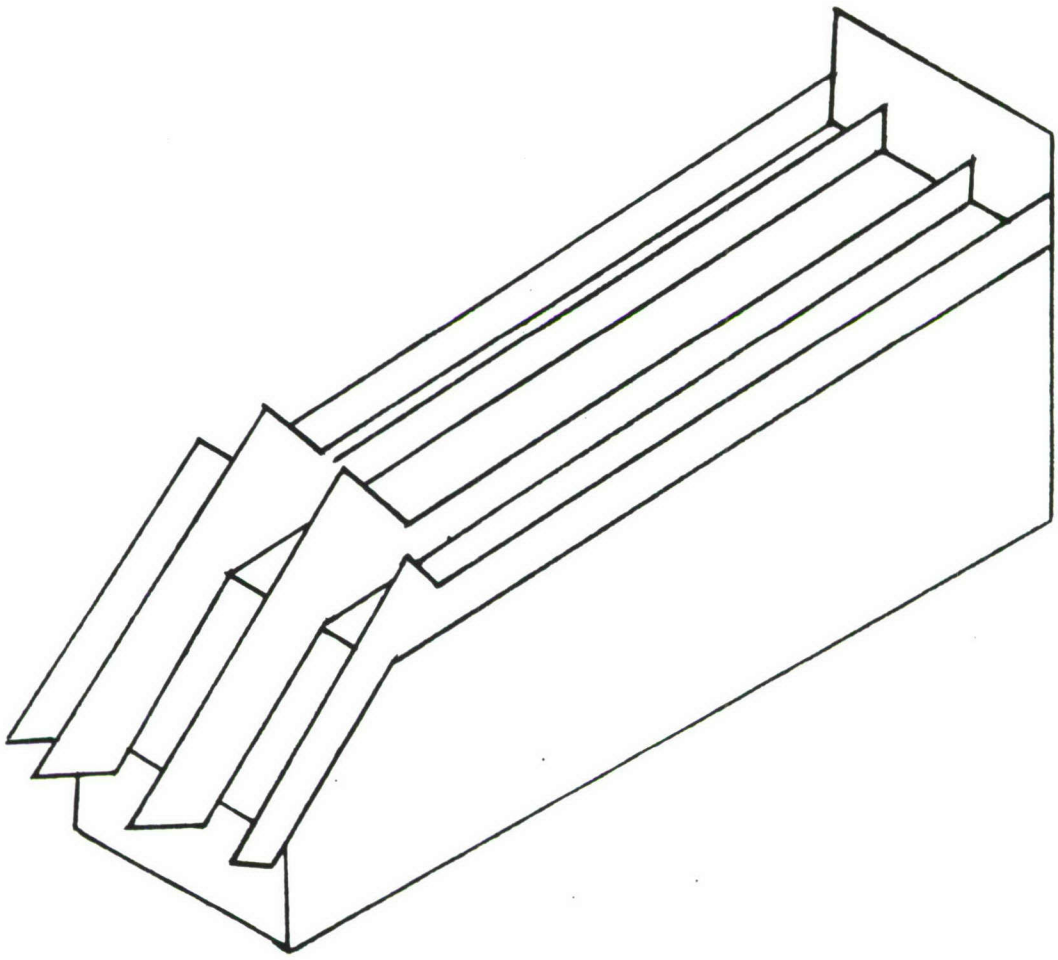

Figure 2-36. Isometric View of Final Canopy

In order to physically examine an approximation of the final canopy design, an experiment was performed at Aberdeen Proving Ground at which baffles were mounted on the existing flat canopy which was designed and fabricated by the Land Warfare Laboratory (LWL). This canopy is illustrated in the photograph in figure 2-37. The LWL canopy design differs from the final canopy design of this report in some very significant respects. The LWL

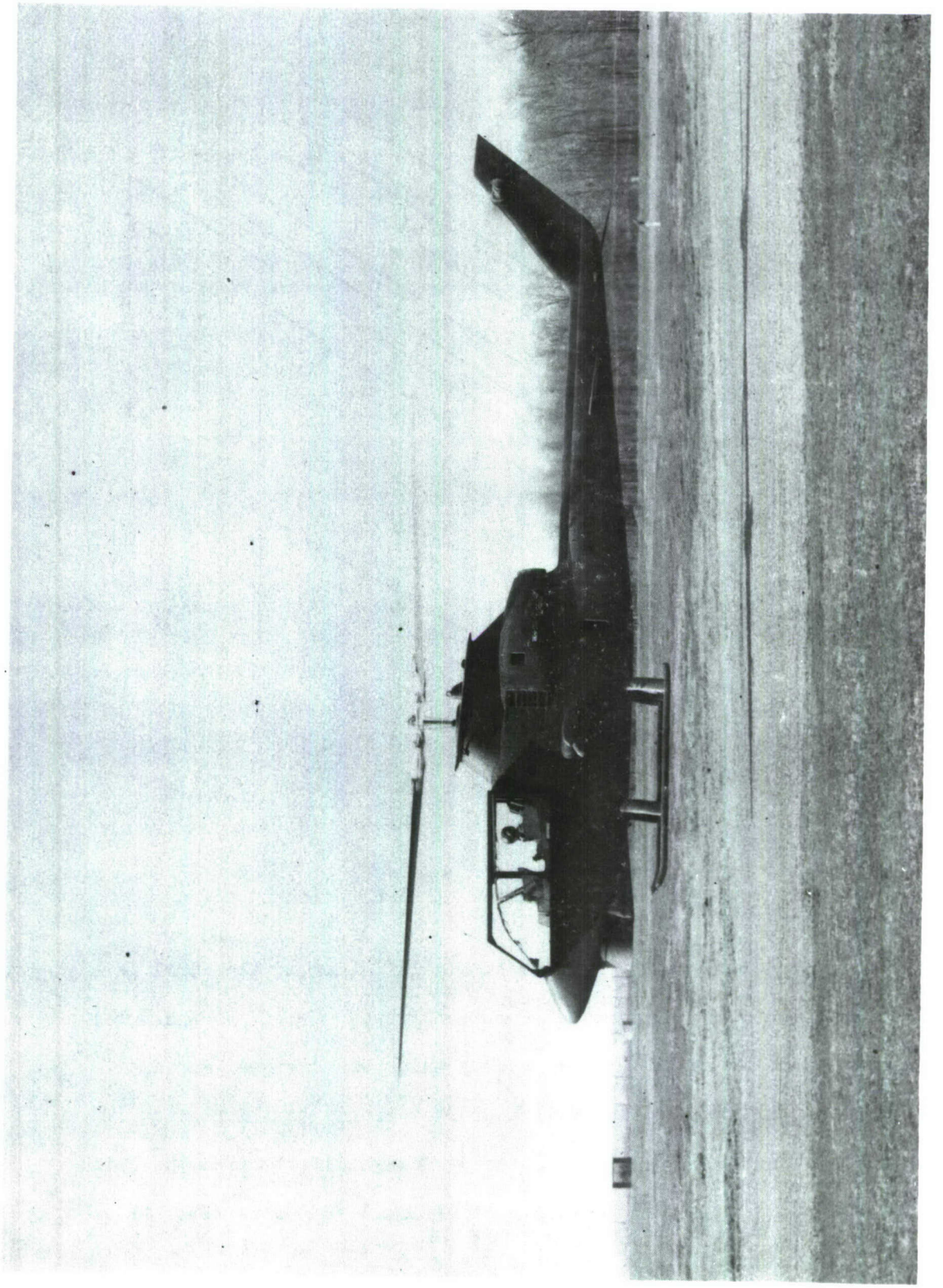

Figure 2-37. Canopy Designed by the Land Warfare Lab

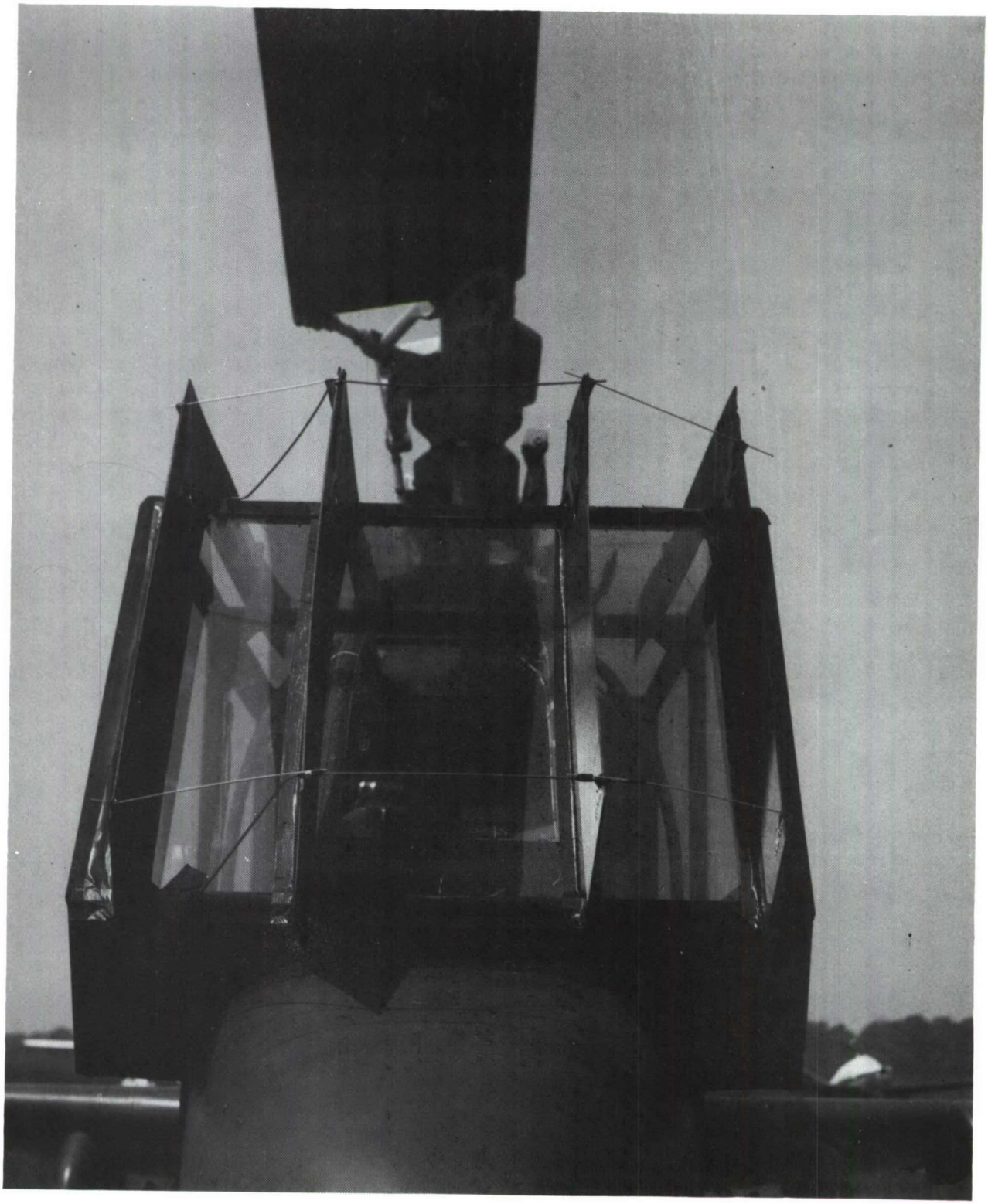

Figure 2-38. External View of Baffles Mounted on LWL Canopy (Front View)

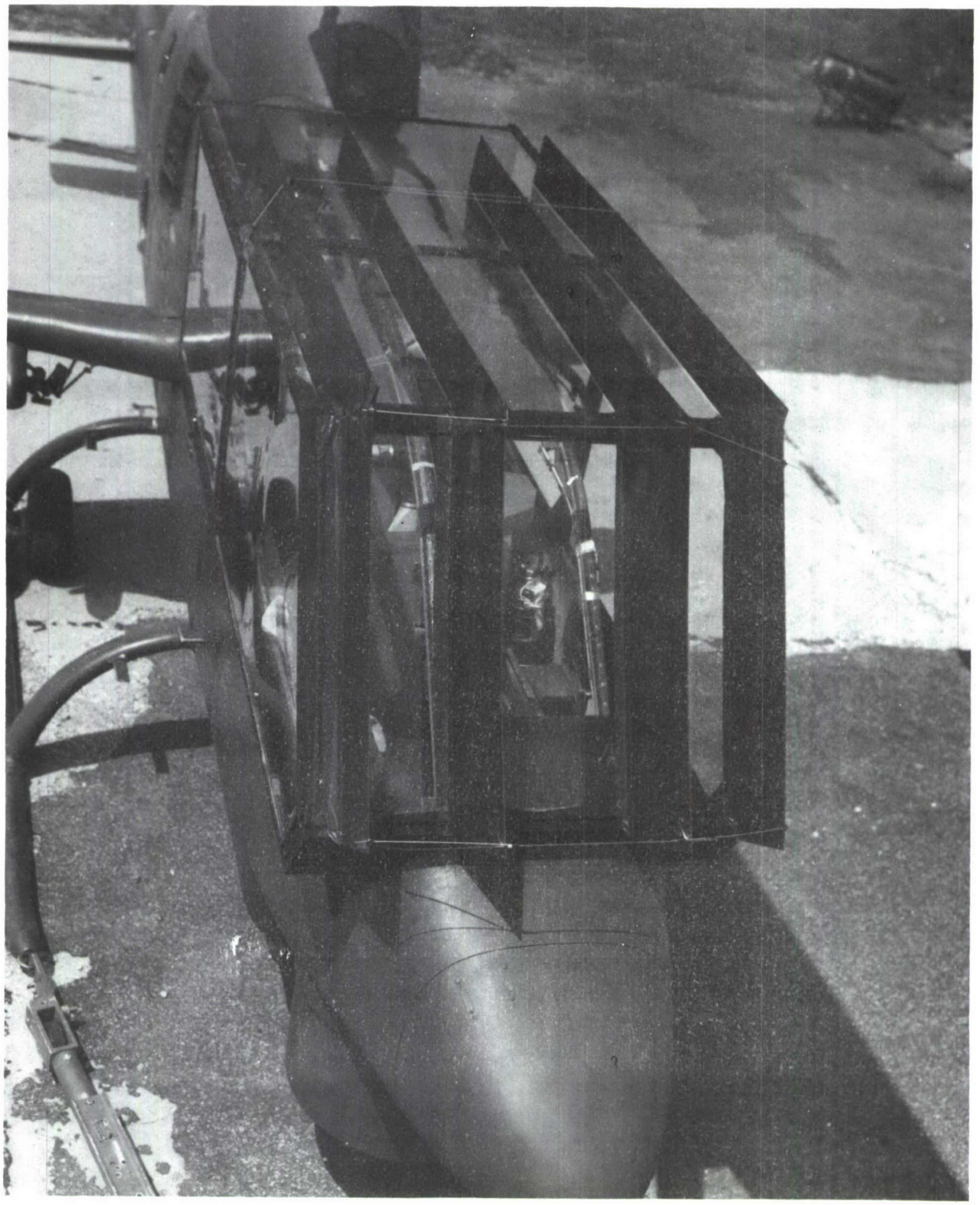

Figure 2-39. External View of Baffles Mounted on LWL Canopy (Front-Top View)

Figure 2-40. External View of Baffles Mounted on LWL Canopy (Illustrating top, side, and front)

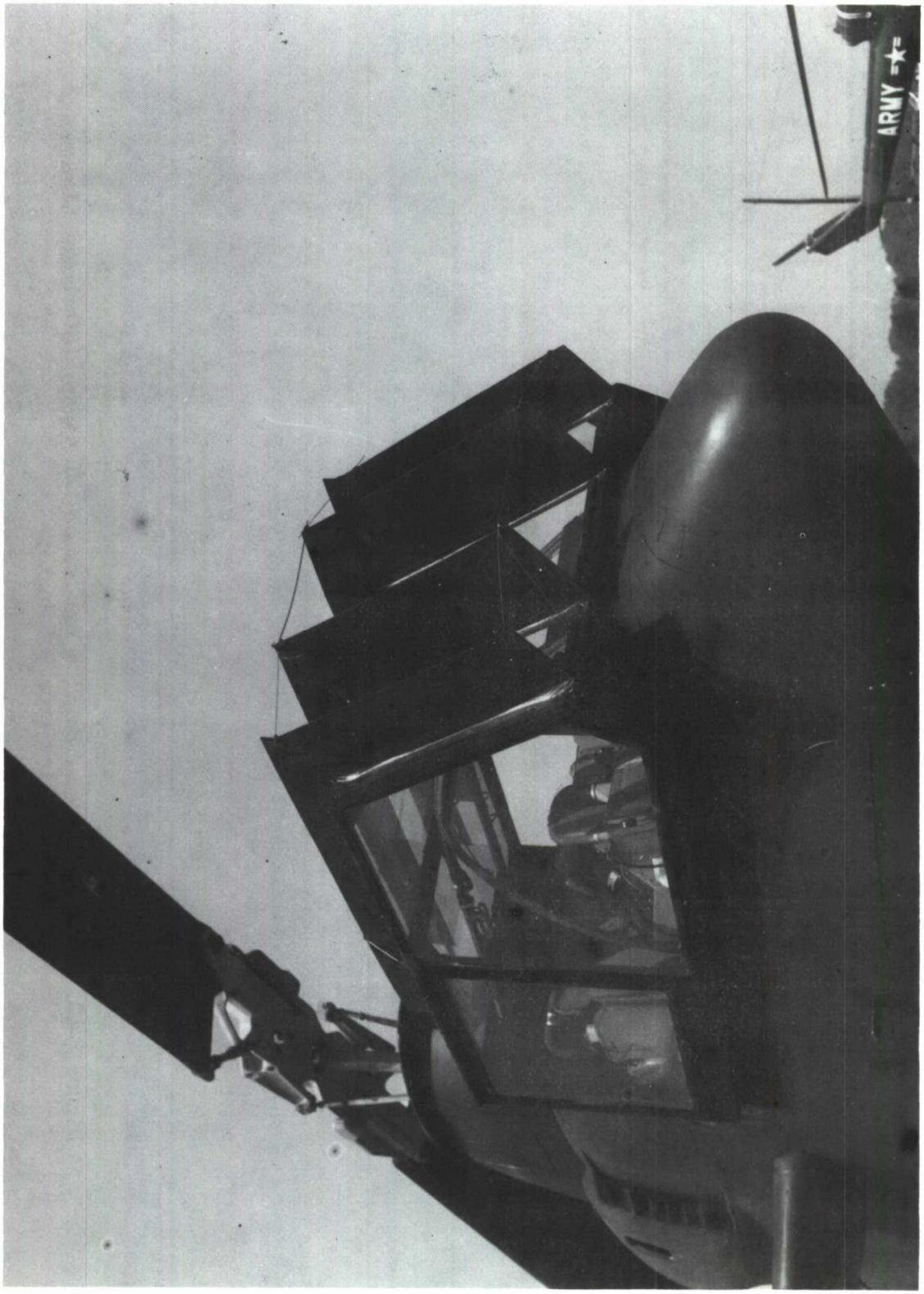

Figure 2-41. External View of Baffles Mounted on LWL Canopy (Starboard Side View from 45° Angle)

Figure 2-42. External View of Baffles Mounted on LWL Canopy (Starboard Side View from 90° Angle)

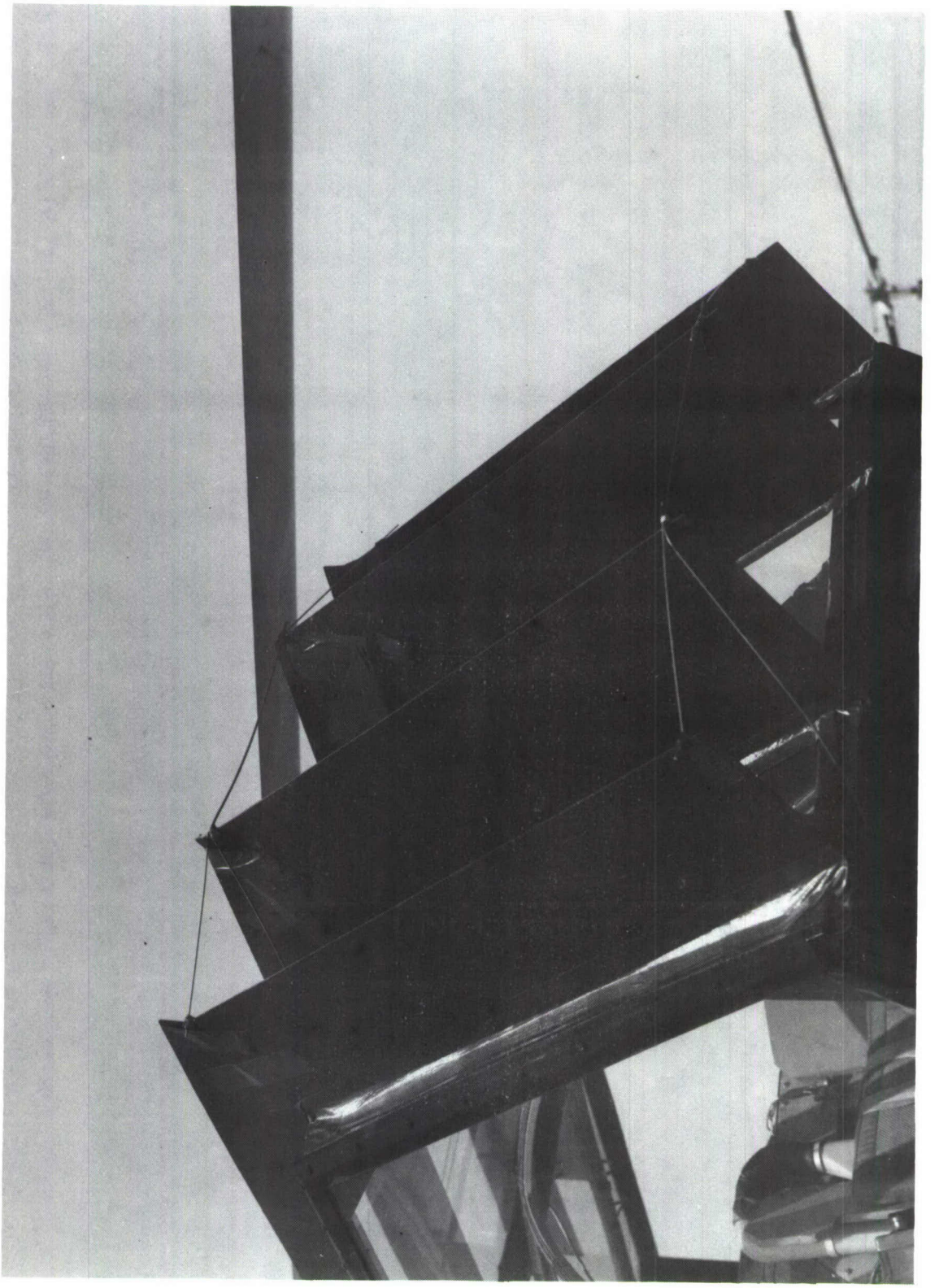

Figure 2-43. External View of Baffles Mounted on LWL Canopy (Starboard Side Close Up View)

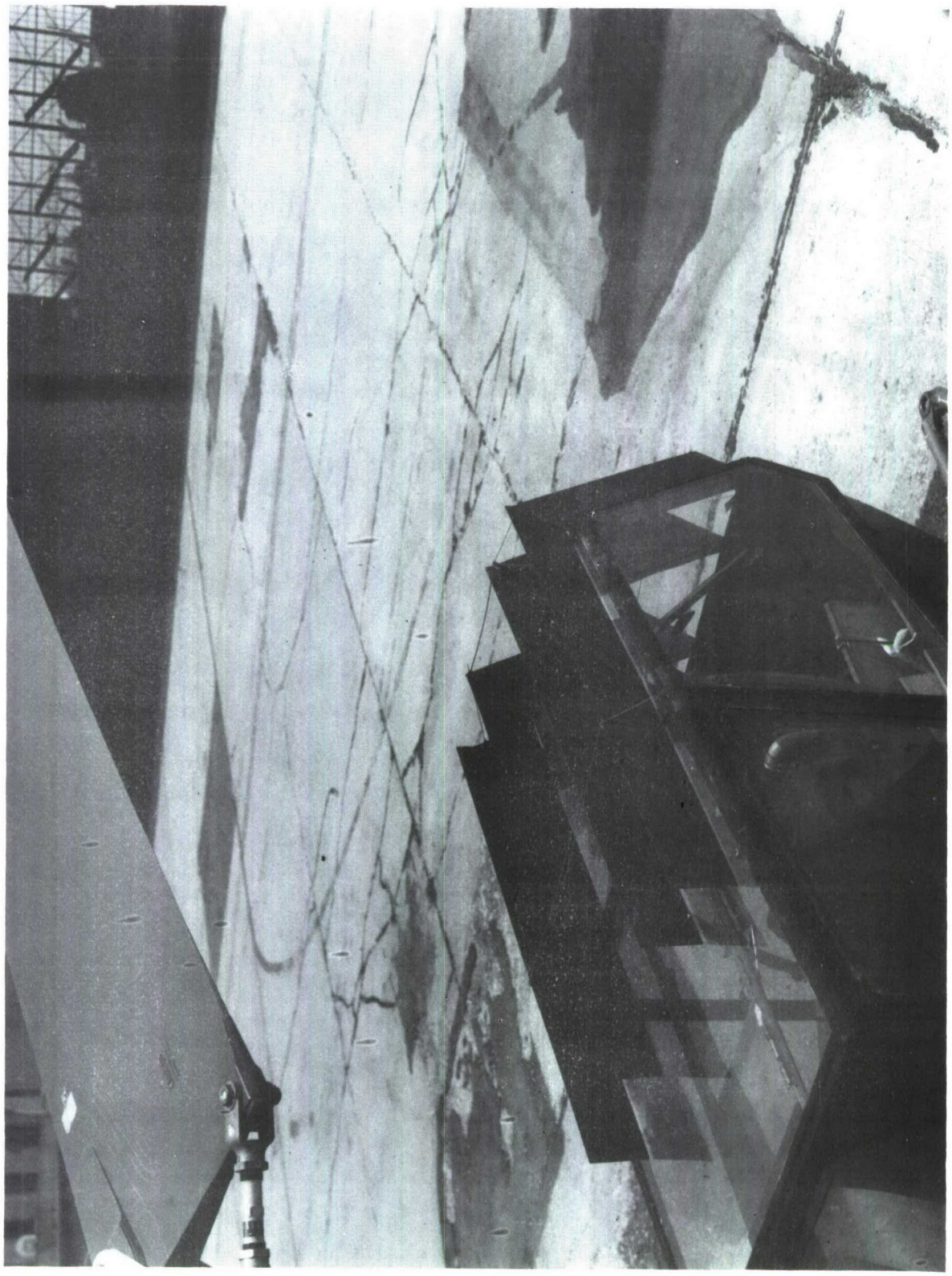

Figure 2-44. External View of Baffles Mounted on LWL Canopy (Rear View)

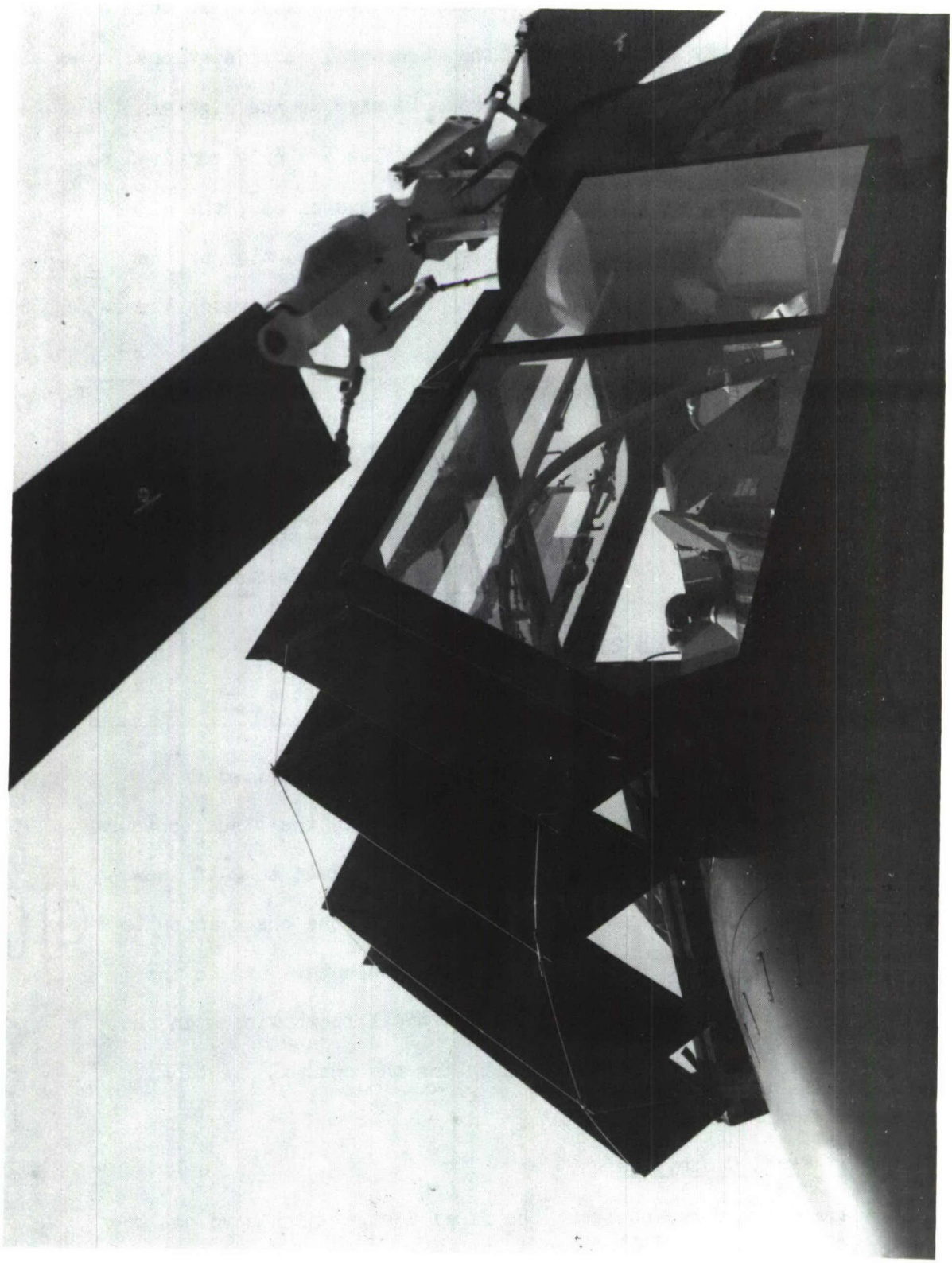

Figure 2-45. External View of Baffles Mounted on LWL Canopy (Port Side View)

report for full shading. This point will require further analysis as this study has not been primarily concerned with the structural considerations. However, table 2-3 shows the approximate decrease in size as the high sun constraints are relaxed. In other words, if the baffles are only required to baffle for sun position below an elevation of 55° instead of 65°, the sizes of the baffles can be reduced as shown in table 2-3. This portion of the analysis requires further attention as time did not permit a thorough investigation of this aspect.

Table 2-3

Baffle Heights Required for Partial Baffling For 40° Window Elevation

Threshold Sun Elevation	Sun Azimuth	Required Baffle Height		Required Baffle Extension	
Above which glints occur from front sloped window.		Inside	Outside	Inside	Outside
55°	91° and 269°	9"	5"	10.5"	6"
45°	91° and 269°	6"	4.5"	9"	5.5"

The second result obtained in this experiment was derived from the photographs in figures 2-46 to 2-51. These illustrate the visual obscuration to the gunner and pilot due to the baffles. Figure 2-46 to 2-48 show the obscuration to the pilot. Figures 2-49 to 2-51 show the obscuration to the gunner. The obscuration to the gunner is more pronounced than to the pilot. These results implied the need for the vertical front window in the final canopy design to allow a baffle-free path for the optical sighting device.

2.9 Discussion of Final Canopy Design

There are a few comments about the final design which have not been mentioned up to this point. The glint reduction aspects of the design are

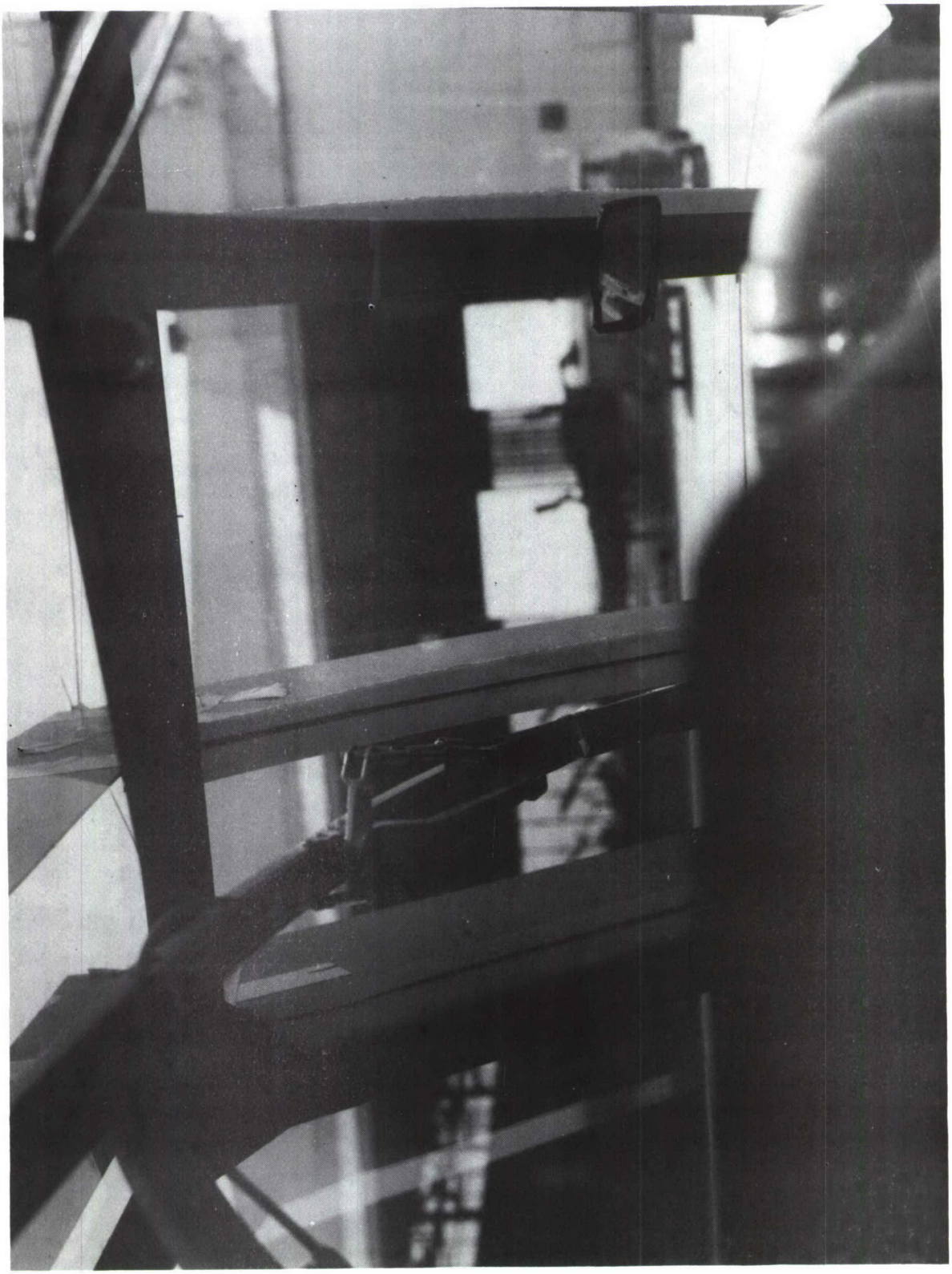

Figure 2-46. Pilot View Through Left Side of Front Window of LWL Canopy With Baffles Mounted

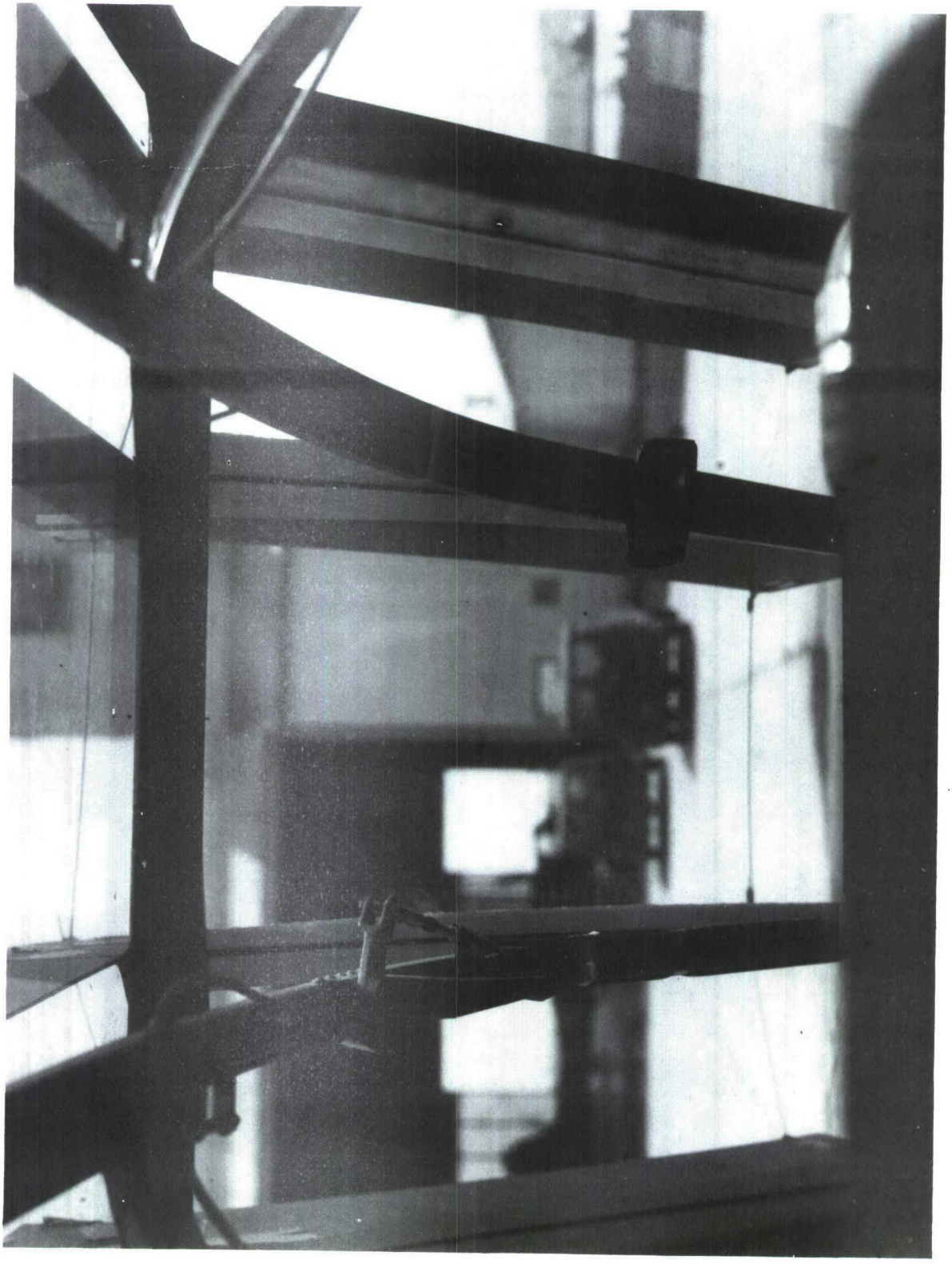

Figure 2-47. Pilot View Straight Ahead Through Front Window of LWL Canopy with Baffles Mounted

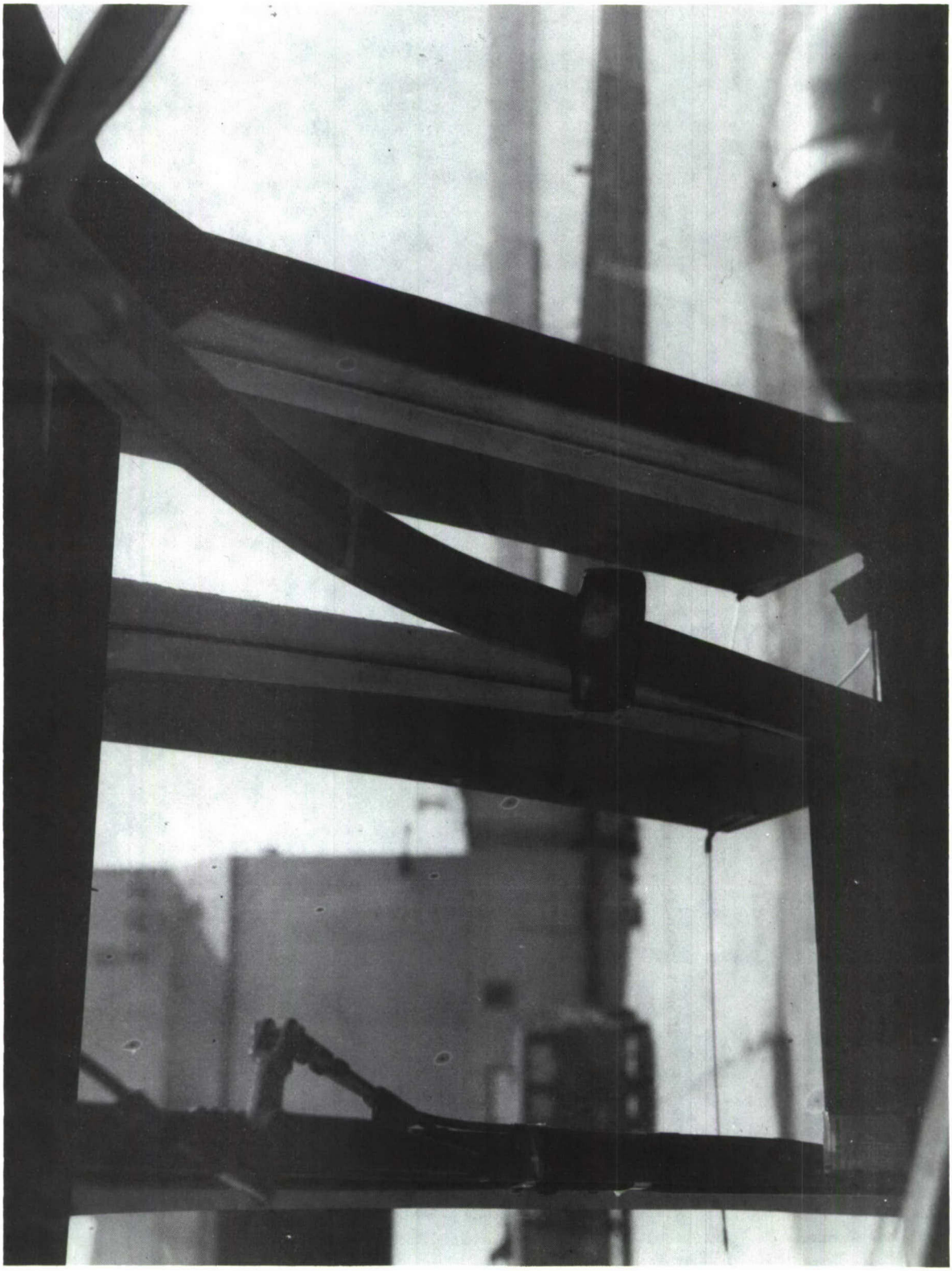

Figure 2-48. Pilot View Through Right Side of Front Window of LWL Canopy with Baffles Mounted

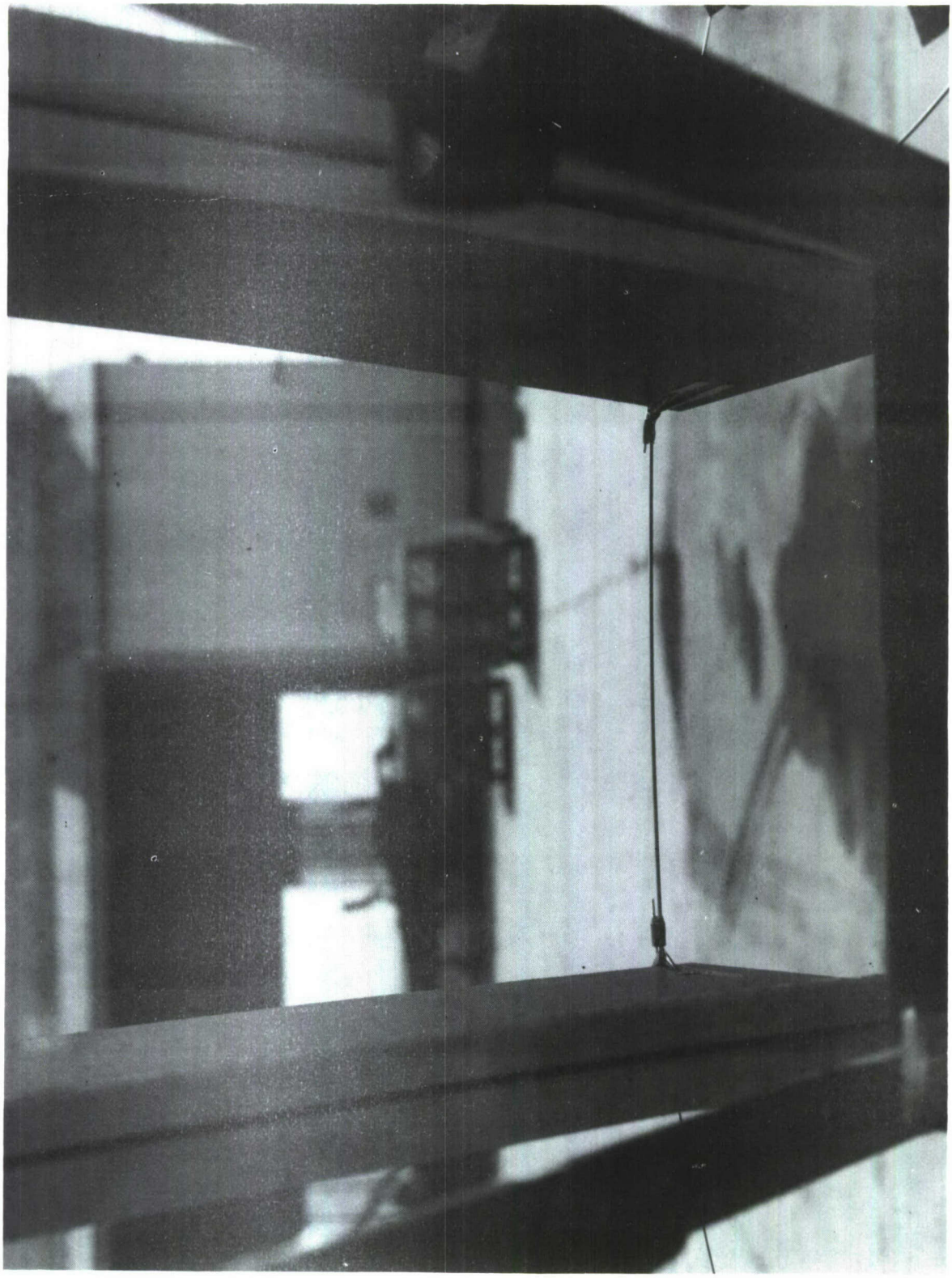

Figure 2-49. Gunner View Straight Ahead Through Front Window of LWL Canopy with Baffles Mounted

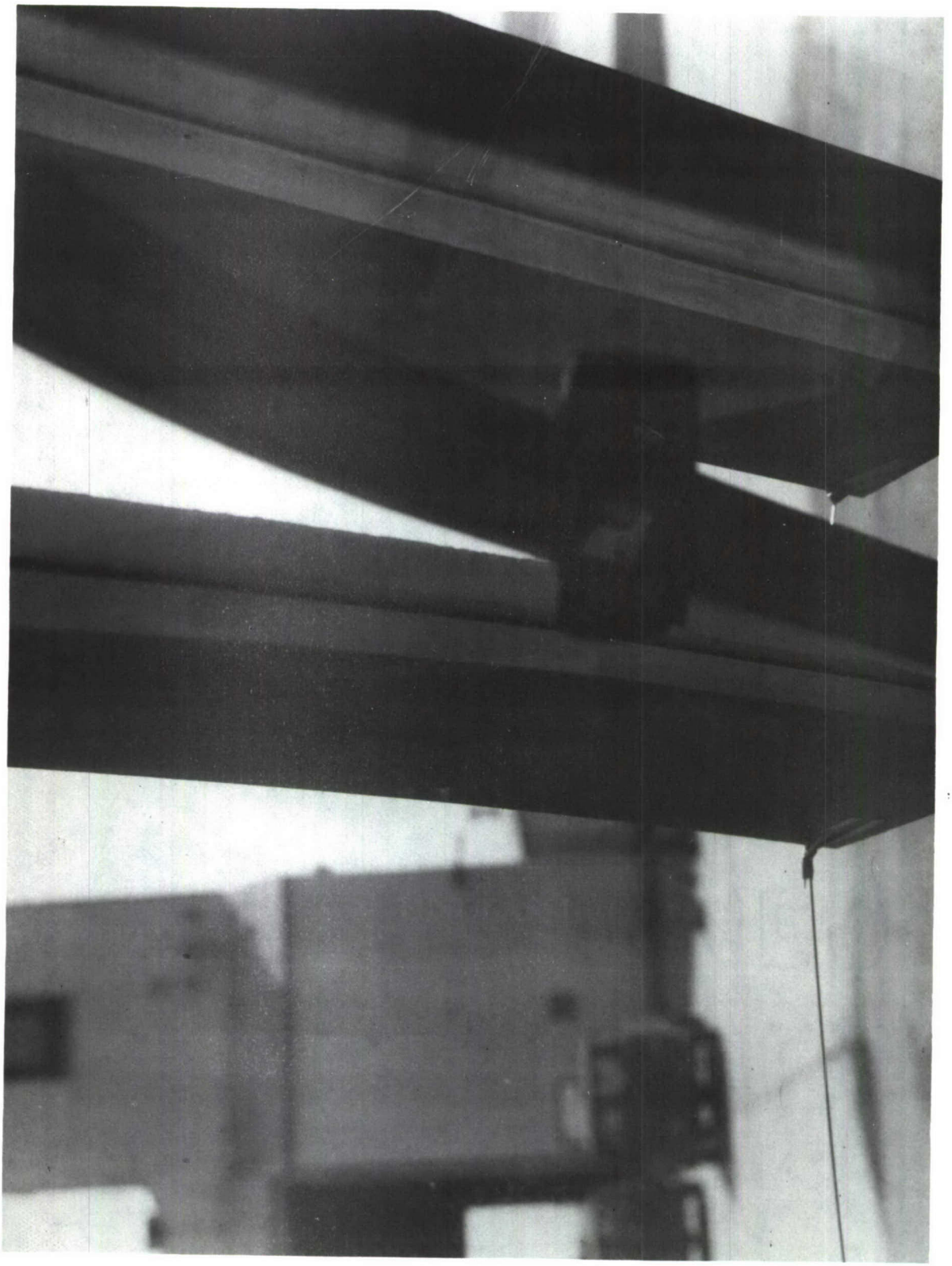

Figure 2-50. Gunner View Through Right Side of Front Window of LWL Canopy with Baffles Mounted

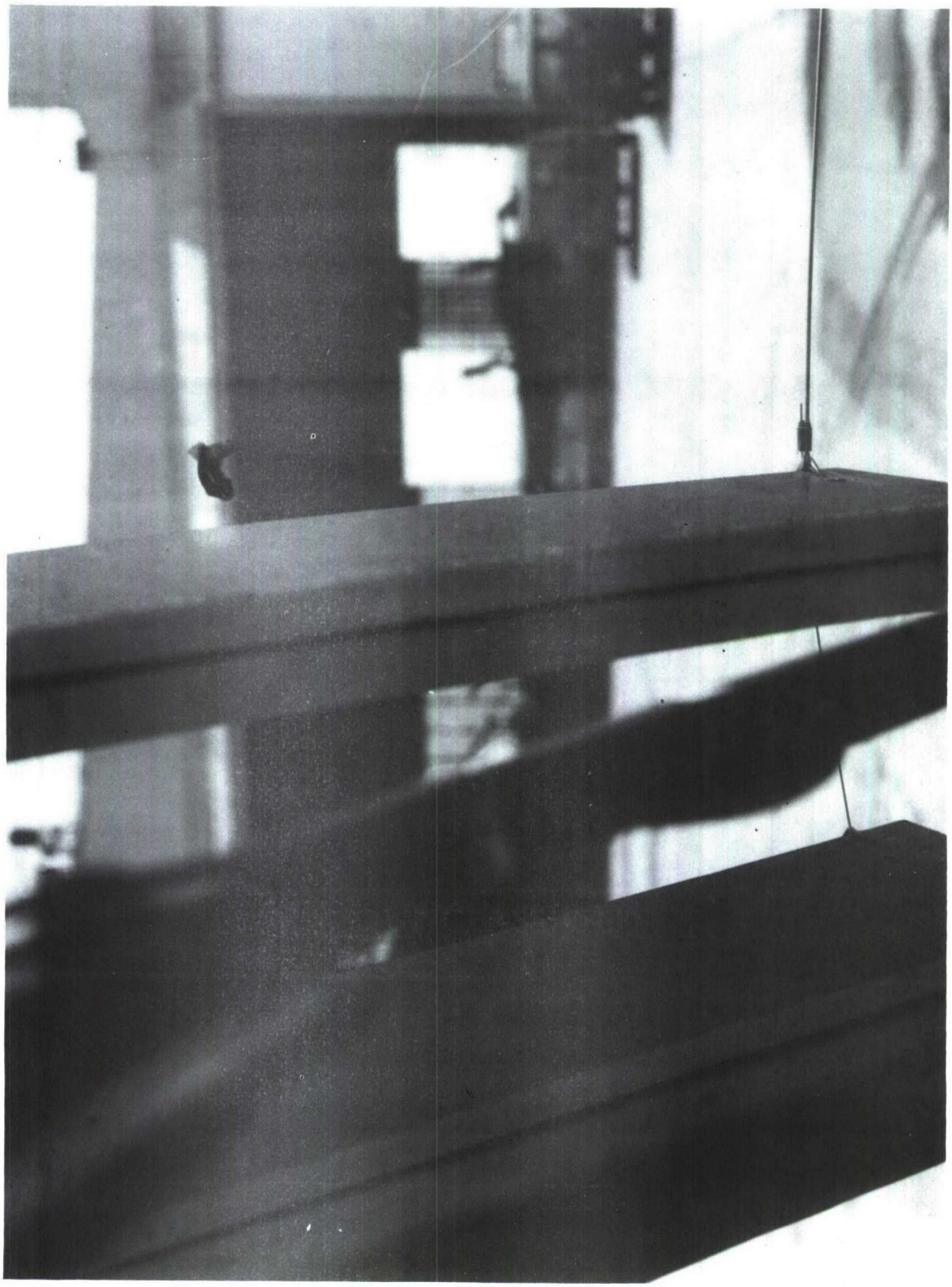

Figure 2-51. Gunner View Through Left Side of Front Window of LWL Canopy with Baffles Mounted

dependent on the 36" width of the structure as well as the slopes of the surfaces and the dimensions of the baffles. The remaining dimensions of the structure can be adjusted to meet other constraints. For example, if the 14.22" vertical front window is not sufficient as a path for the optical sighting device, it can be enlarged without affecting the glint characteristics of the canopy. The following general equations and figure 2-52 can be used in adjusting the dimensions of the basic structure.

The 15 inch rear baffle is obviously included to reduce glints caused by low sun rays approaching the craft from the rear. It can be rounded for aerodynamic reasons.

2-10 Adjustment of Baffle Sizes for the Basic Canopy Design

The canopy structure illustrated in figures 2-35 and 2-36 has been designed primarily for effectiveness in minimizing glints in the region of interest. In the event that it is decided that the baffle sizes are physically infeasible, it is important to estimate the effect of reducing baffle sizes on the effectiveness of the baffles in reducing glints. It is expected that if the sizes are prohibitive, the front baffles will be the problem. Hence, the bulk of this discussion will pertain to the adjustment of baffle sizes for the front sloped window.

There are two dimensions which can be adjusted without changing the basic shape of the baffles: the length and the height. These will be the only parameters adjusted for the following reasons. The baffle design in figures 2-35 and 2-36 was examined using the SEEHC3 model discussed later. The analysis of the adjustments in the baffle parameters being discussed here was done by means of the shadowing map technique discussed earlier but because of time limitations, the adjusted baffle sizes were not analyzed by SEEHC3.

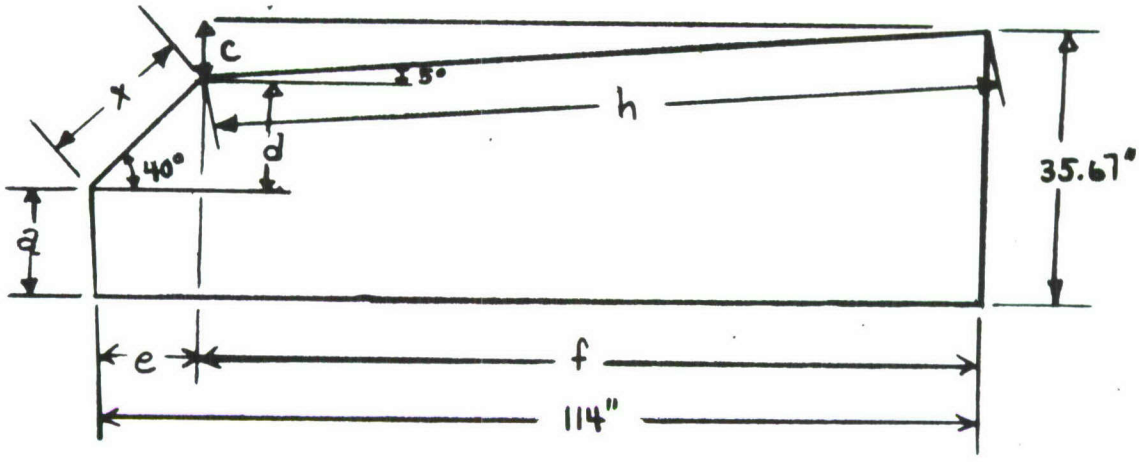

CALCULATION OF BASIC PARAMETERS

$d = X \sin 40°$
$e = X \cos 40°$
$f = 114 - e$
$c = f \tan 5°$
$a = 35.67 - (d + c)$
$h = f / \cos 5°$

Figure 2-52. Design Criteria for Adjusting the Parameters of the Final Canopy Design

Therefore, to maintain consistency with the analysis done by SEEHC3, the basic shape of the baffles was not changed for the analysis presently being discussed. Also, the slopes of the windows will not be changed.

The height of the baffle and the distance that it must be extended are not independent. As the height of the baffle above the window surface is decreased, the amount that it must be extended decreases. Hence, the output of this analysis is tabular data showing the height of the baffles, the amount that they must be extended and an estimated sun elevation above which sun glints will occur in the region of the given azimuth.

Before presenting the results, the method used for generating the results will be discussed. Consider figures 2-53, 2-54 and 2-55. Note that the following analysis uses feet as the basic unit.

The first step in the analysis is to refer to figures 2-6 and 2-7 and obtain the offending sun rays for a window elevation of 45° and the corresponding reflected vector for each offending sun ray. Then the baffle heights are fixed at a given height and the corners A, b, d are mapped into the window plane along the sun vector as shown in figure 2-53 and corners C, D, b are mapped into the plane along the reflected vector as shown in figure 2-54. The object is to obtain the locus of intercepts of the points as a function of the sun positions and the baffle heights. Note that corners A, B, d can be analyzed together along the sun vector since as they are mapped along the sun vector, their locus of intercepts will differ only by a constant. Also, for the same reason, corner C is used to obtain the locus of intercepts for corners C, D, a, b along the reflected vector. The loci of the y-coordinates intercepts for corner A are shown in figure 2-56 and the loci of the y-coordinates of the intercepts for corner C are shown in figure 2-57.

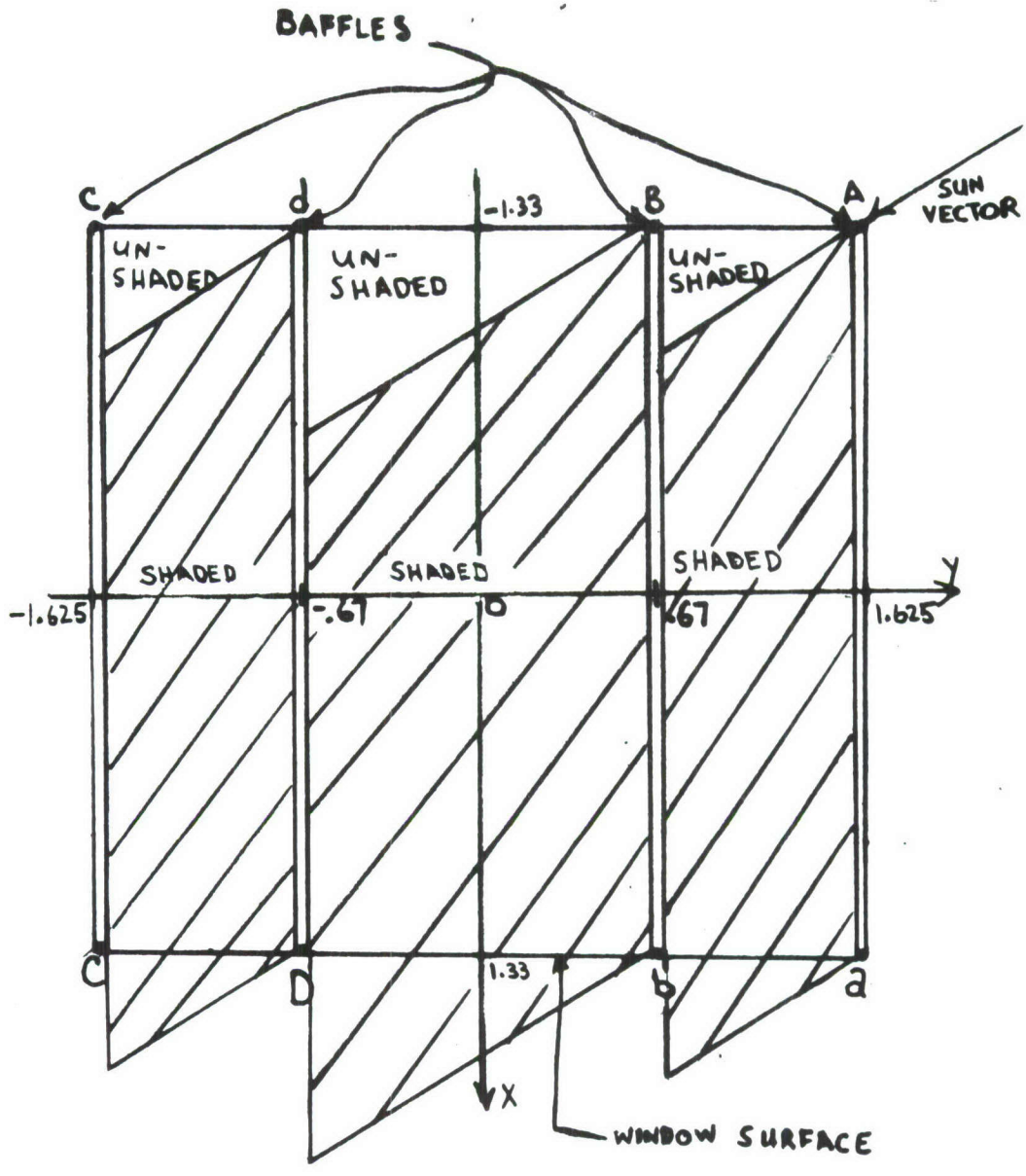

WINDOW ELEVATION AT 45° TO SIMULATE TOTAL PITCH OF WINDOW WITH RESPECT TO EARTH COORDINATES WHEN MOUNTED ON AN AIRCRAFT PITCHED BY 5°

Figure 2-53. Illustration of Shadow Mapping Technique Along Sun Ray for Analyzing Baffle Height and Extension Adjustments

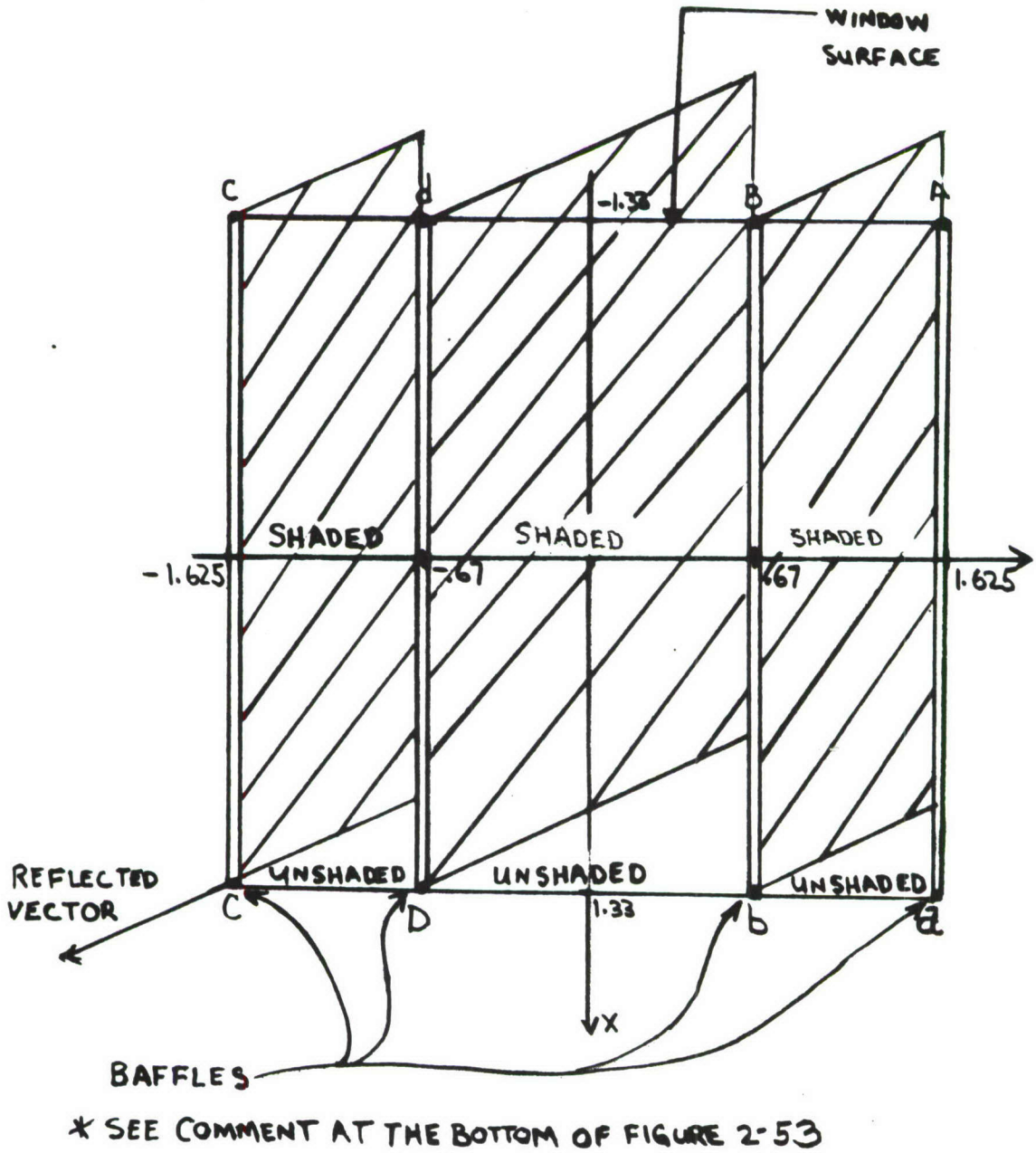

Figure 2-54. Illustration of Shadow Mapping Technique Along Reflected Ray for Analyzing Baffle Height and Extension Adjustments

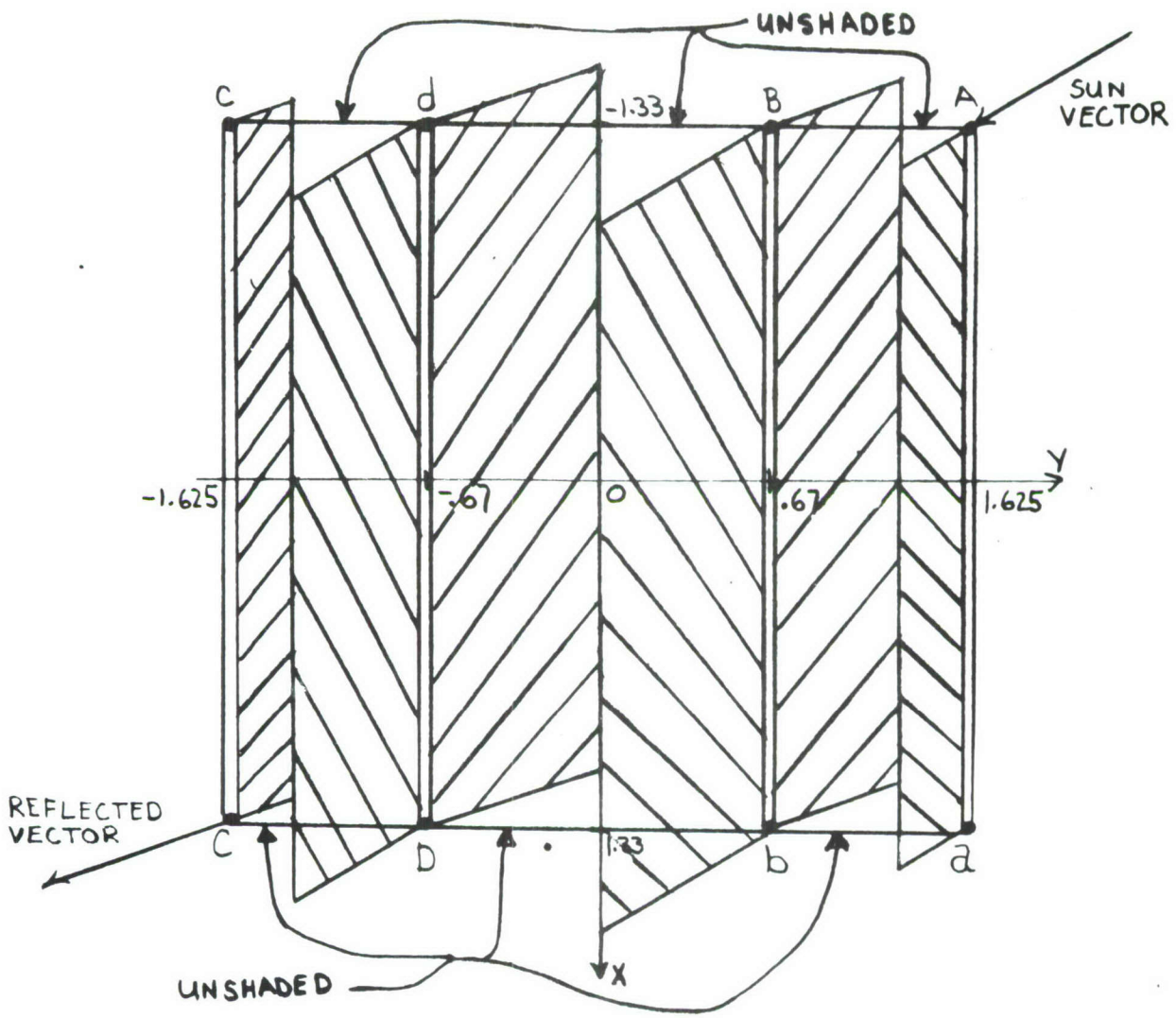

* SEE COMMENT AT THE BOTTOM OF FIGURE 2-53

Figure 2-55. Illustration of Shadow Mapping Technique Along Sun Ray and Reflected Ray

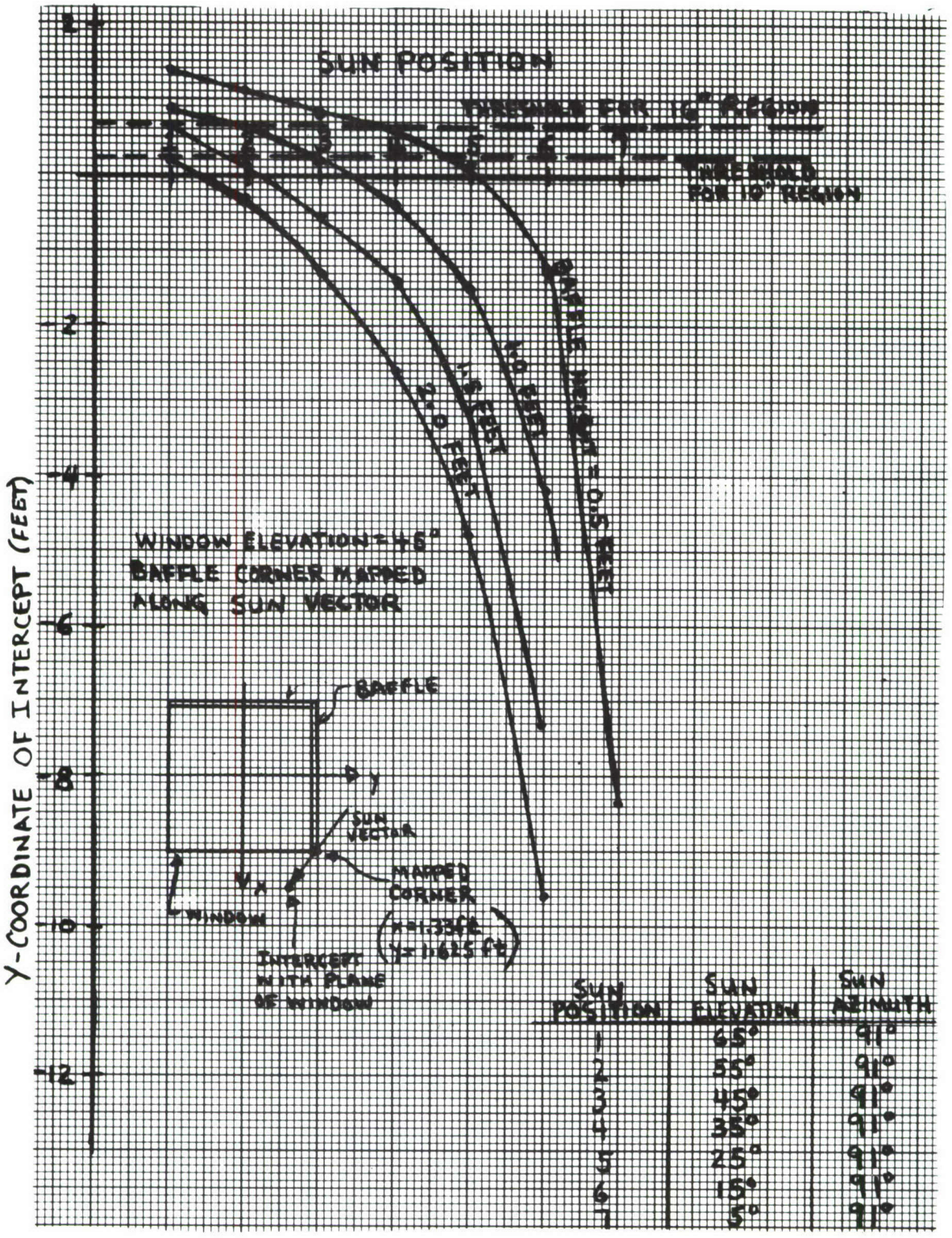

Figure 2-56. Y-Coordinate of Sun Ray Intercept with the Window Plane vs. Sun Position For Various Baffle Heights

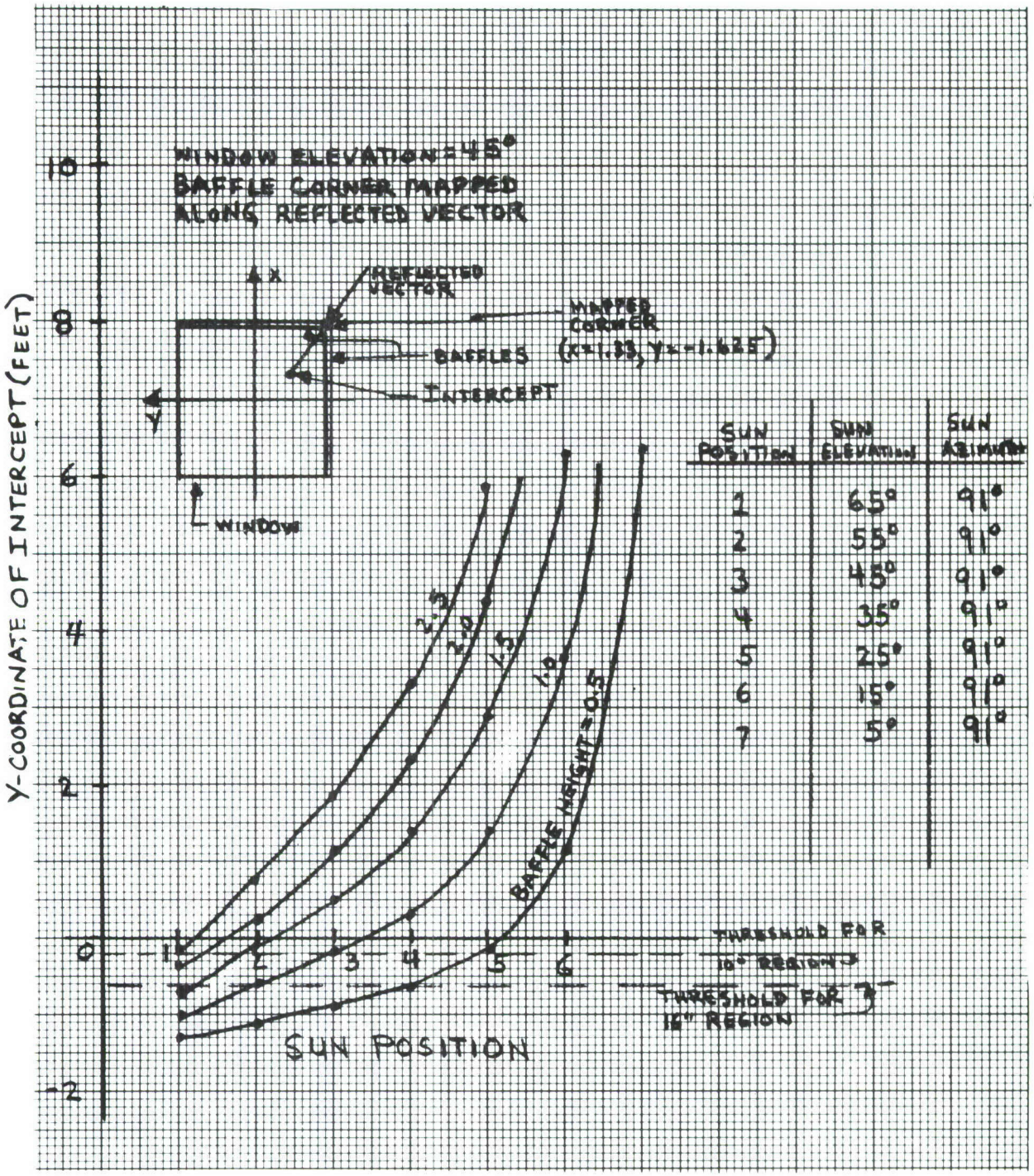

Figure 2-57. Y-Coordinate of Reflected Ray Intercept With the Window Plane vs. Sun Position for Various Baffle Heights

The loci of the x-coordinates for corner A are shown in figure 2-58 and the loci of the x-coordinates for corner C are shown in figure 2-59.

Referring to figure 2-53, note that a necessary condition for the shade of baffle A-a to overlap with baffle B-b is that the intercept of corner A with the plane must have a y-coordinate of .67 or less. This number specifies a threshold for the height of baffle A-a on the curves of figure 2-56. All points of the loci which have y-coordinates less than this threshold represent conditions under which the shadow of baffle A-a overlaps with baffle B-b. Notice also in figure 2-53 that the y-coordinate of the intercept of corner B must be less than -.67 in order to overlap with baffle d-D. In order to use the data for corner A, this y-coordinate must be translated by .955 in the positive y direction so that corner B coincides with corner A. This means that y-intercept of corner A must be less than

$$-.67 + .955 = .285$$

in order to simulate the condition for the shadow of baffle B-b to overlap with baffle d-D. Hence, this establishes another threshold on the loci in figure 2-56 such that below the threshold the shadow of baffle B-b along the sun vector overlaps with baffle d-D. Similarly, thresholds can be determined for the corners being mapped along the reflected vector in figure 2-54.

Figure 2-55 illustrates the combination of the approaches in figures 2-53 and 2-54, taking advantage of the shade of the baffles along the sun vector and the reflected vector. Note that there are 6 regions labeled "unshaded". The x-coordinate of the intercept of corners A, B, and d along the sun vector must be less than or equal to -1.33 ft in order to eliminate the triangular region. These regions can be eliminated by extending the baffles in the negative x-direction. The unshaded regions at the bottom of the window

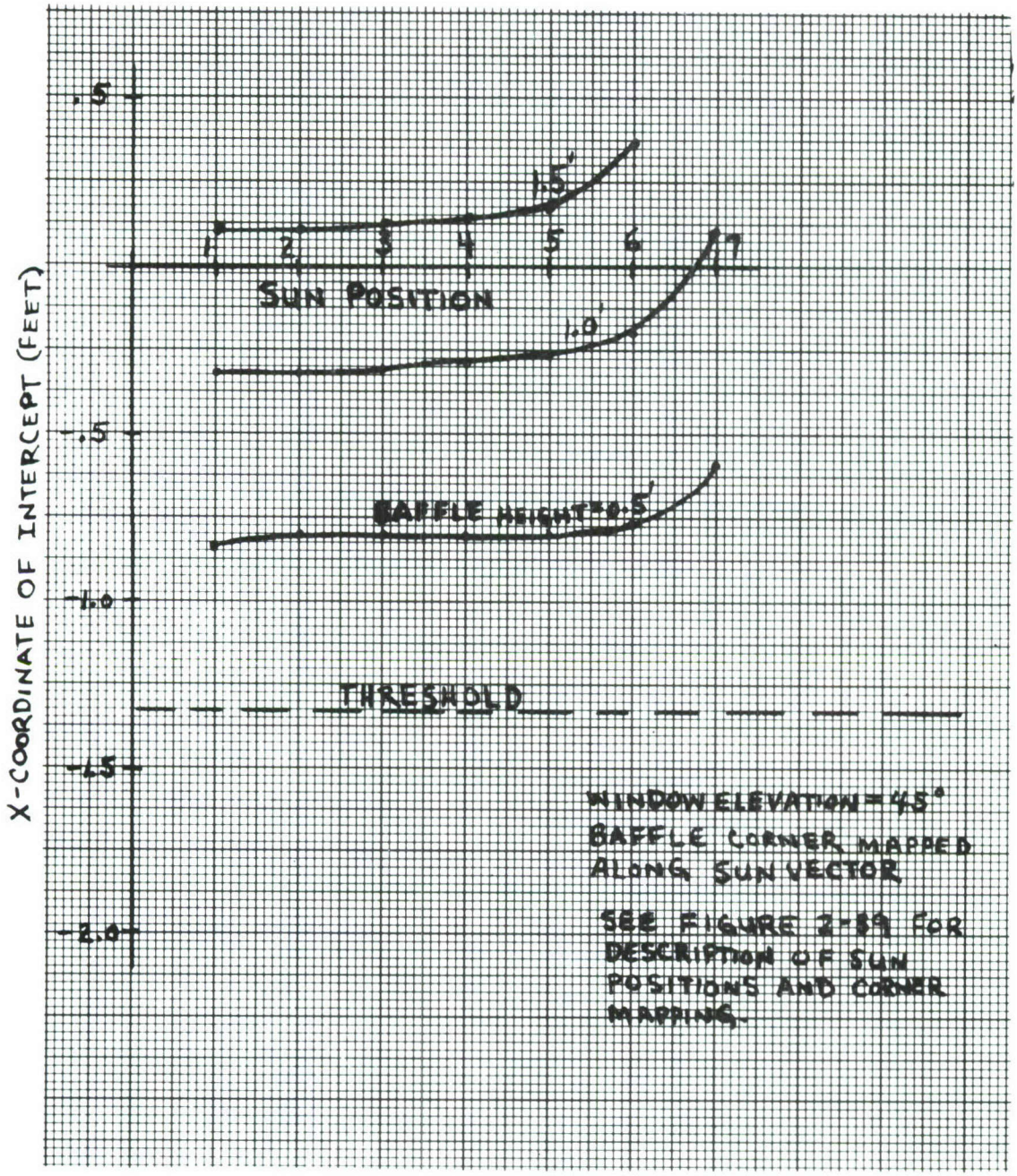

Figure 2-58. X-Coordinate of Sun Ray Intercept with Window Plane vs. Sun Position for Various Baffle Heights

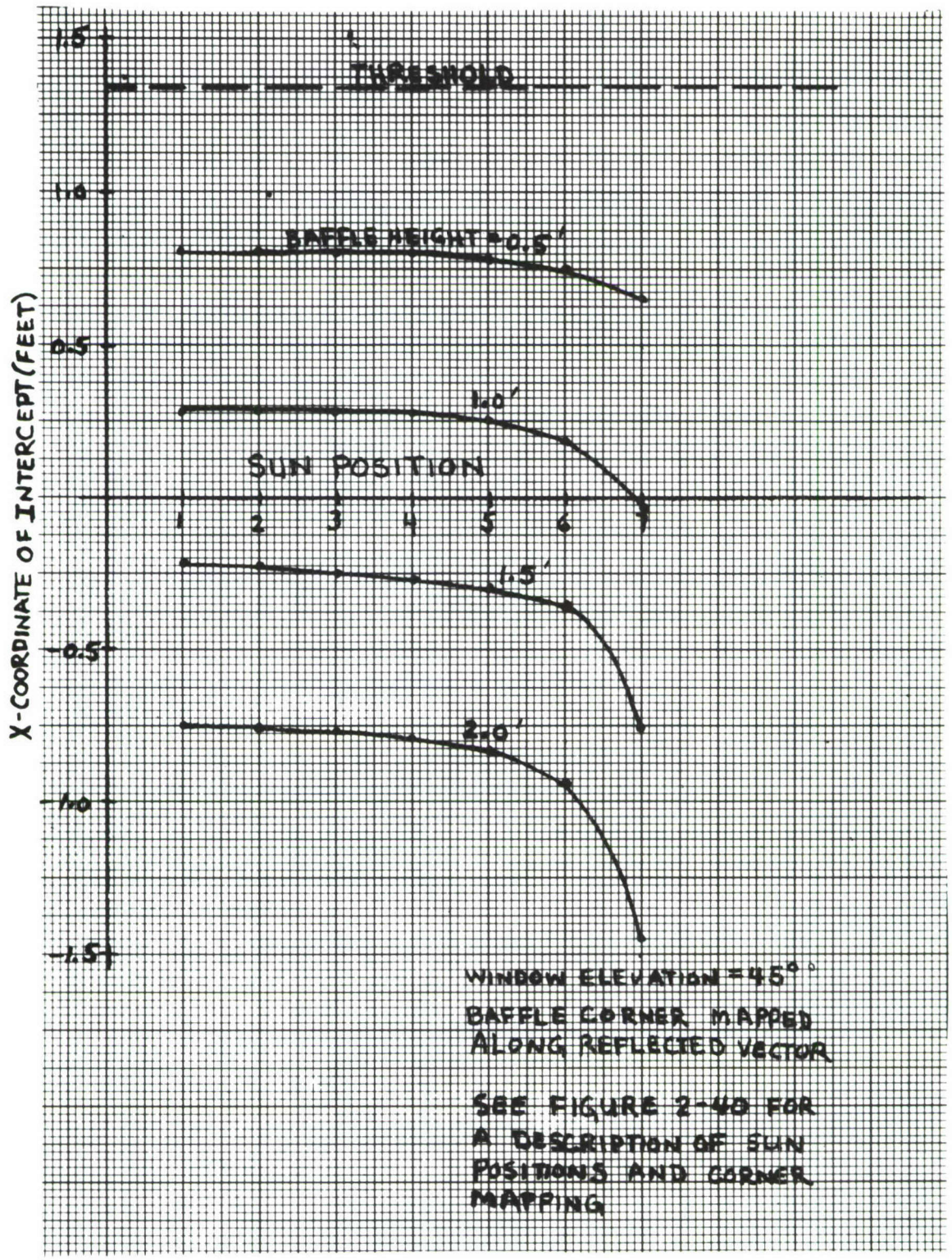

Figure 2-59. X-Coordinate of Reflected Ray Intercept with Window Plane vs. Sun Position For Various Baffle Heights

can be eliminated by extending the baffles in the positive x-direction. As mentioned before, the amount of the extension is dependent on the heights of the baffles. Figures 2-58 and 2-59 show the loci of the x-coordinate of the intercepts of the corners in the window plane as the baffle heights and sun positions are varied. Note that the loci should be below the threshold in figure 2-58 and above the threshold in figure 2-59. Hence, the baffles must be extended to accomplish this for the linear portions of the curves. Notice that the X-intercept is almost independent of the sun position for the first four sun positions. It depends almost entirely on the height of the baffle for high suns. (The x-coordinate begins to vary at low suns (position 5, 6 and 7), but at these low sun positions, the y-coordinate is so large that the x-coordinate is no longer of interest.) Hence the required heights of the baffles can be found as a function of sun position and then the required extension of the baffles can be determined as a function of baffle height. The results of this analysis are shown in tabular form in table 2-3. It should be recalled that the baffle sizes in table 2-3 were not analyzed by SEECH3 due to time restrictions and represent only estimates obtained from the mapping technique. These illustrate the manner in which baffle sizes change as the range of high suns which are allowed to give glints in the region of interest is increased. (High suns are the most demanding sun positions in the design of the present baffle system.)

2-11. Flat Canopy Conclusions and Recommendations

In the event that it is decided that baffles are to be initially avoided in the final canopy design, it is important to choose the "best" slopes for the windows based on some criteria. It is here that the front window should receive the closest attention. Figure 2-6 shows that the

adjustment of the elevation of the front window has little effect on the size of regions of sun positions that cause glints in the 91° zenith region. In other words, adjustment of the elevation of the front window between 40° and 60° only changes the sun positions which cause glints in the region of interest. Hence, if baffles are not going to be mounted, the slope of the front window can be adjusted to any elevation desired. However, if it is possible that baffles may be added in the future, it is desirable to fix the elevation of the window (plus helicopter pitch) at 45° so that the baffle configuration in this study (see figures 2-35 and 2-36) can be used. There is another reason for the recommendation of 45° elevation for the front window. Notice from figure 2-6 that the sun positions which cause glints in the 91° zenith region, with respect to earth coordinates, all have 91° azimuths with respect to helicopter coordinates (or 269° azimuths by symmetry). This is a very useful piece of information from a prediction point of view. All that is necessary is that when the helicopter is in a hovering position, the pilot must avoid allowing the sun position with respect to the helicopter x-axis to be 91° or 269° in azimuth if it does not interfere with the mission. This will eliminate the possibility of a glint in the 91° zenith region (with respect to earth coordinates). Hence, it is recommended that the canopy design in figure 2-35 be used even if the baffles are not mounted.

THIS PAGE INTENTIONALLY LEFT BLANK

3.0 MODELS FOR COMPARING CANOPIES

3.1 SEEHC2

3.1.1 Description

The SEEHC2 model is a modification of the COBWIN model used in evaluating anti-reflective coatings in Work Assignment #2 of contract #DAAD05-72-C-0284. This model was described in the final report for that work assignment[1].

The modifications to the model consisted of modifying the output so that x-y plots of the glint pattern on the ground were generated.

An example of this output is provided in figure 3-1. The helicopter is headed from left to right and is located at the 0,0 coordinate of the map. The sun's zenith measured in degrees from the vertical and its azimuth measured in degrees in counterclockwise rotation from the helicopter heading are noted at the top of the chart. The brightness plot of sun rays at discrete positions on the x-y plot is shown. Using figure 3-2 which was generated from a special SEEHC run, we can extrapolate to find that a 50% probability of detection exists for just about all rays on the plot. Then using figure 3-1, we can generate a butterfly pattern such as shown in figure 3-3 to show the areas on the ground which can see the sun glint.

3.1.2 Verification of SEEHC2

This output was used to verify the model by setting up inputs similar to conditions existing during a test at MASSTER, Ft. Hood, Texas in late August and early September of 1972 where observers stationed at a range of 50

---

[1] Final Report Cobra Glint Model AH-1G, Westinghouse Electric Corporation, December 1972.

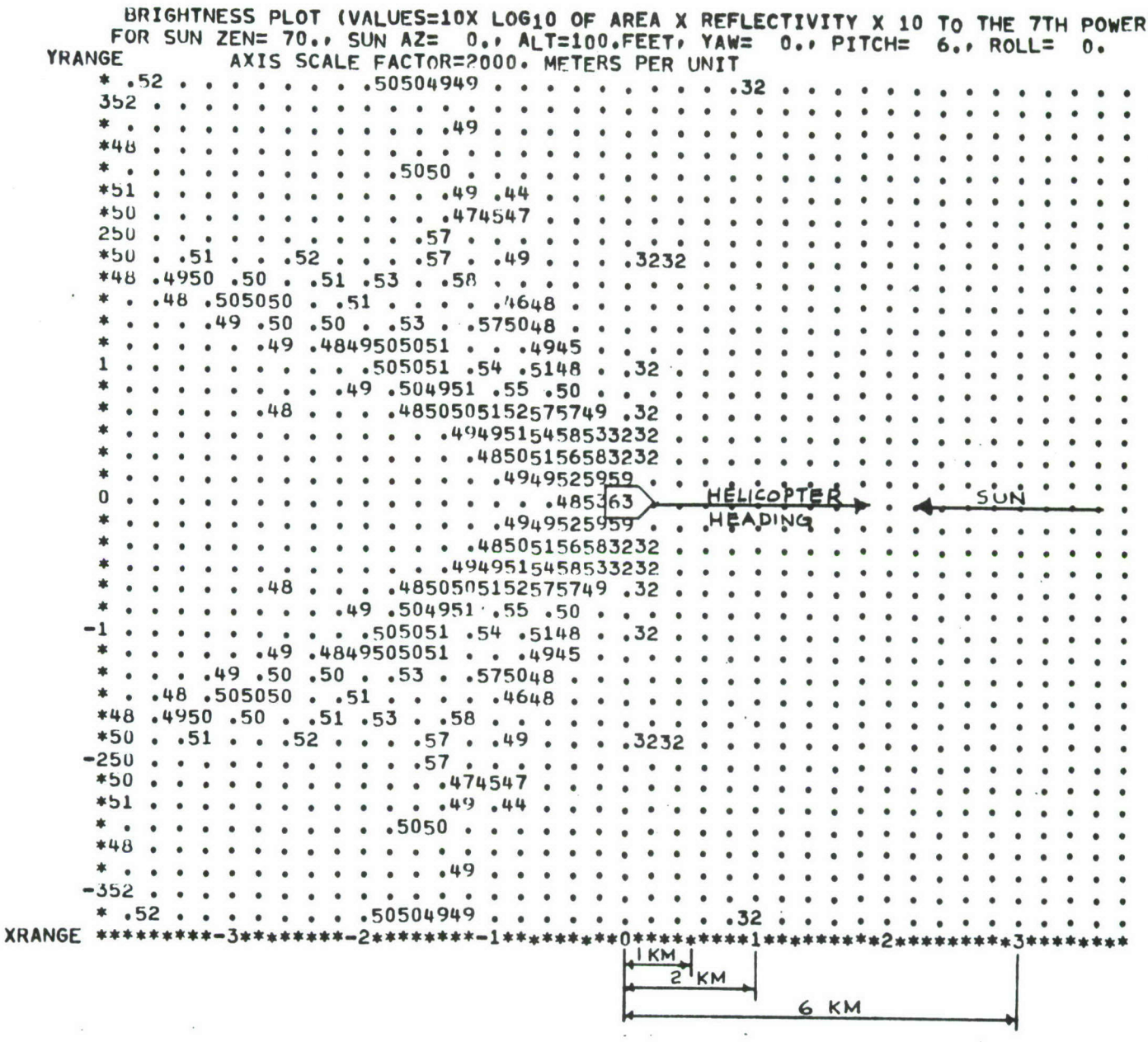

Figure 3-1. Glint Pattern of Existing Canopy with Sun Elevation of 20° and Sun Azimuth of 0°

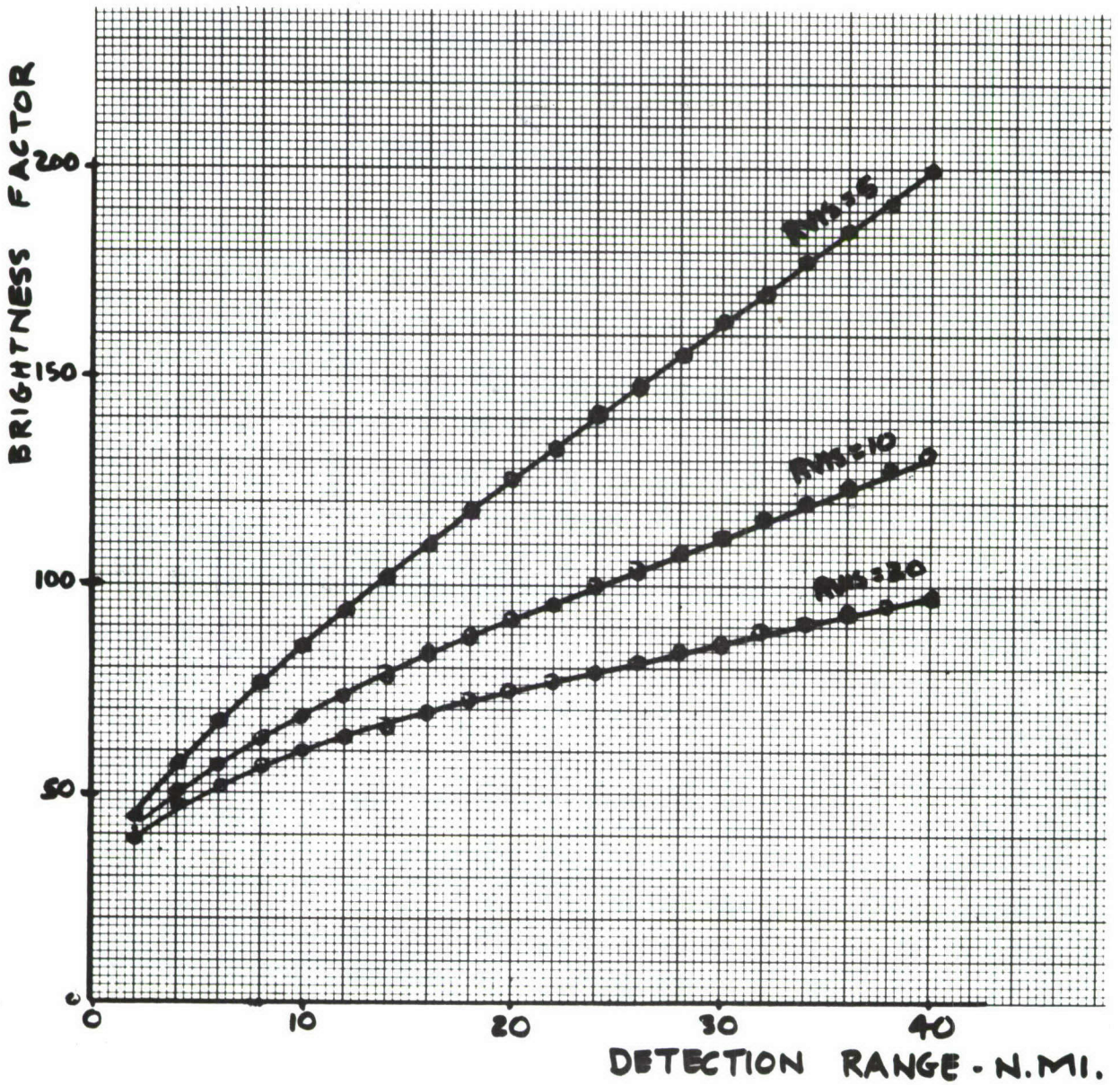

Figure 3-2. Brightness Factor vs. Detection Range

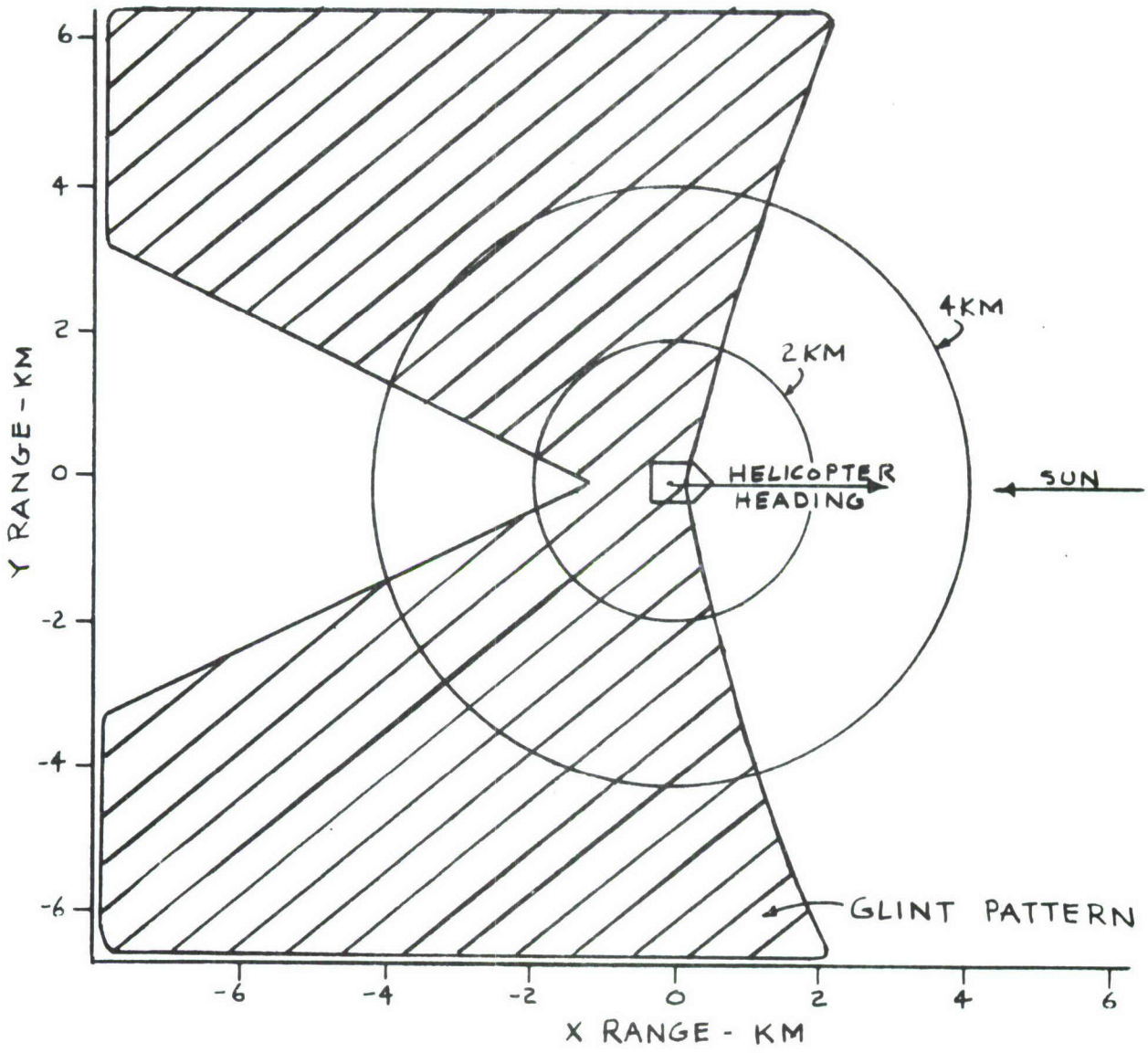

Figure 3-3. "Butterfly" Pattern for Existing Canopy with Sun Elevation of 20° and Sun Azimuth of 0°

yds. from a Cobra noted where glints occurred. Data was taken with the helicopter facing north, east, south and west at three times of the day. The results of this verification are shown in figure 3-4. The plots are oriented with north up and the sun position shown by the arrow on the outside of the plot. The three times of day are noted at the top of each column. The helicopter position is shown by the pentagon. MASSTER glint detections are shown on the inner ring. Westinghouse predicted detections are shown on the outer ring. Over 70% of all detections were seen by MASSTER and predicted by the SEEHC model.

3.2 SEEHC3

The general purpose of the SEEHC3 model is the same as that of SEEHC2. That is, it is used to examine ground glint patterns emanated from canopy surfaces when illuminated by the sun. However, there are a few basic differences and it is the object of this section to discuss these differences.

There are three basic differences between the two models:

(1) Canopy surface descriptions

(2) Capability of SEEHC3 to analyze surfaces with baffles

(3) Computation of the brightness factor and glint range

In SEEHC2 the surface description utilized a basic canopy coordinate system and each surface was described by the direction of its normal and a parameter which gives a measure of the energy emanated in the direction of the reflected ray. The parameter was primarily useful for curved surfaces. In SEEHC3, the canopy is assumed to be constructed of flat surfaces. The method for describing the canopy structure in SEEHC3 utilizes the concept of a generalized flat surface. The concept, in SEECH3, uses three coordinate systems:

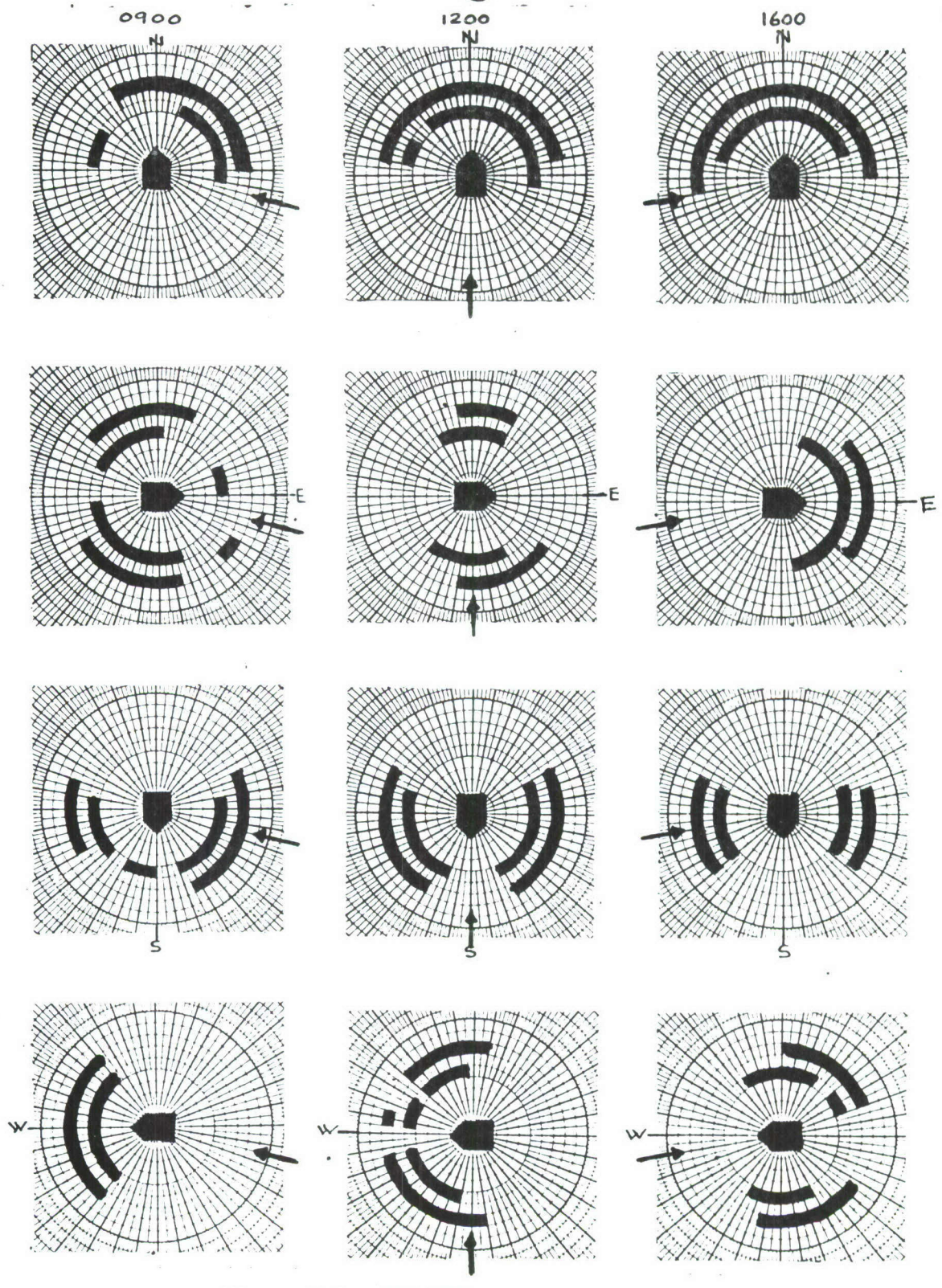

Figure 3-4. MASSTER Verification Data

a reference coordinate system, a canopy coordinate system, and a surface coordinate system. The first step is to describe the surface in its own coordinate system as is shown in figure 3-5. This is done for each surface and

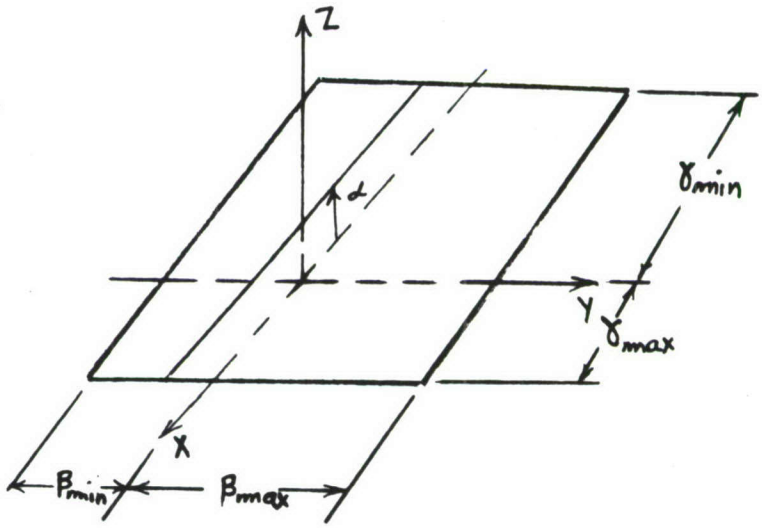

Figure 3-5. Window Surface Description

baffle to be used in the canopy. The next step is to position each surface with respect to the canopy coordinate system. This is done by specifying x, y, z coordinates of the center of the surface coordinate system with respect to the canopy system as well as by specifying the yaw, pitch, and roll of the surface system with respect to the canopy system. The final step is to specify the position and orientation of the canopy system with respect to the reference coordinate system. The technique is illustrated in figure 3-6. Note that in using this technique each surface is uniquely positioned in space.

The second difference in SEEHC3 is the capability to analyze baffle structures. This is accomplished by use of an algorithm which will be referred

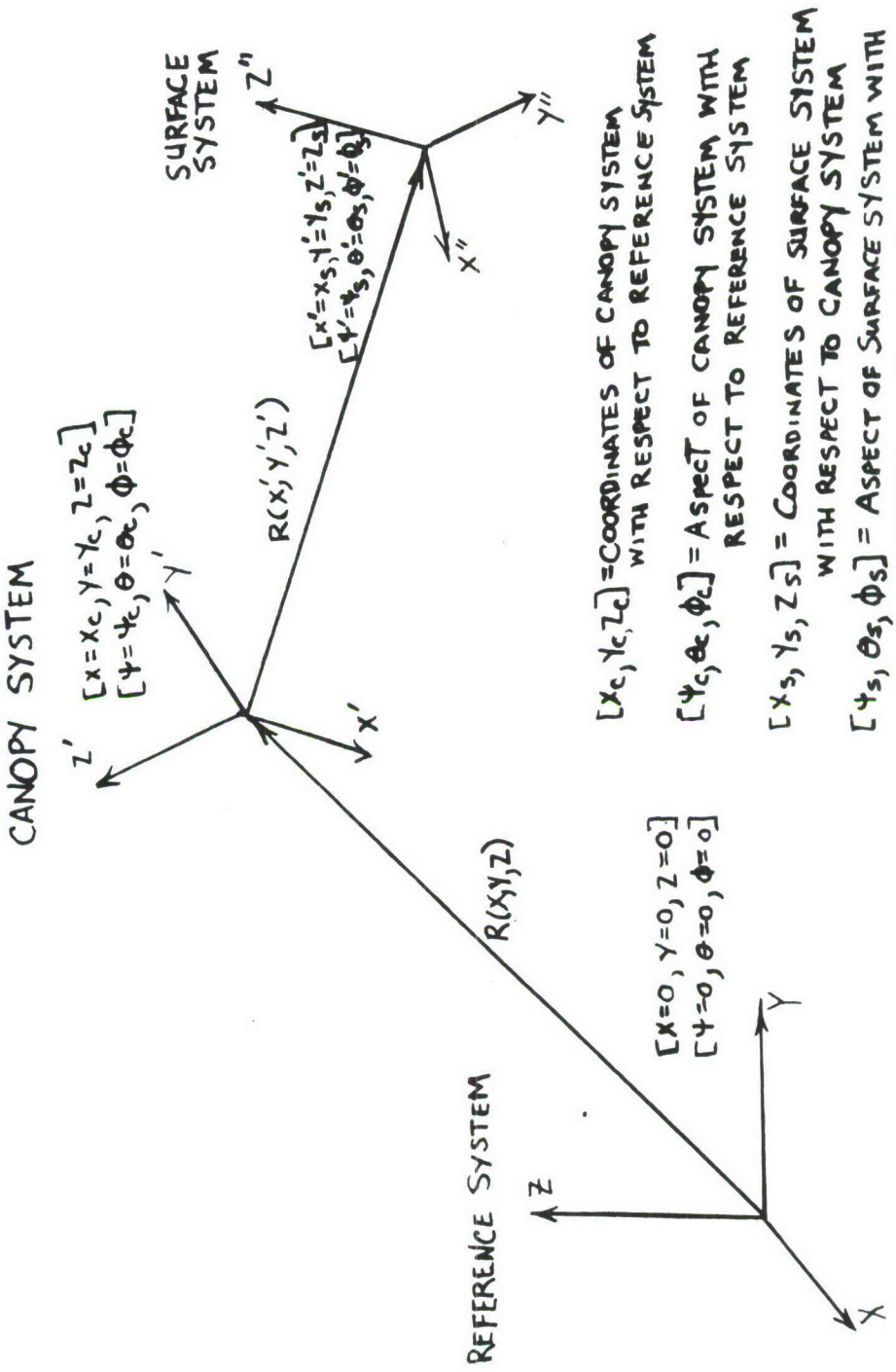

Figure 3-6. Canopy Construction and Helicopter Positioning

to as RAYINT. The purpose of RAYINT is to determine if a surface is entirely shaded by a baffle. The inputs to the algorithm are the surface location and size, the baffle locations and sizes, and direction of the ray to be traced. RAYINT begins by quantizing the surface into a specified number of elements. Then, for each element, RAYINT traces the sun ray and the reflected ray from the center of the element to determine if they intercept any baffles. If the sun ray or reflected ray from a given element intercept a baffle, then the routine iterates to the next element. If the rays from every element intercept a baffle, then the surface does not show a glint and the routine goes on to the next surface. In the event that the sun ray and the reflected ray from a particular element do not intercept baffles, then the routine acknowledges that a glint has been produced by the surface being considered. In this case, the pertinent data for the glint is computed and the glint is registered on an α-β plot in the same manner as was done in SEEHC2.

The final difference between SEEHC2 and SEEHC3 is the computation of brightness factor and glint range. Since SEEHC2 considered curved surfaces, it was necessary to compute a measure of the effective energy emitted in the direction of the reflected ray by a flat surface whose area is equivalent to the effective area of the appropriate curved surface element. This measure is called the brightness factor. SEECH3 considers only flat surfaces and assigns a nominal value of 99 to the brightness factor. The reason for choosing 99 is due to the fact that the window surface areas being considered by SEEHC3 are so large that the brightness factor was expected to be over 100. Since the maximum in the range of brightness factor in SEEHC2 was 99, it was arbitrarily set at 99 in SEEHC3 in order to indicate the large surface areas being considered. The glint range was arbitrarily set at 5 nautical miles,

since this is well beyond the ranges for which glints are of interest. Notice that the maximum range inside the border on the glint plots is slightly greater than 6 km or less than 4 nautical miles.

4.0 CANOPY CONFIGURATION COMPARISONS

4.1 Canopy Configurations

4.1.1 Existing Canopy

The existing canopy has been described in the final report on Work Assignment #2 of contract number DAAD05-72-C-0284. It is represented by 1464 segments in the COBWIN and SEEHC2 models. The glint coverage for the existing canopy configuration will be considered as the baseline from which other canopies will be judged. There must be a significant reduction for any other canopy configuration, as compared to the existing canopy, before it can be given serious consideration.

4.1.2 "Porthole" Canopy

The Porthole Canopy was an approach developed by LWL on a visit to Ft. Hood, Texas on March 12 and 13, 1973 by G. Cook and P. Ferrara of LWL and R. Daumit of Westinghouse. It involves blocking of all of the side windows except for a section on each side near the pilot which is approximately 44" long and 9" high and a section on each side near the gunner which is approximately 25" long and 9" high. The overhead remains unblocked. Thus, two 'portholes' on each side and the overhead are the only window areas which can provide both glints and vision. Figures 4-1 and 4-2 are photographs taken at Ft. Hood which show a Cobra with the portholes cut out of a paper mask for the canopy. This canopy was simulated in SEEHC2 by removing those portions of the canopy which would be blocked out from the window descriptions. The window was represented in the SEEHC2 program by 282 segments as compared to 1464 segments for the existing window.

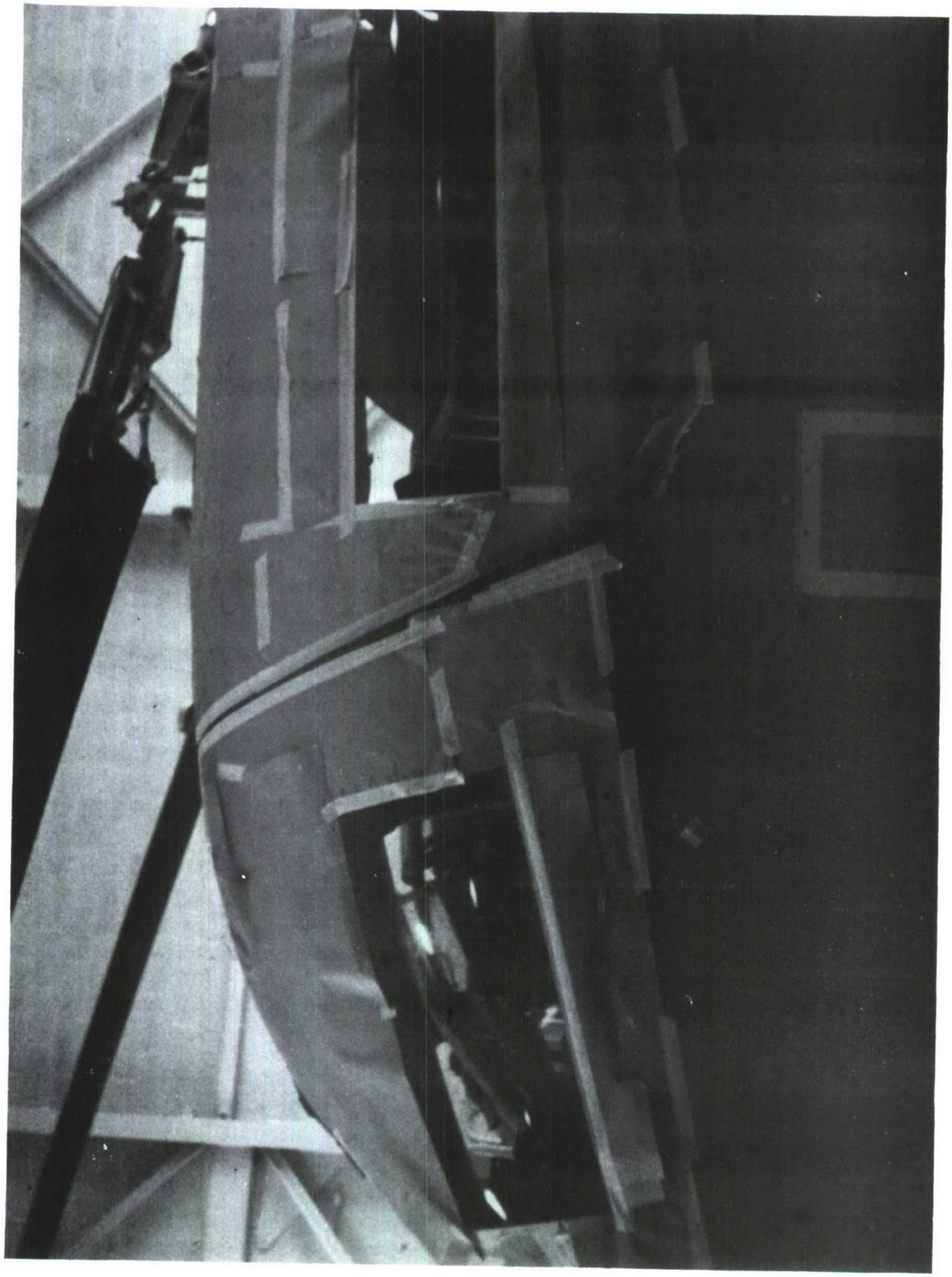

Figure 4-1. Porthole Canopy (Side View)

Figure 4-2. Porthole Canopy (Front View)

4.1.3 "LWL-35" Canopy

The LWL-35 canopy was designed by the Land Warfare Laboratory under AVSCOM direction for use in a demonstration of the flat plate canopy concept. As shown in figure 4-3, the LWL-35 canopy consists of 4 flat plates; two vertical plates on the sides, a horizontal plate on the top and a front plate sloped 35° back from the vertical.

A flight test demonstration side by side with a standard Cobra proved the great reduction in sun glint signature possible by the use of flat plates. As shown later in section 5, this effect was predicted by the SEEHC2 model.

4.1.4 Westinghouse Recommended Configuration

4.1.4.1 40° Baffled Canopy

The 40° baffled canopy was described in section 2.8 and sketched in figures 2-35 and 2-36. Figures 2-37 through 2-51 show the 40° baffled canopy baffles on the LWL-35 canopy. The "40° baffled" canopy is Westinghouse's recommended design for a baffled canopy which reduces solar glint on the ground to a minimum.

4.1.4.2 40° Canopy

The 40° canopy was included to demonstrate the differences in baffled and non-baffled canopies of an otherwise equal design.

4.2 Method of Comparison

Using the glint patterns generated by SEEHC2 and SEEHC3, it is possible to compare the glint signatures of different canopy configurations as a function of sun elevation.

Glint patterns are generated for each sun elevation and show all downward glints from the given sun elevation as the sun is rotated from 0°

Figure 4-3. LWL-35 Canopy

to 330° in azimuth in 30° increments. For each pattern, elevation is held constant at 100 feet and the roll, yaw, and pitch of the helicopter is cycled through ±2° around a basic attitude of 0° yaw and roll and 5° to 6° down pitch. For each glint pattern, a butterfly pattern is drawn which encompasses all points at which a glint occurs.

Two conditions are considered. The first considers all glints in the 360° azimuth coverage which are at a range of 1 km or more. Glints at ranges of less than 1 km are not considered harmful because the helicopter would be either visually detected or heard at that range. The second condition considers all glints within ±70° of the nose of the helicopter and at a range of 1 km or more.

4.3 Comparison Data

The data for each set of patterns is plotted on linear graphs in figures 4-4 and 4-5 and on semilog graphs in figures 4-6 and 4-7 and is tabulated in Table 4-1. The actual glint patterns are shown in Appendix A.

The linear plots of figures 4-4 and 4-5 are included to show the great improvement of a flat plate canopy, i.e. the LWL-35 canopy, over curved canopies, i.e. the Existing and Porthole canopies. This difference is greatest at lower sun elevations which, as will be shown in section 5.2, occurs more often than higher sun elevations. The 40° and 40° baffle curves are included as additional flat plate cases.

The semilog plots of figures 4-6 and 4-7 are included to compare the 40° and 40° Baffled canopies to show the improvement when baffling is used on a flat plate canopy. Curves for the LWL-35, Existing and Porthole canopies are also included in these figures for comparison. It may be noted that the LWL-35 curves show better results than the 40° curves. This may be

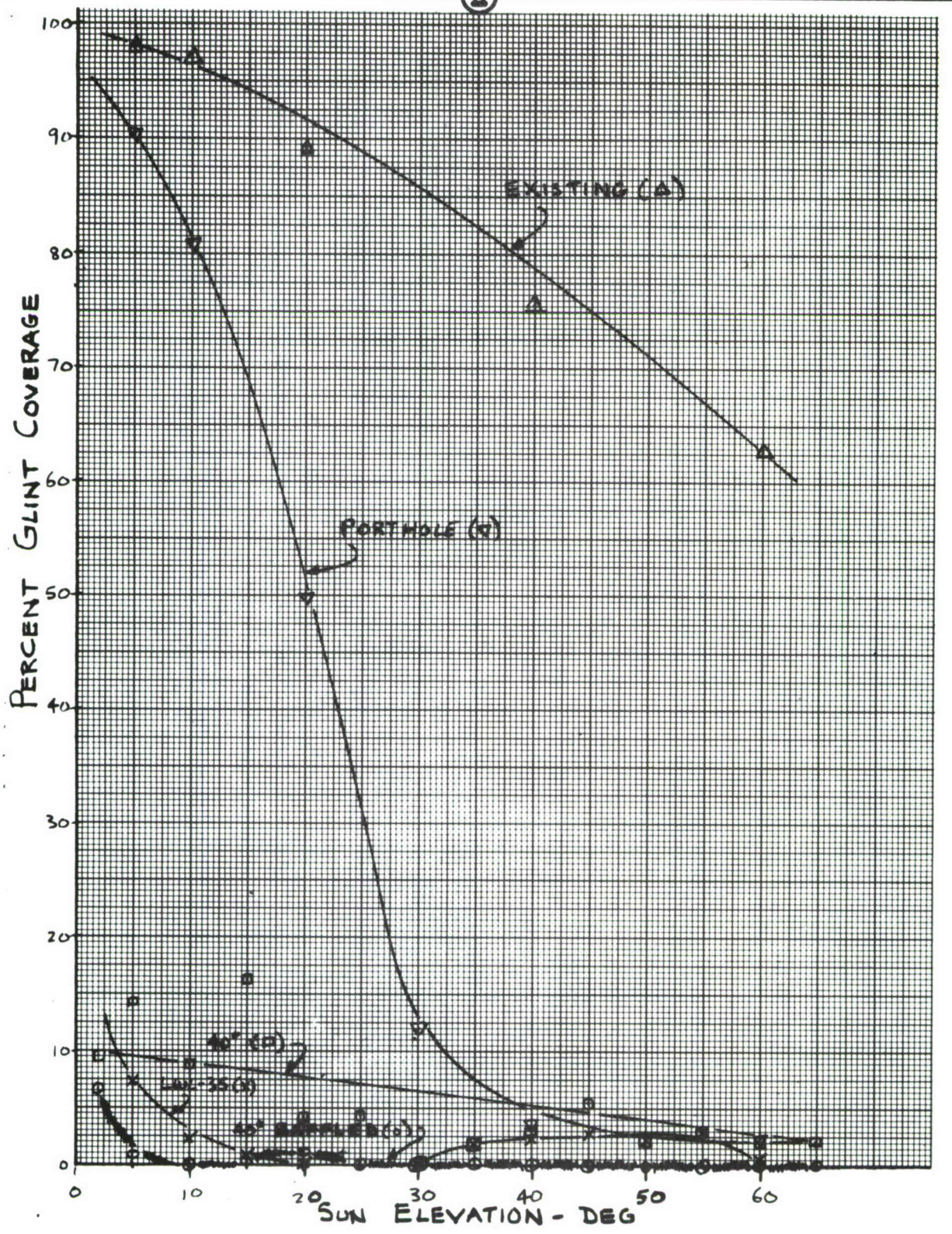

Figure 4-4. Linear Plot of Glint Coverage for 360° Case

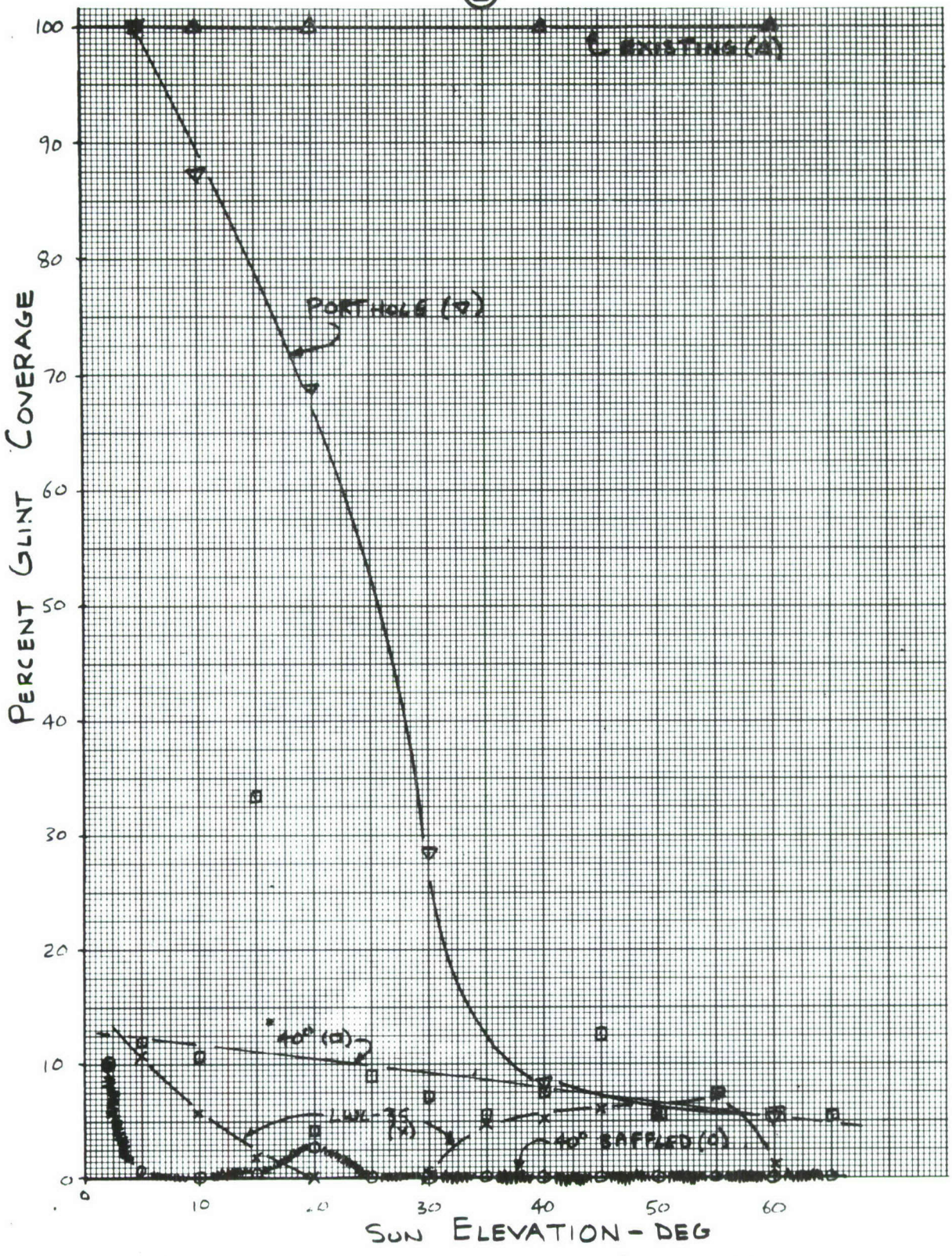

Figure 4-5. Linear Plot of Glint Coverage for ±70° Case

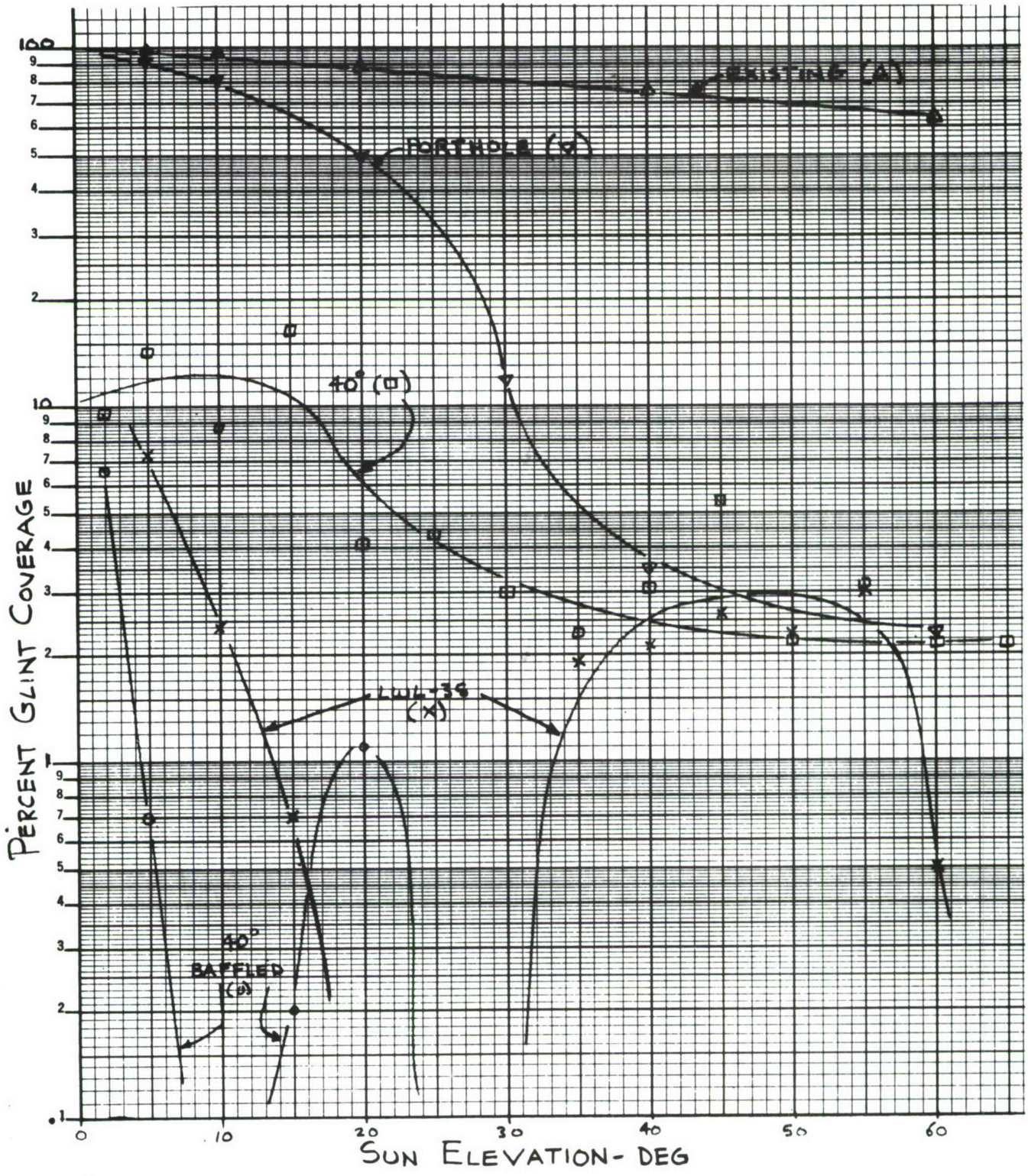

Figure 4-6. Semilog Plot of Glint Coverage for 360° Case

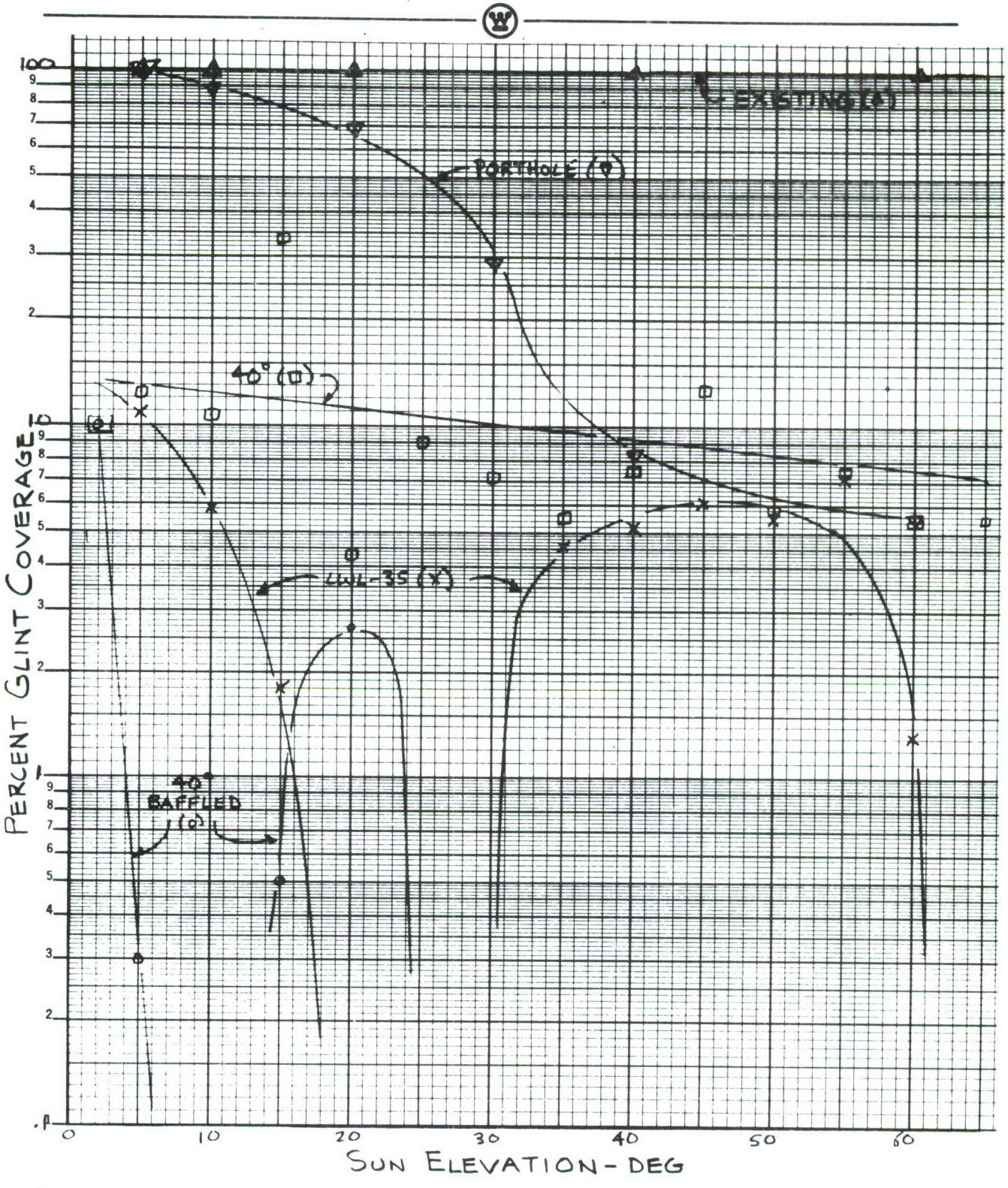

Figure 4-7. Semilog Plot of Glint Coverage for 70° Case

Table 4-1

Comparison of Percent Glint Coverage For Five Canopy Configurations

Canopy	Existing		Porthole		LWL-35		Unbaffled 40°		Baffled 40°	
Azimuth Area	360°	±70°	360°	±70°	360°	±70°	360°	±70°	360°	±70°
Sun Elevation										
2°							9.5	10.0	6.6	10.0
5°	97.7	100	90.4	100	7.4	10.9	14.1	12.2	.7	.3
10°	96.9	100	80.9	87.3	2.4	5.8	8.7	10.6	0	0
15°					.7	1.8	16.1	33.4	.2	.5
20°	89.2	100	49.8	68.8	0	0	4.1	4.3	1.1	2.7
25°							4.4	9.0	0	0
30°			11.9	28.4	0	0	3.0	7.1	0	0
35°					1.9	4.6	2.3	5.5	0	0
40°	75.5	100	3.5	8.3	2.1	5.1	3.1	7.5	0	0
45°					2.6	6.1	5.4	12.8	0	0
50°					2.3	5.5	2.4	5.8	0	0
55°					3.0	7.1	3.1	7.5	0	0
60°	62.7	100	2.3	5.5	.5	1.3	2.3	5.5	0	0
65°							2.3	5.5	0	0

due to the fact that the data points taken for the 40° case included points only 10° in azimuth away from a worst case condition. Such a condition may also exist for the LWL-35, but it was not investigated. If it exists, it would modify the LWL-35 curve upwards.

From the above data, we observe that:

- The Flat Plate Canopies have a much smaller glint signature than the curved canopies, and
- The Baffled Flat Plate Canopy has a much smaller glint than the Unbaffled Flat Plate Canopy.

5.0 ADDITIONAL WORK PERFORMED

5.1 Aid in Flat Plate Demonstration

Westinghouse assisted LWL in the demonstration of a flying flat plate canopy by modeling the LWL-35 canopy and putting it into SEEHC2 to show the reduction in glints. In addition, runs were made with the existing canopy to show its glint pattern so that LWL would know where to be to see its glints. The results of this data were used by LWL to help determine the format of a movie film made of the demonstration.

Figures 5-1 through 5-7 show some glint patterns made for LWL. They show the glint patterns out to 2 km for the existing canopy at 12 noon in late March when the sun was at an elevation of 50° with the helicopter at a 100 foot altitude. The dashed lines in figures 5-5 and 5-6 represent the predicted LWL-35 glint. The box in the lower right hand corner identifies the time on the first line, the compass direction in which the nose of the helicopter is pointing on the second, the helicopter altitude on the third line and the computer run identifier on the fourth line. North is shown by the letter N. The sun direction is south in all cases and the arrow points to the helicopter's heading. The circle represents the 1 km range mark. The patterns were sized to provide a scaled overlay on a 1:25,000 scale map.

5.2 Sun Elevation Data

The amount of time which the sun is at given elevations is a matter of importance if one is to properly evaluate the output of this study. If the sun is at one elevation for only a small fraction of the time, then a design which is enlarged just to block reflections from that sun elevation may not be justifiable. Thus, in accordance with paragraph 5b of the statement

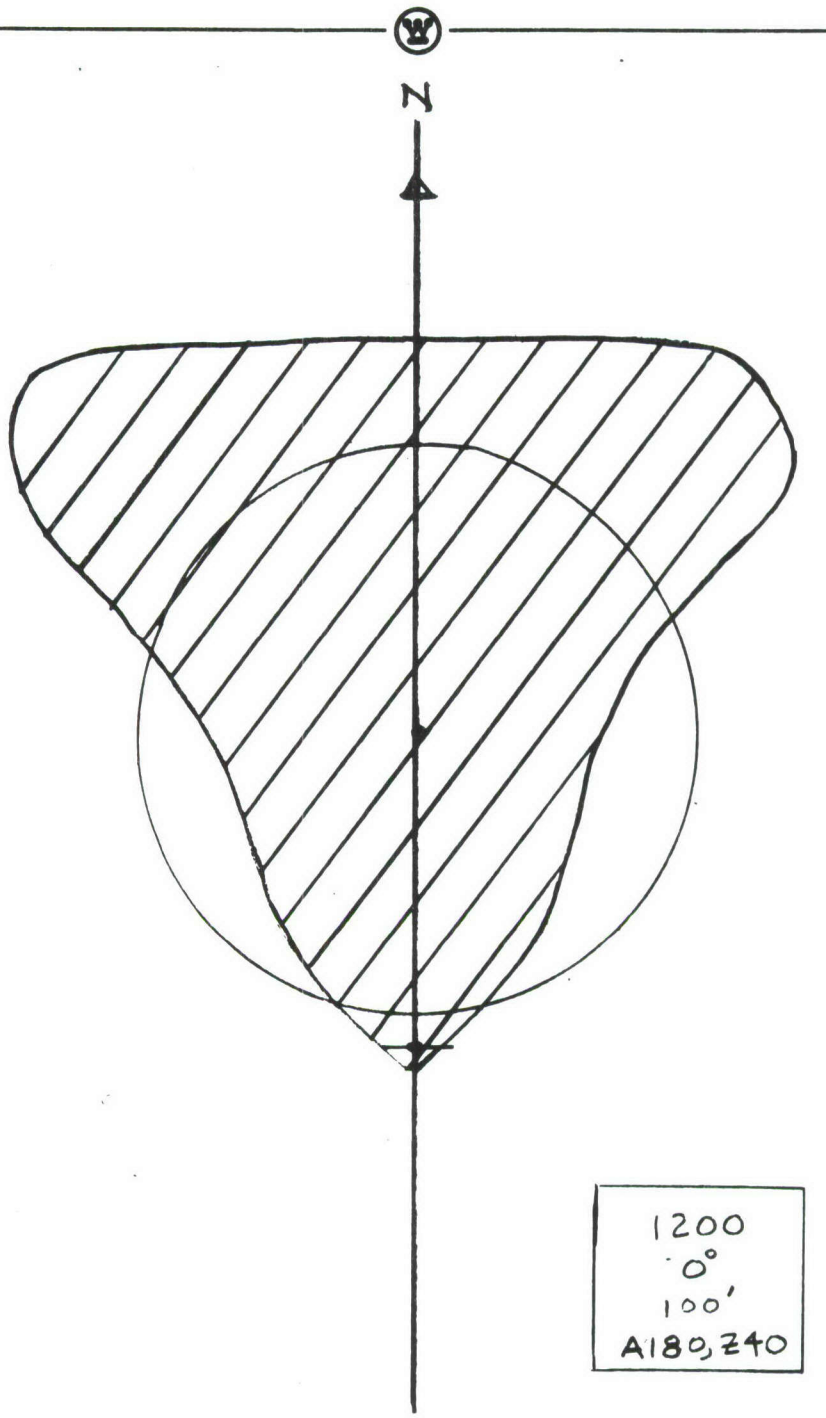

Figure 5-1. Glint Pattern for 0° Heading

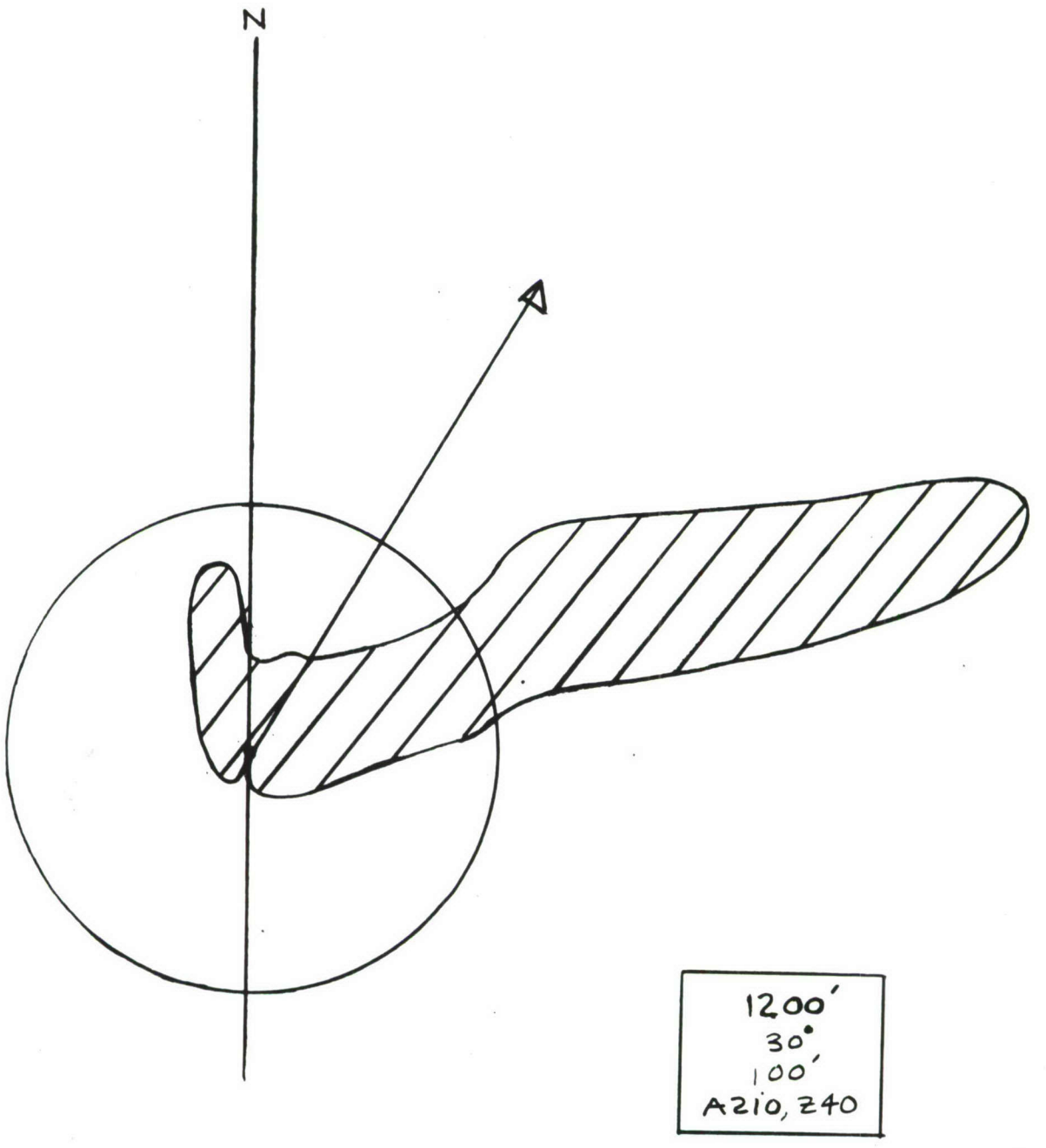

Figure 5-2. Glint Pattern for 30° Heading

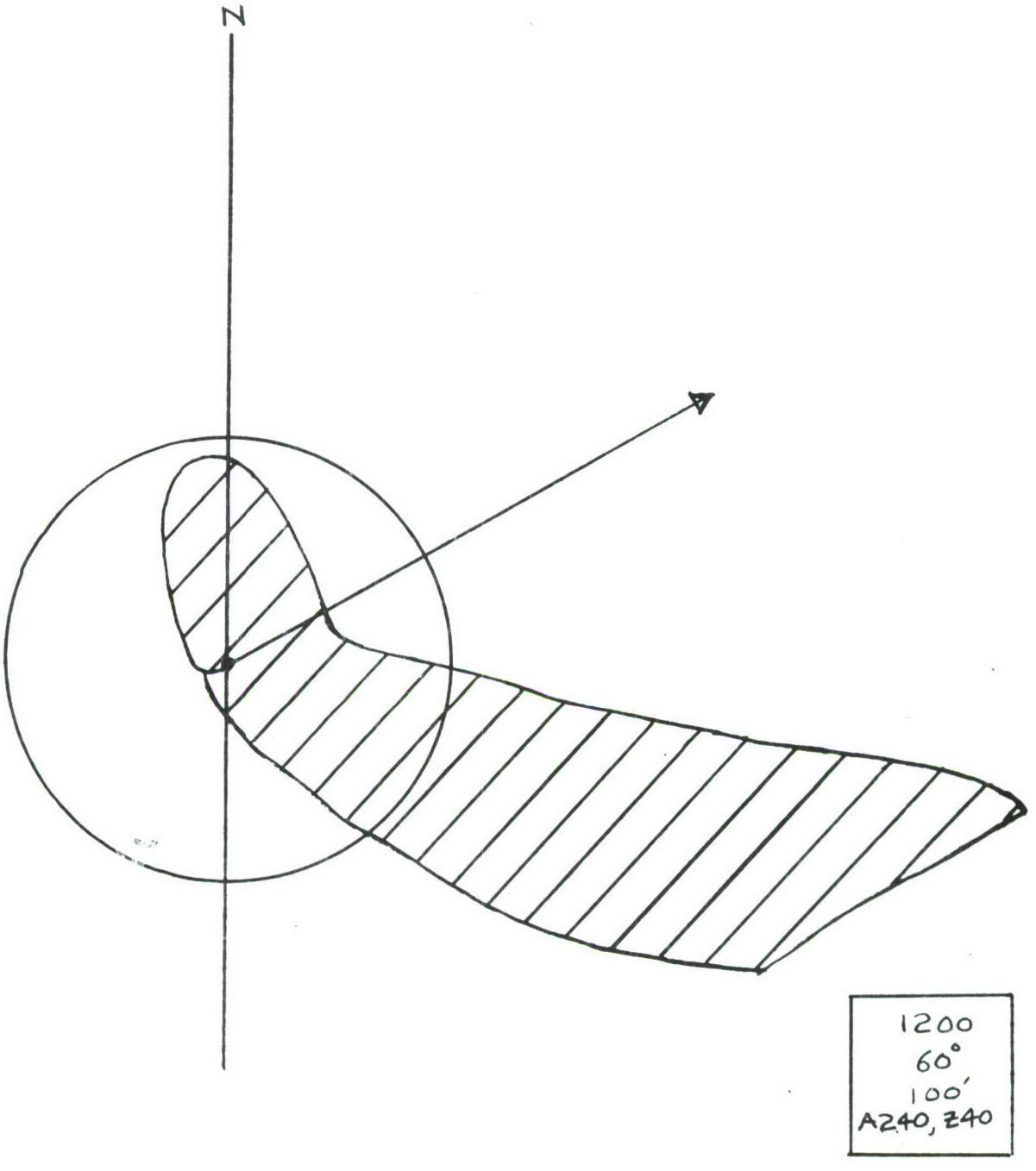

Figure 5-3. Glint Pattern for 60° Heading

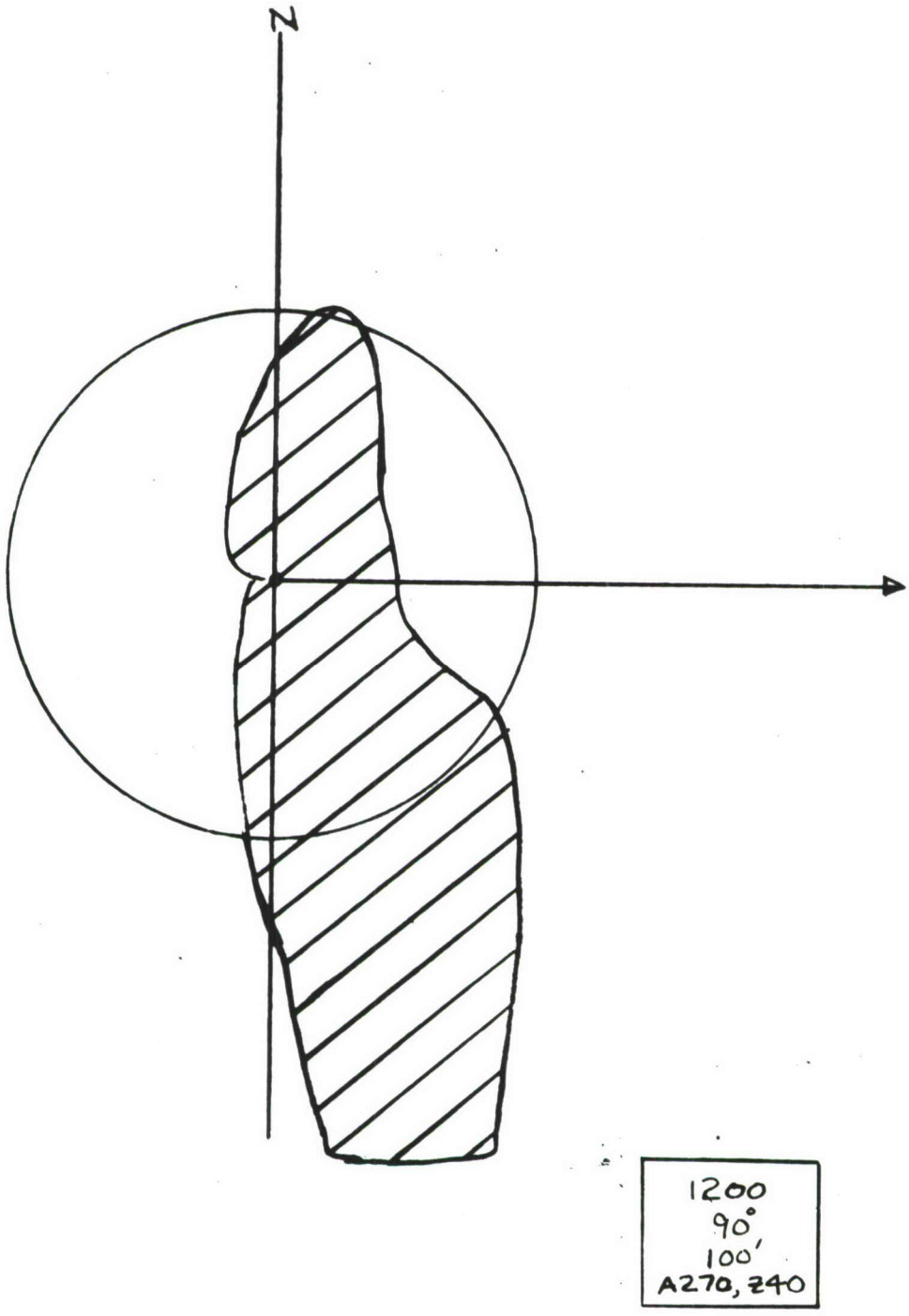

Figure 5-4. Glint Pattern for 90° Heading

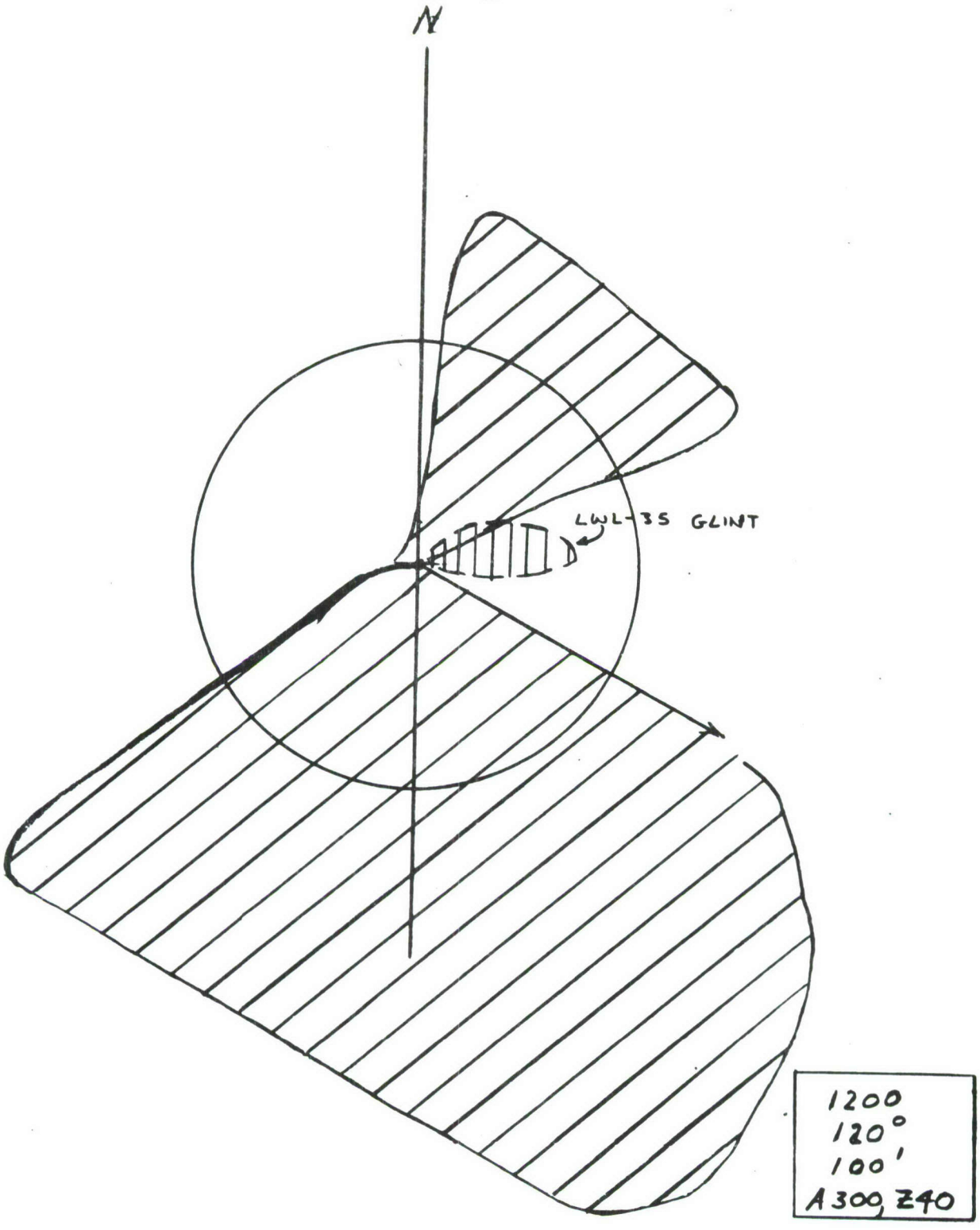

Figure 5-5. Glint Pattern for 120° Heading

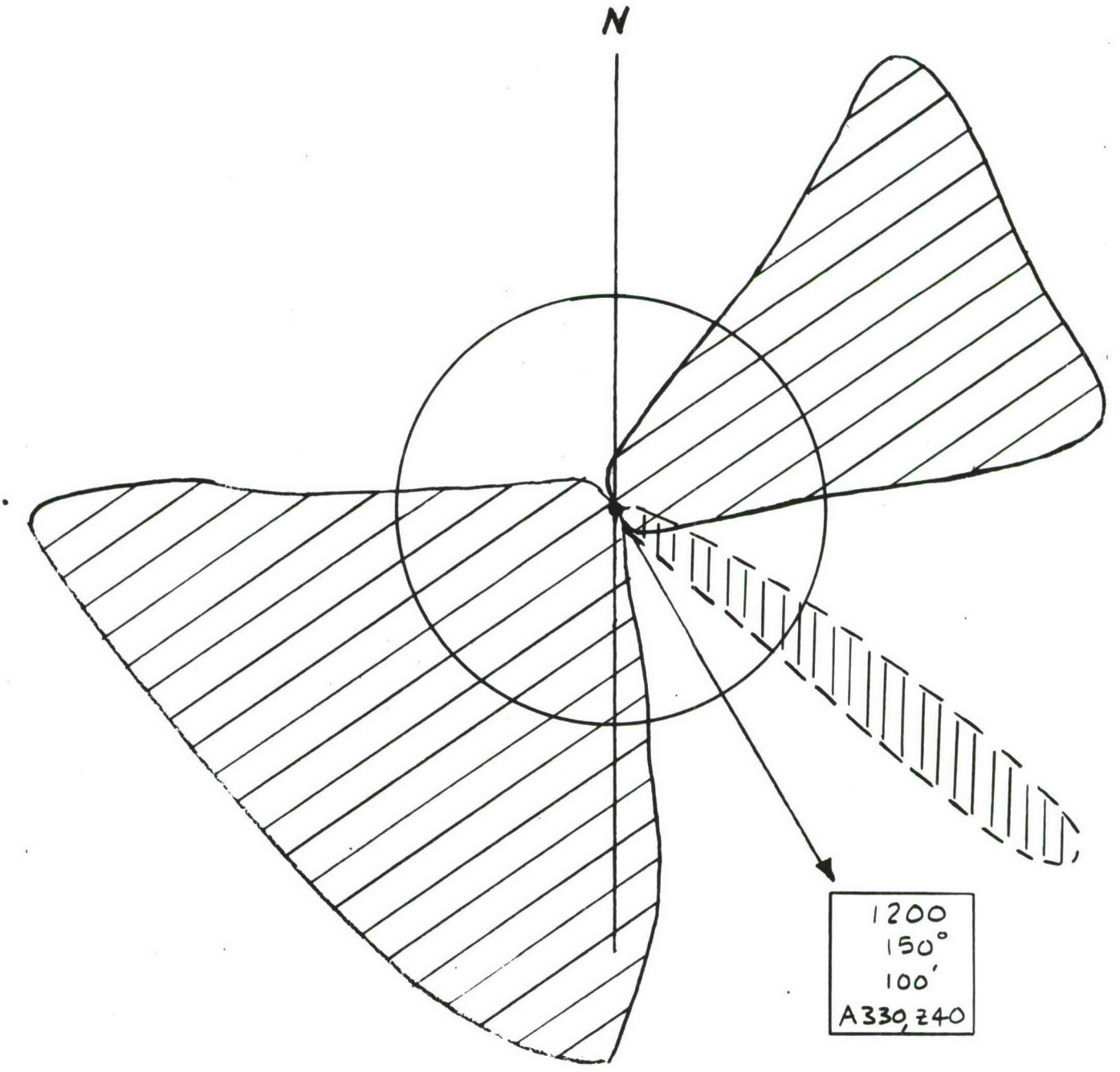

Figure 5-6. Glint Pattern for 150° Heading

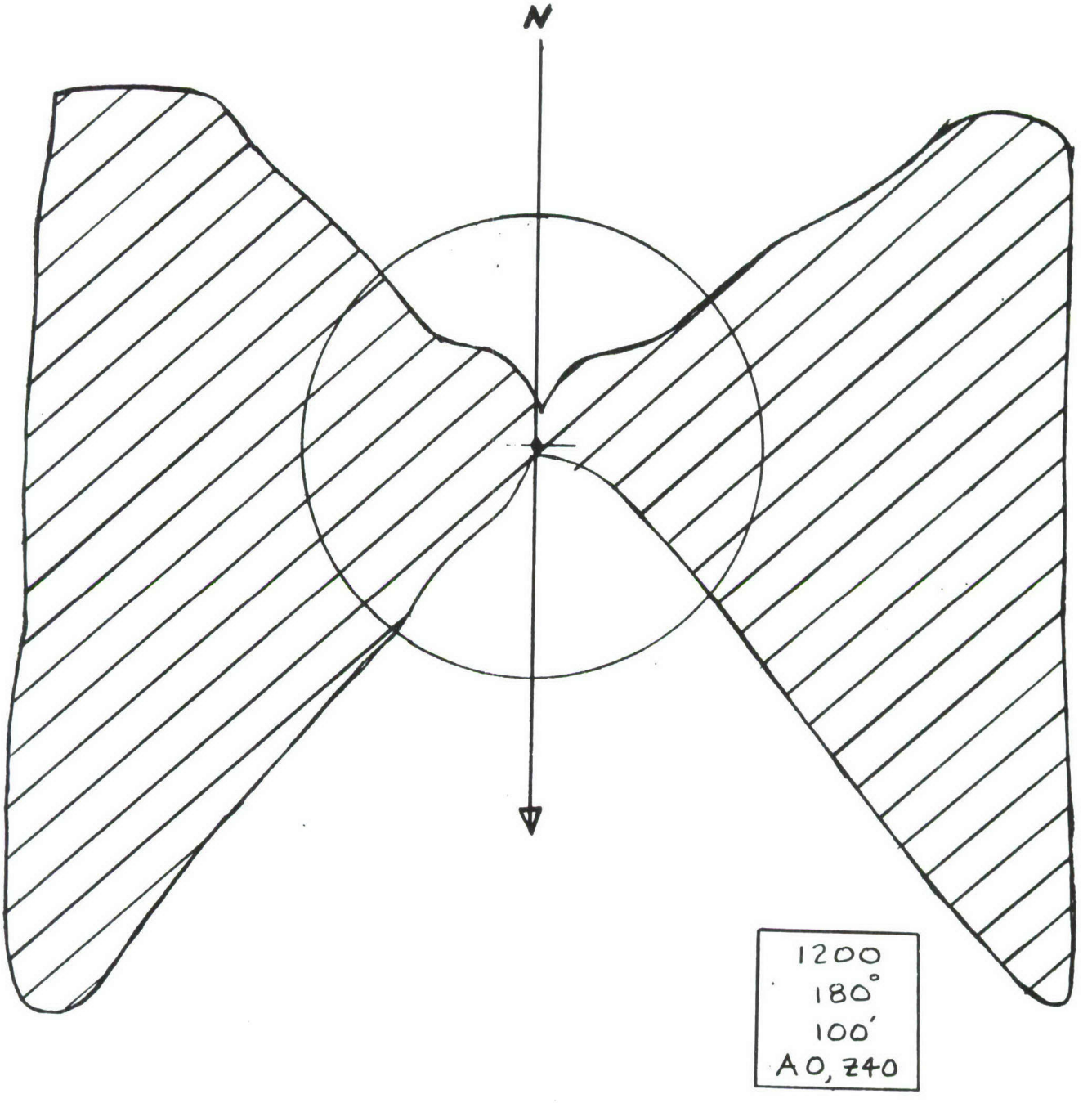

Figure 5-7. Glint Pattern for 180° Heading

of work for Work Assignment #3 of contract DAAD05-73-C-0305, Westinghouse generated a table showing the percentage of time that the sun spent at different elevations between the latitudes of 20° and 60° north.

This data, shown in Table 5-1 and figure 5-8, was generated using a digital computer program containing the equation:

$$\sin A = \sin B \sin C + \cos C + \cos B \cos C \cos H$$

where

A = altitude of the sun

B = latitude of the observer

C = declination of the sun

H = hour angle of the sun.

Table 5-1

Percentage of Sun Elevations From 20° to 60° North Latitudes

Sun Elevation	Percentage of Occurence
0-5°	8.78
5-10°	9.28
10-15°	9.22
15-20°	9.04
20-25°	8.77
25-30°	8.43
30-35°	8.01
35-40°	7.52
40-45°	6.95
45-50°	6.29
50-55°	5.05
55-60°	3.96
60-65°	3.04
65-70°	2.26
70-75°	1.59
75-80°	1.03
80-85°	.58
85-90°	.20

Table 5-1 shows that, in the 20° to 60° latitude, the sun elevation distribution is nearly uniform from 0° to approximately 50°. Also, the table indicates that the sun is above 65° elevation for only 5.66 percent of the time. Therefore, in considering the sun glint problem regarding canopy surfaces, the designer should concentrate his efforts primarily on sun elevations from 0° to 65°.

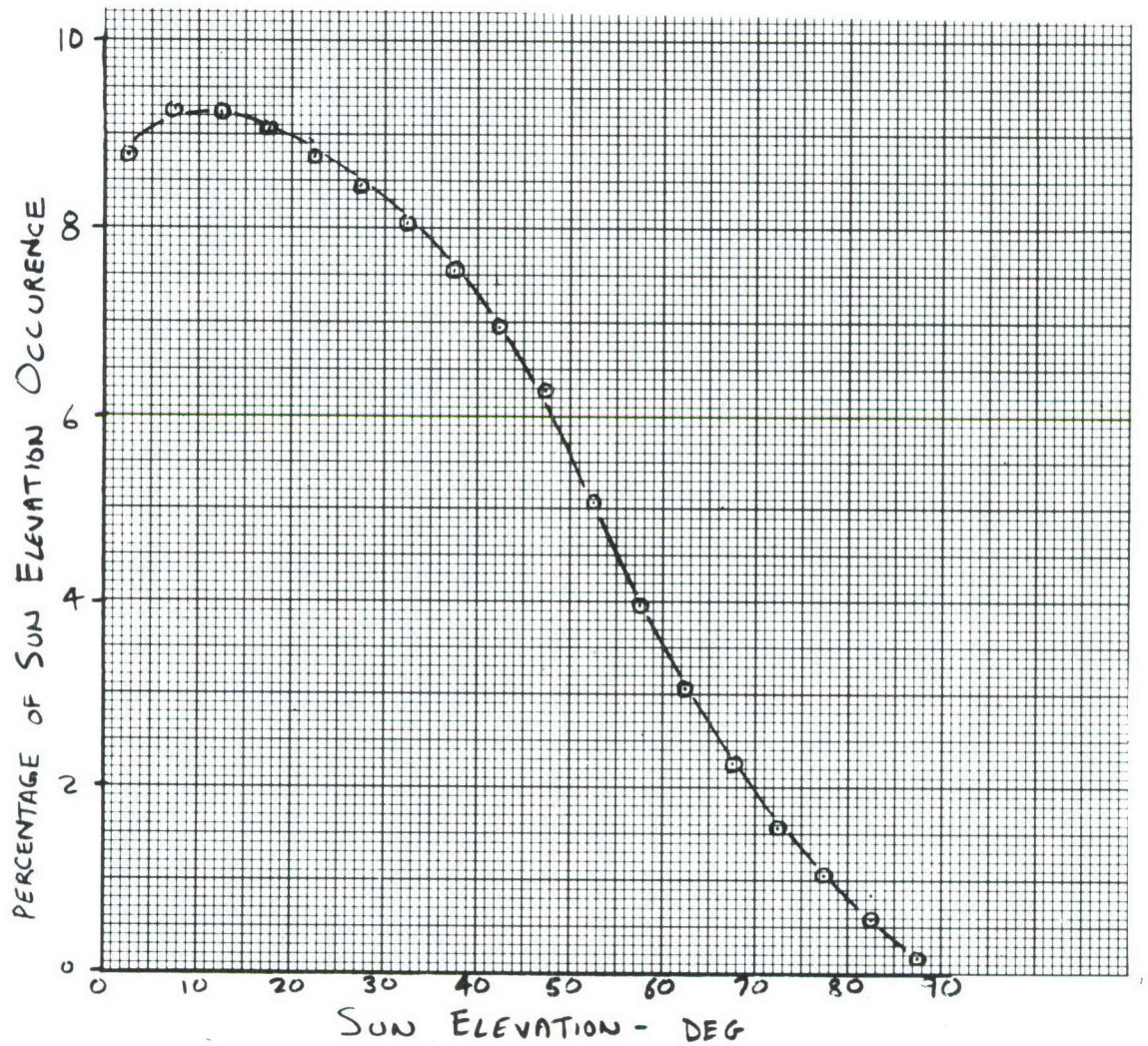

Figure 5-8. Probability of Sun Elevation Occurance

APPENDIX A

Glint Patterns

The glint patterns for 5 canopies and 14 sun elevations are presented in this appendix. The patterns for a given sun elevation make up a glint pattern set which is shown on one page. The set includes patterns for two to five canopy configurations with the patterns for any one canopy always in the same location on the page. Figure A-1 shows these locations.

Each pattern includes twelve azimuth cuts from 0° to 330°, integrated to give one pattern. The scales on the left and bottom of the pattern convert into kilometers as follows:

Scale Value	-3	-2	-1	0	1	2	3
Kilometers	-6	-4	-2	0	2	4	6

The circle in the middle of the pattern is the 1 km range ring. The pentagon inside shows the helicopter position and heading (always to the right). The two lines drawn out from the 1 km range ring are the $+70^{\circ}$ and -70° azimuth lines. The glint patterns are shown in figures A-2 through A-15.

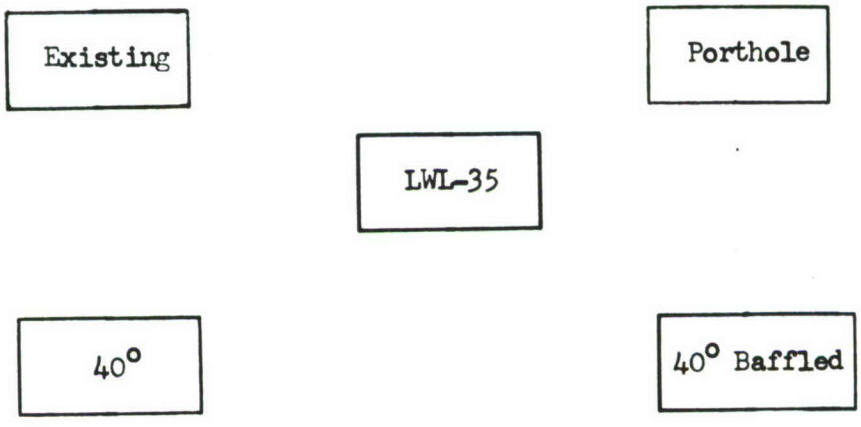

Figure A-1. Glint Pattern Arrangement

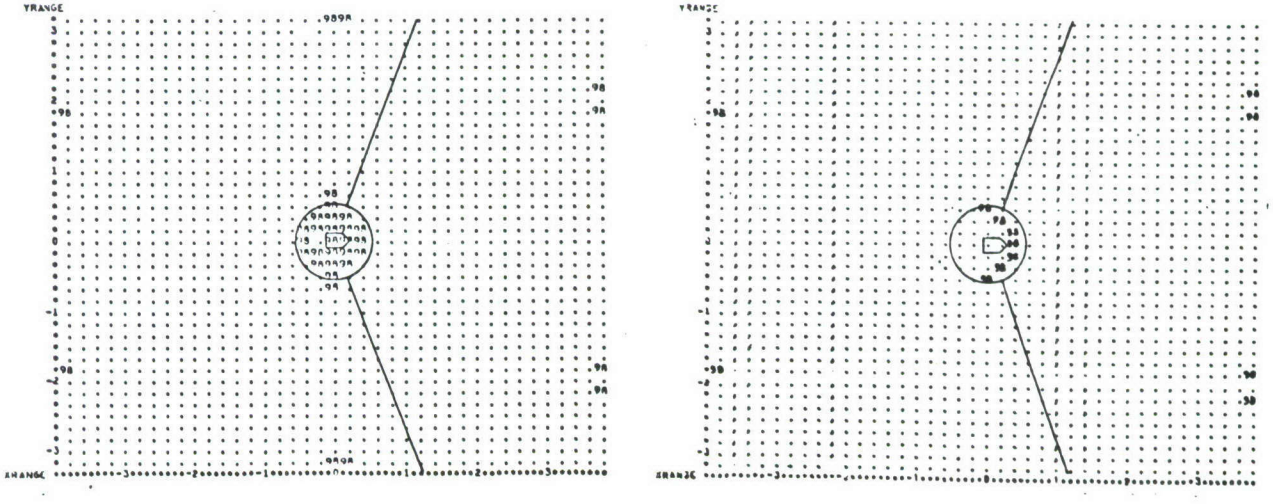

Figure A-2. 2° Sun Elevation Patterns

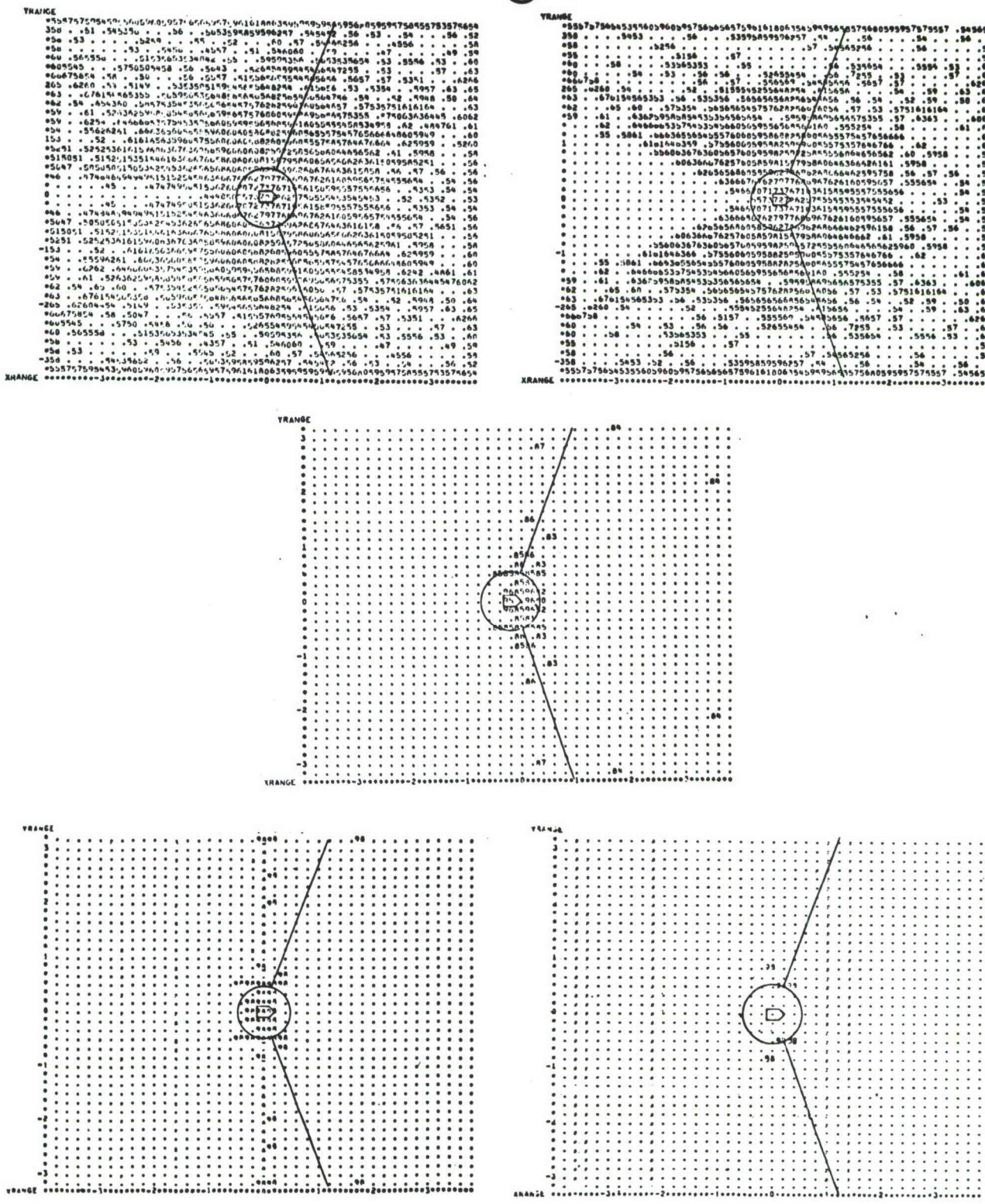

Figure A-3. 5° Sun Elevation Patterns

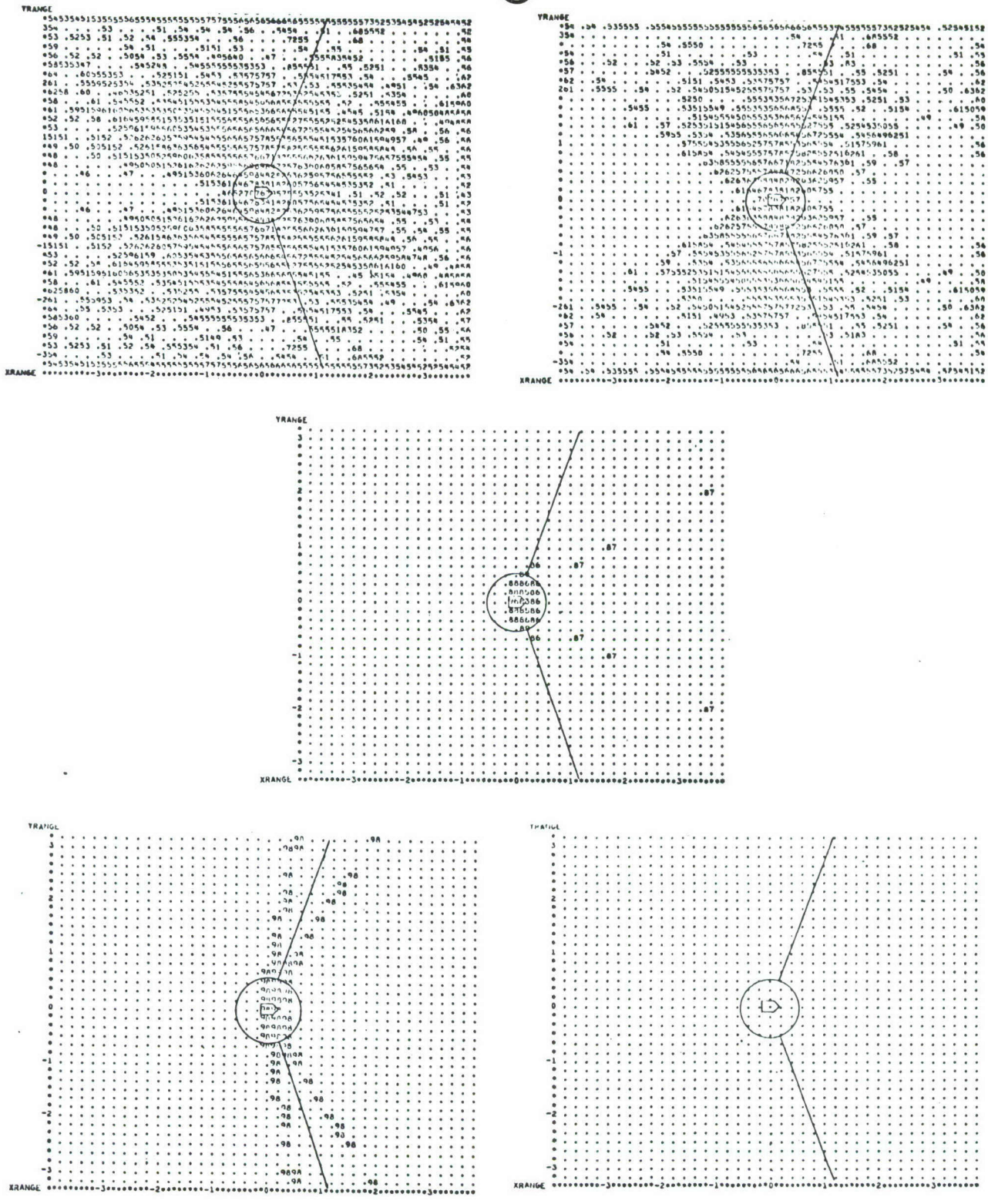

Figure A-4. 10° Sun Elevation Patterns

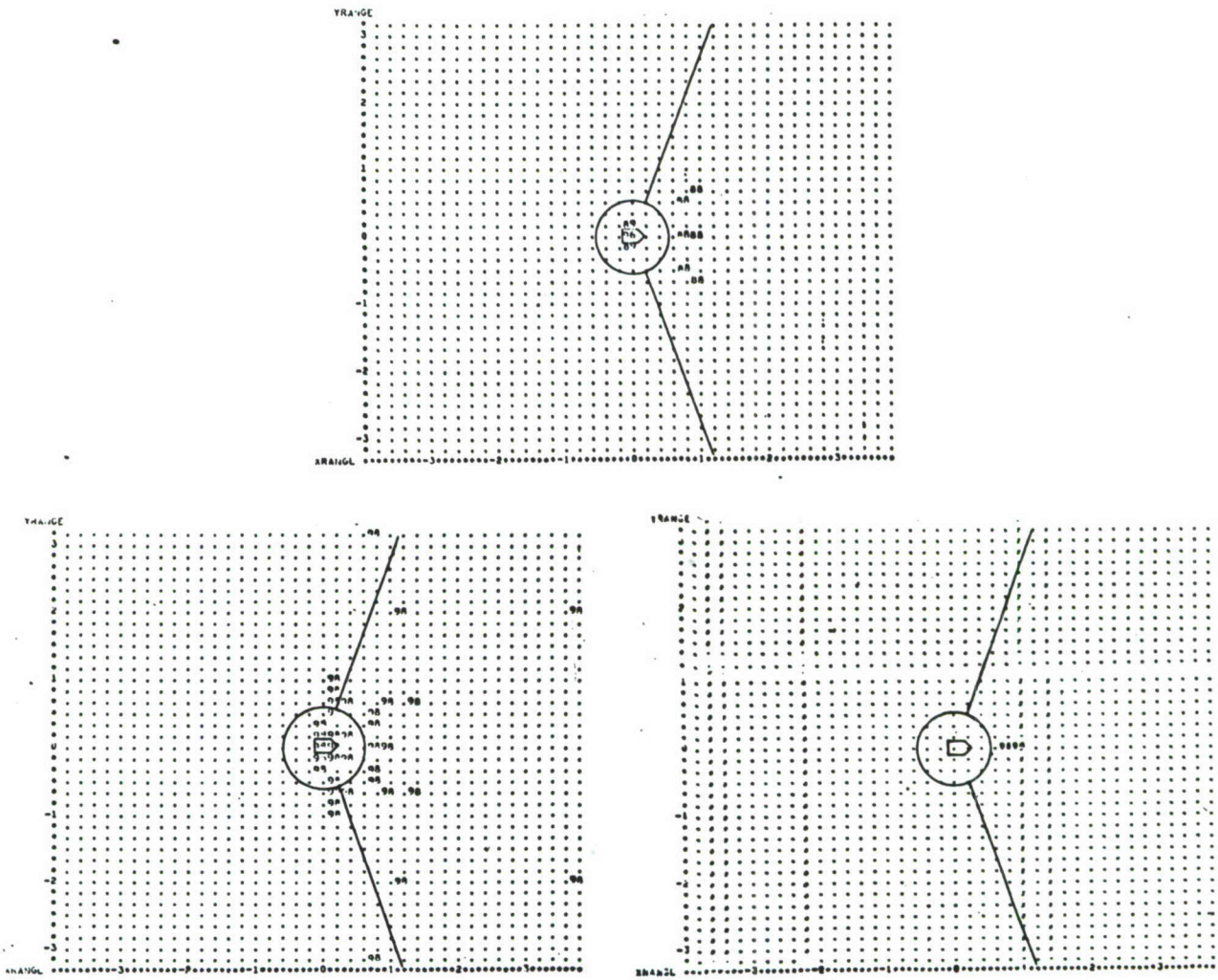

Figure A-5. 15° Sun Elevation Patterns

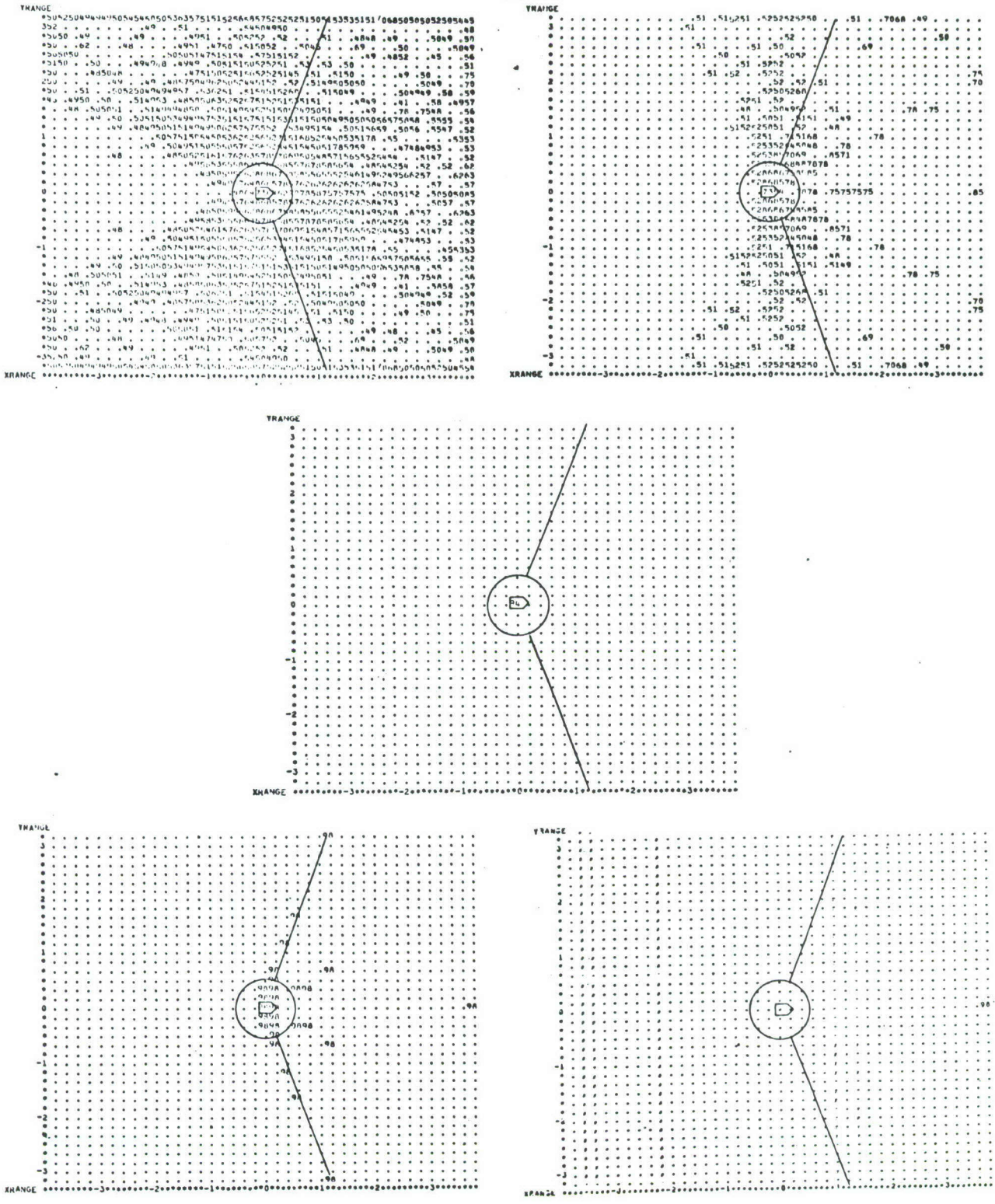

Figure A-6. 20° Sun Elevation Patterns

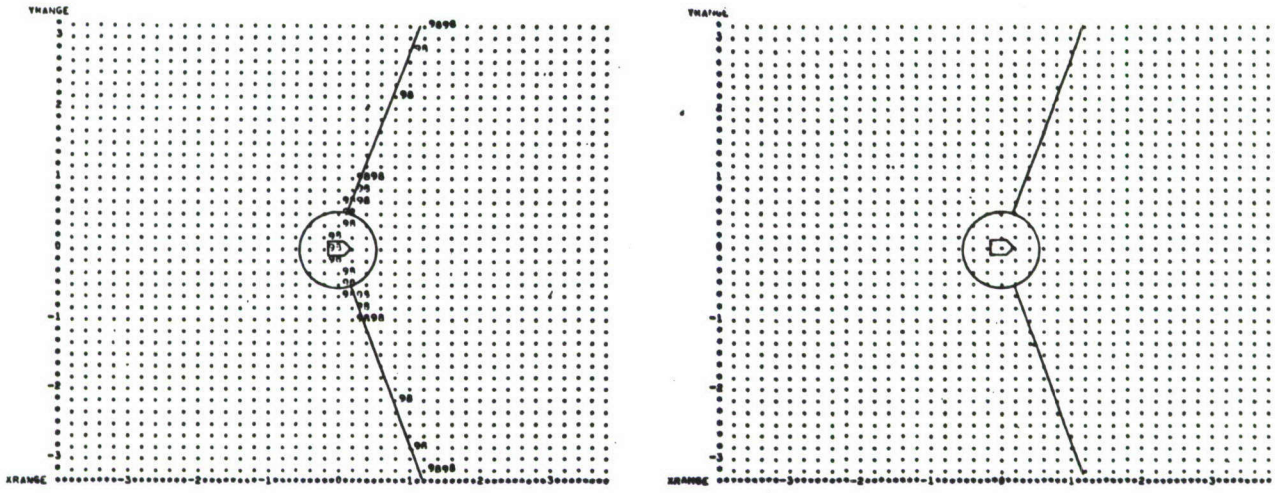

Figure A-7. 25° Glint Patterns

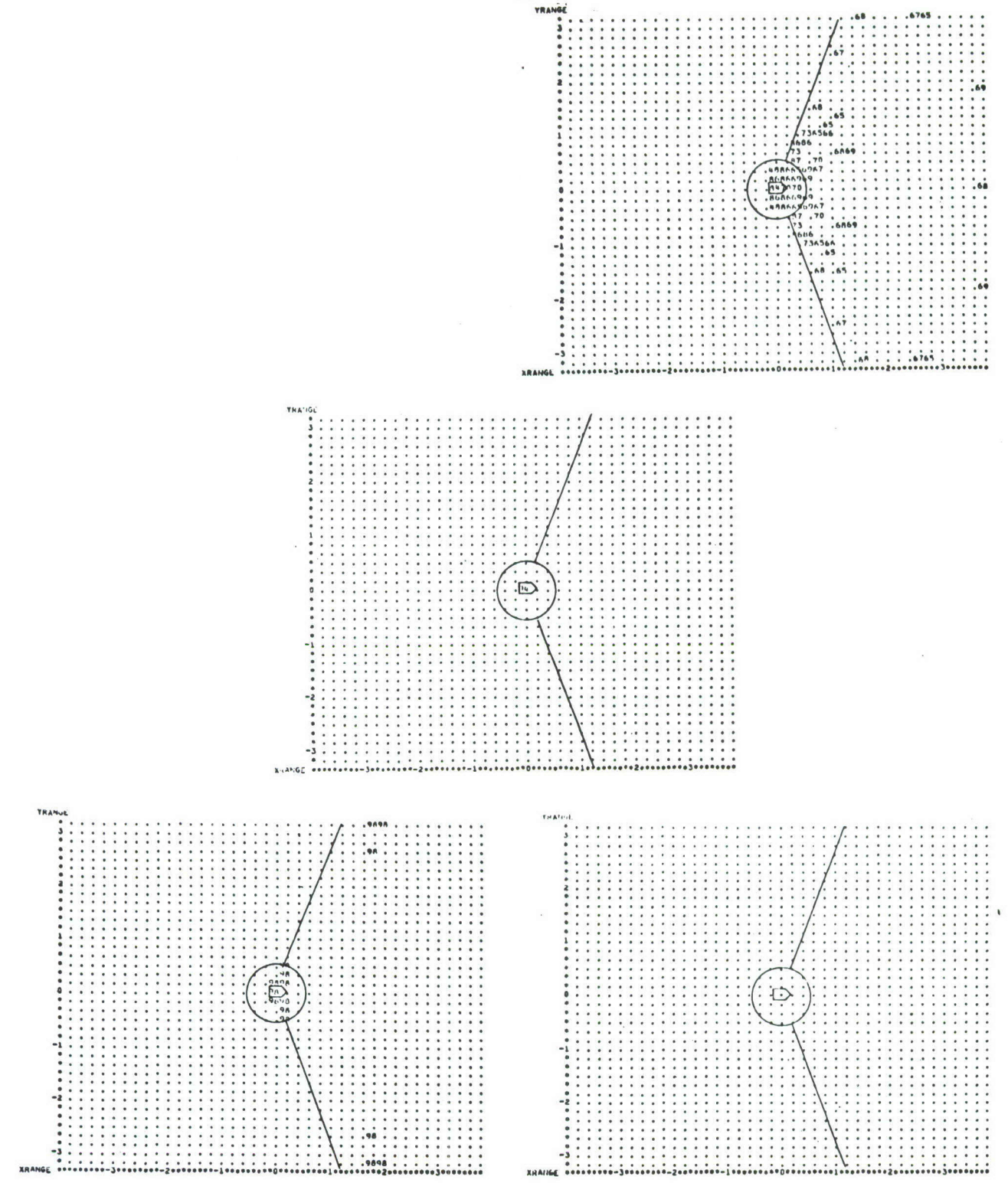

Figure A-8. 30° Glint Patterns

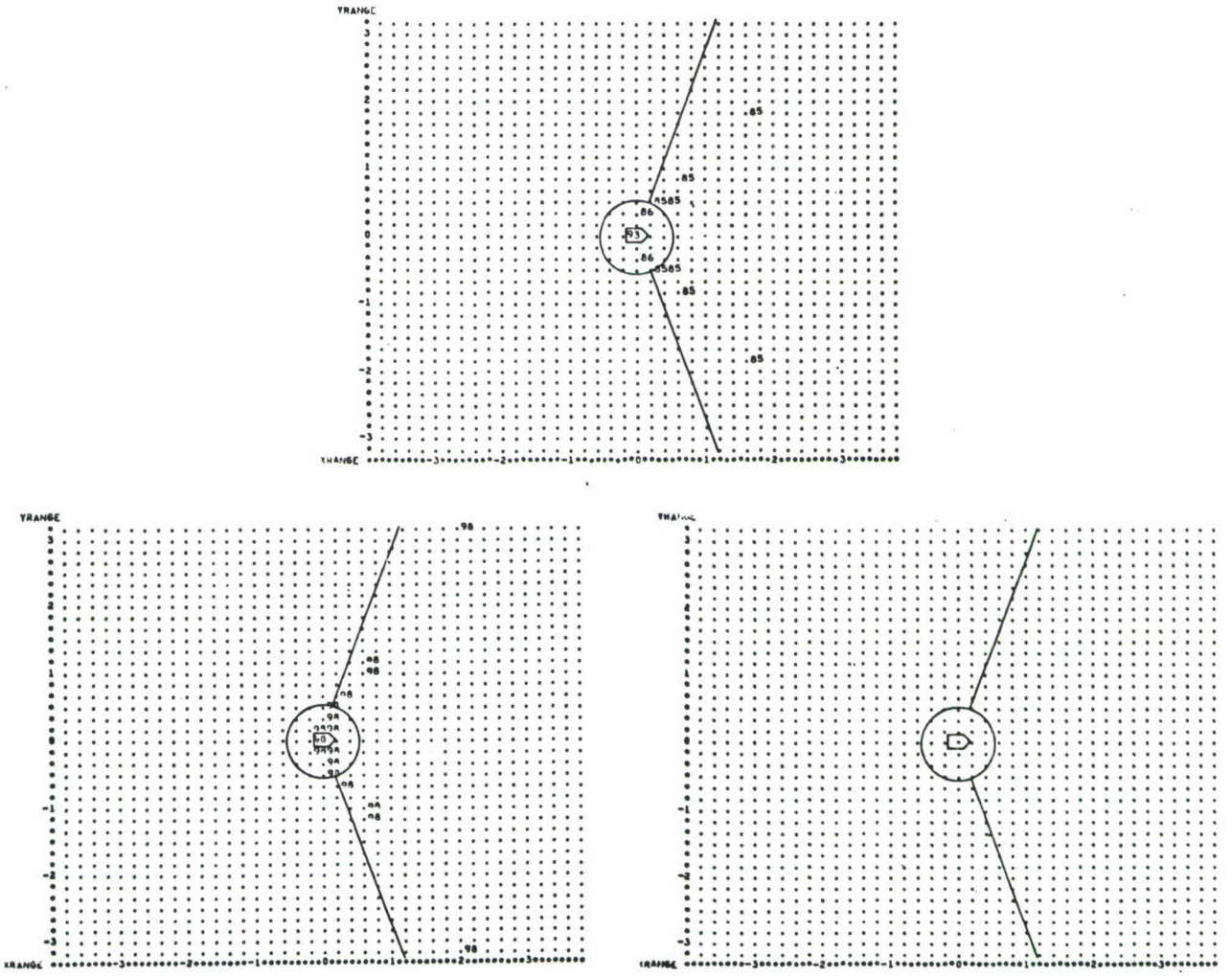

Figure A-9. 35° Glint Patterns

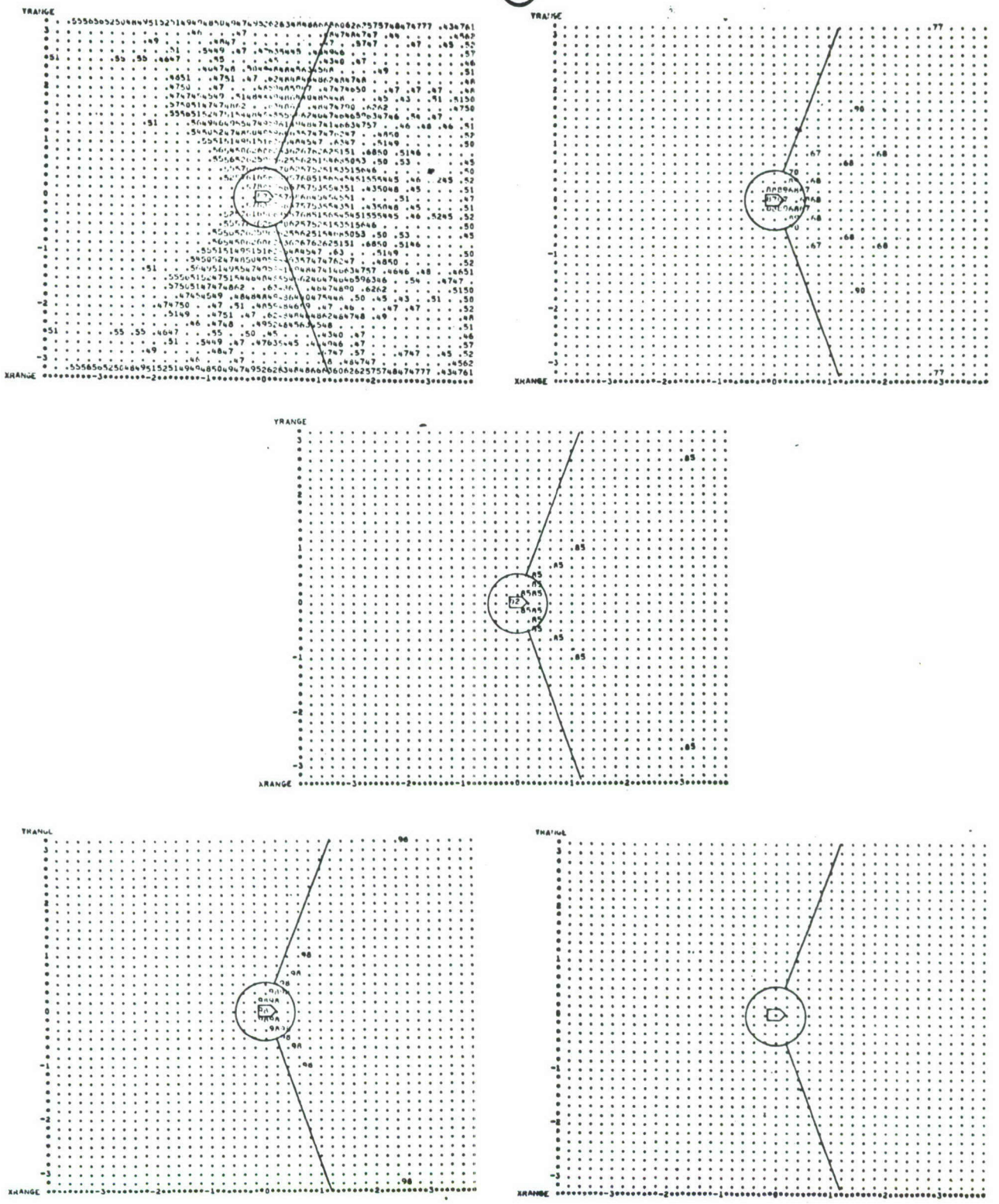

Figure A-10. 40° Glint Patterns

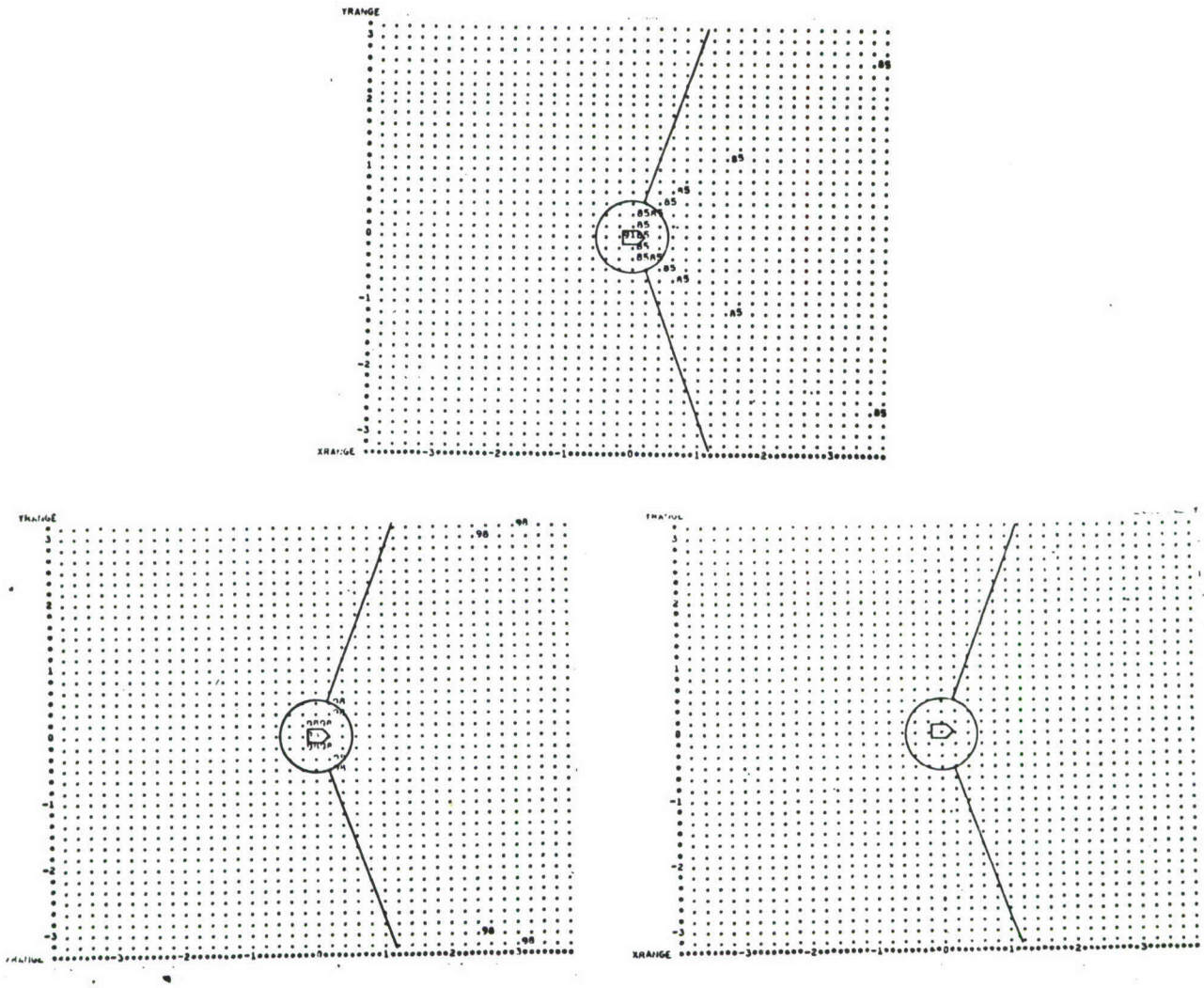

Figure A-11. 45° Glint Patterns

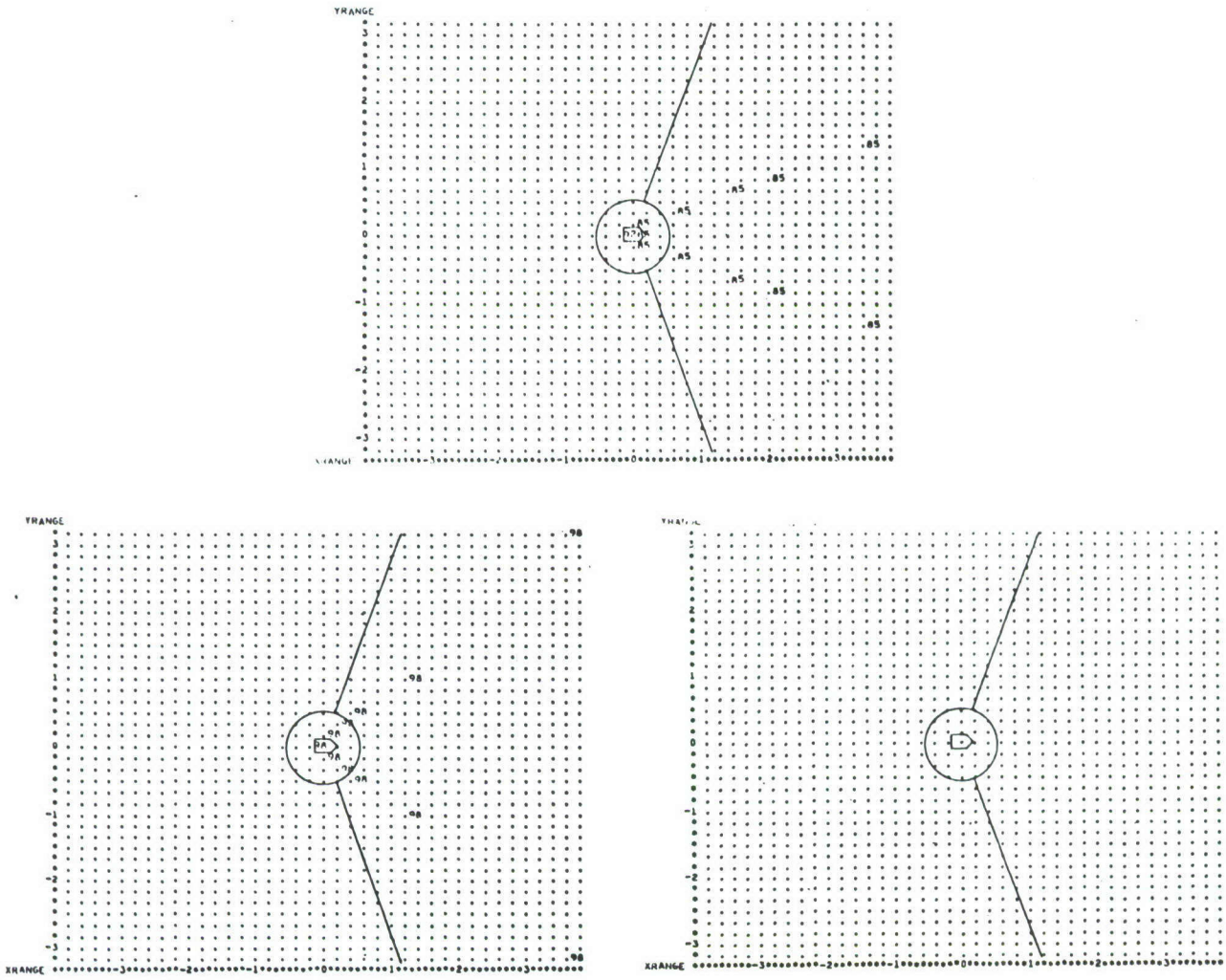

Figure A-12. 50° Glint Patterns

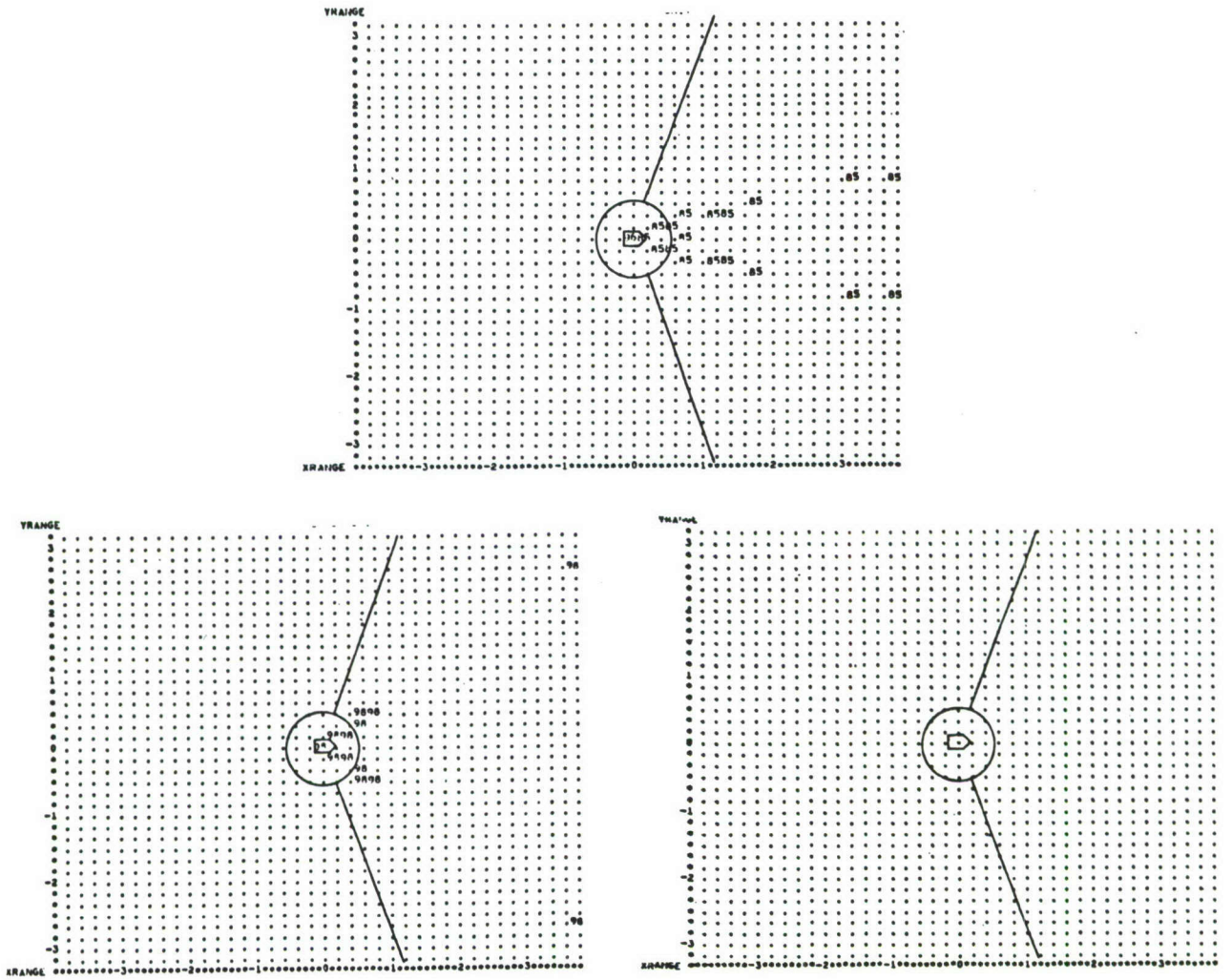

Figure A-13. 55° Glint Patterns

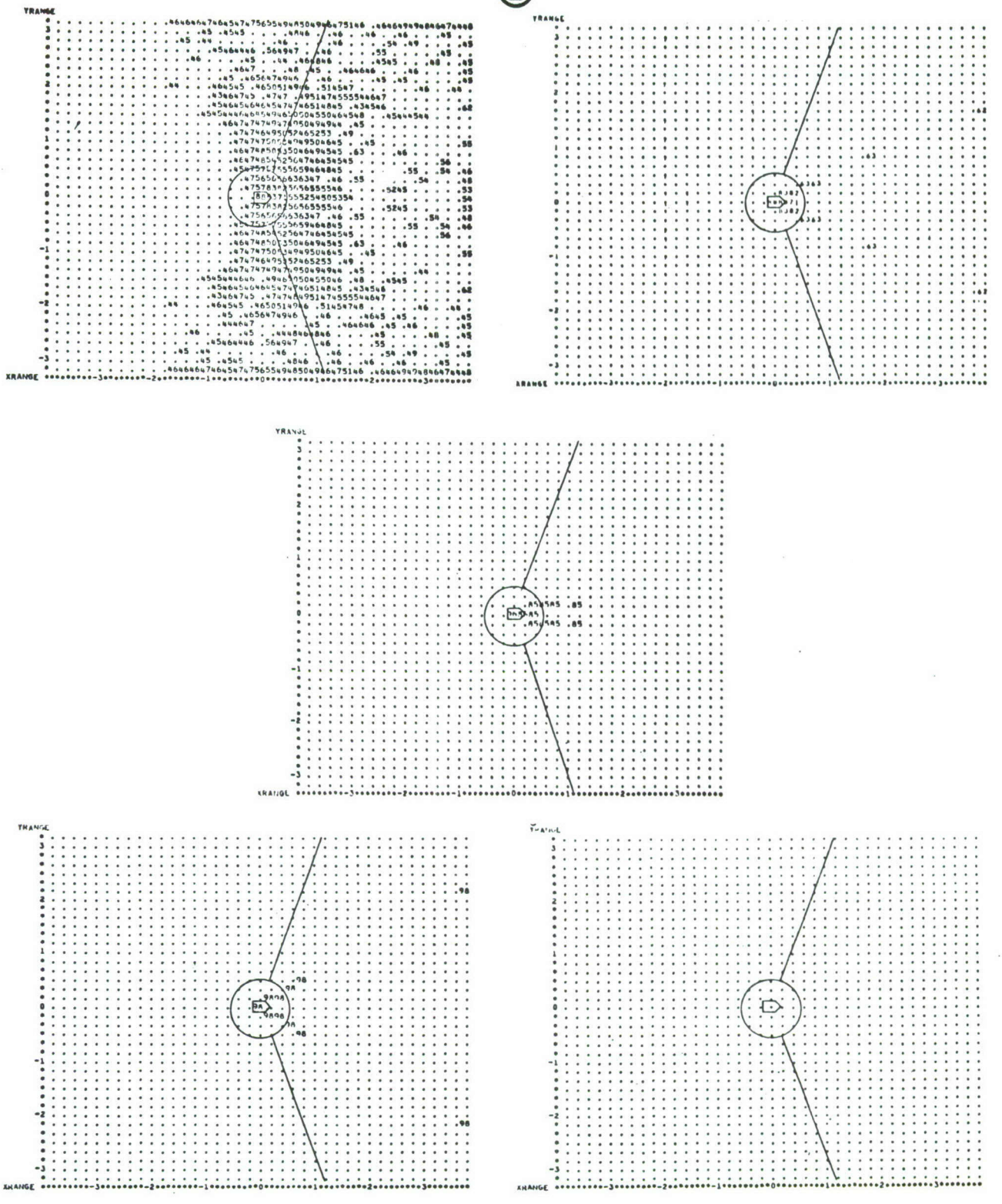

Figure A-14. 60° Glint Patterns

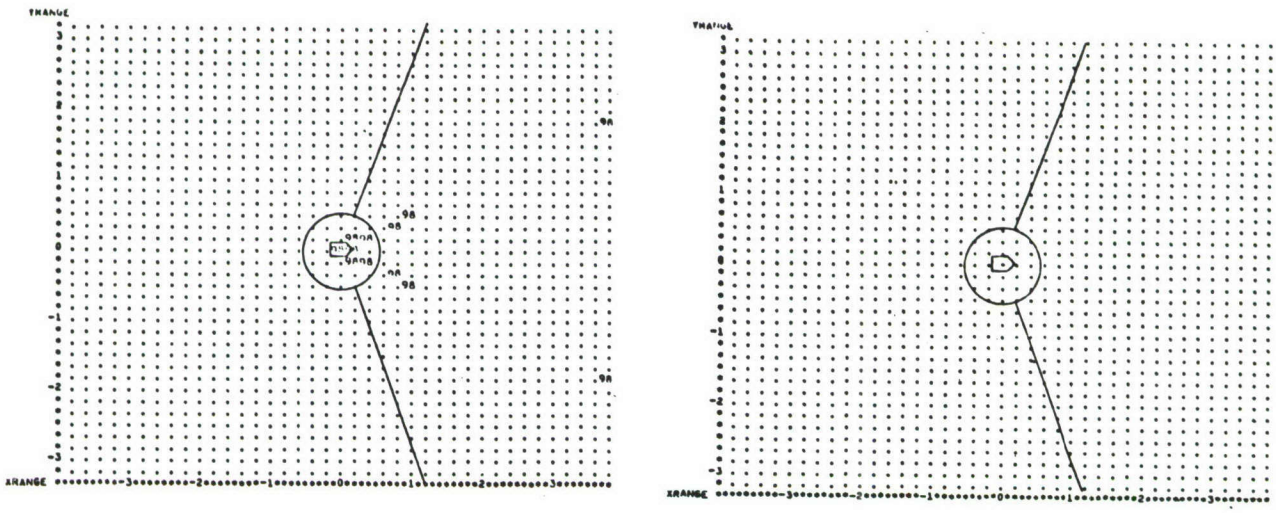

Figure A-15. 65° Glint Patterns

THIS PAGE INTENTIONALLY LEFT BLANK

DISTRIBUTION LIST

	Copies
Commander US Army Materiel Command ATTN: AMCDL 5001 Eisenhower Avenue Alexandria, VA 22304	1
Commander US Army Materiel Command ATTN: AMCRD 5001 Eisenhower Avenue Alexandria, VA 22304	3
Commander US Army Materiel Command ATTN: AMCRD-P 5001 Eisenhower Avenue Alexandria, VA 22304	1
Director of Defense, Research & Engineering Department of Defense WASH DC 20301	1
Director Defense Advanced Research Projects Agency WASH DC 20301	3
HQDA (DARD-DDC) WASH DC 20310	4
HQDA (DARD-ARZ-C) WASH DC 20310	1
HQDA (DAFD-ZB) WASH DC 20310	1
HQDA (DAMO-PLW) WASH DC 20310	1
HQDA (DAMO-IAM) WASH DC 20310	1
Commander US Army Training & Doctrine Command ATTN: ATCD Fort Monroe, VA 23651	1

Commander US Army Combined Arms Combat Developments Activity (PROV) Fort Leavenworth, KS 66027	1
Commander US Army Logistics Center Fort Lee, VA 23801	1
Commander US Army CDC Intelligence & Control Systems Group Fort Belvoir, VA 22060	1
TRADOC Liaison Office HQS USATECOM Aberdeen Proving Ground, MD 21005	1
Commander US Army Test and Evaluation Command Aberdeen Proving Ground, MD 21005	1
Commander US Army John F. Kennedy Center for Military Assistance Fort Bragg, NC 28307	1
Commander-In-Chief US Army Pacific ATTN: GPOP-FD APO San Francisco 96558	1
Commander Eighth US Army ATTN: EAGO-P APO San Francisco 96301	1
Commander Eighth US Army ATTN: EAGO-FD APO San Francisco 96301	1
Commander-In-Chief US Army Europe ATTN: AEAGC-ND APO New York 09403	4
Commander US Army Alaska ATTN: ARACD APO Seattle 98749	1

Commander
MASSTER
ATTN: Combat Service Support & Special Programs Directorate
Fort Hood, TX 76544 — 1

Commander
US MAC-T & JUSMAG-T
ATTN: MACTRD
APO San Francisco 96346 — 2

Senior Standardization Representative
US Army Standardization Group, Australia
c/o American Embassy
APO San Francisco 96404 — 1

Senior Standardization Representative
US Army Standardization Group, UK
Box 65
FPO New York 09510 — 1

Senior Standardization Representative
US Army Standardization Group, Canada
Canadian Forces Headquarters
Ottawa, Canada K1A0K2 — 1

Director
Air University Library
ATTN: AUL3T-64-572
Maxwell Air Force Base, AL 36112 — 1

Battelle Memorial Institute
Tactical Technical Center
Columbus Laboratories
505 King Avenue
Columbus, OH 43201 — 1

Defense Documentation Center (ASTIA)
Cameron Station
Alexandria, VA 22314 — 12

Commander
Aberdeen Proving Ground
ATTN: STEAP-TL
Aberdeen Proving Ground, MD 21005 — 2

Commander
US Army Edgewood Arsenal
ATTN: SMUEA-TS-L
Aberdeen Proving Ground, MD 21010 — 1

US Marine Corps Liaison Officer
Aberdeen Proving Ground, MD 21005 — 1

Director
Night Vision Laboratory
US Army Electronics Command
ATTN: AMSEL-NV-D (Mr. Goldberg)
Fort Belvoir, VA 22060 — 1

Commander
US Air Force Special Communications Center (USAFSS)
ATTN: SUR
San Antonio, TX 78243 — 1

Commander
US Army Armament Command
ATTN: AMSAR-ASF
Rock Island, IL 61201 — 1

Eustis Directorate
US Army Air Mobility R & D Laboratory
ATTN: SAVDLEU-MOS (E. Gilbert, J. Ladd)
Fort Eustis, VA 23604 — 2

Commander
US Army Aviation Systems Command
ATTN: AMCPM-ASE
P.O. Box 209
St. Louis, MO 63166 — 2

Commander
US Army Aviation System Command
ATTN: AMCPM-AAH
P.O. Box 209
St. Louis, MO 63166 — 2

Commander
US Army Aviation Systems Command
ATTN: AMCPM-CO
P.O. Box 209
St. Louis, MO 63166 — 2

Hughes Helicopters
Div. of Summa Corp.
ATTN: Mr. Robert Beagles
Culver City, CA 90230 — 2

CALSPAN Corporation
P.O. Box 235
ATTN: Mr. A. Akerman
Buffalo, NY 14221 — 1

CALSPAN Corporation
P.O. Box 235
ATTN: Mr. Harry Hammill
Buffalo, NY 14221 — 1

Dept. of the Air Force
Headquarters, ASD
ATTN: ASD/ENADE/P. G. Wiegert
Wright Patterson AFB, OH 45433 — 1

Bell Helicopter Company
P. O. Box 482
ATTN: Mr. Charles M. Seibel
Fort Worth, TX 76101 — 1

Commander
US Air Force Avionics Laboratory
ATTN: AFAL/WRD (J. D. MacAulay)
Wright Patterson AFB, OH 45433 — 1

Bell Helicopter Company
P.O. Box 482
ATTN: Mr. Jerry Jaggers
Fort Worth, TX 76101 — 2

Commander
US Army Aviation Systems Command
ATTN: AMSAV - EFA (L. Howard)
P.O. Box 209
St. Louis, MO 63166 — 1

Commander
US Army Aviation Systems Command
ATTN: AMSAV - EFS (R. Lutz)
P.O. Box 209
St. Louis, MO 63166 — 1

Commander
US Army Aviation Systems Command
ATTN: AMSAV - EEH (J. McDermott)
P. O. Box 209
St. Louis, MO 63166 — 1

The Franklin Institute Research Laboratories
20th & Race Streets
ATTN: John A. DeBenedictis
Philadelphia, PA 19103 — 2

The Franklin Institute Research Laboratories
20th & Race Streets
ATTN: William Collins
Philadelphia, PA 19103 — 2

Commander
US Army Mobility Equipment R & D Center
ATTN: STSFB - M (R. Murphy)
Ft. Belvoir, VA 22060 — 2

Bell Helicopter Company
P.O. Box 482
ATTN: Mr. R. Norwine, Govt Marketing
Ft. Worth, TX 76101 — 1

Bell Helicopter Company
P.O. Box 482
ATTN: Mr. Kenneth Bradford
Ft. Worth, TX 76101 — 1

Headquarters
Dept. of the Army
ATTN: DARD - ZC
Washington, DC 20310 — 1

Headquarters
Dept. of the Army
ATTN: DARD - DDA
Washington, DC 20310 — 1

Headquarters
Dept. of the Army
ATTEN: DARD - ZCA
Washington, DC 20310 — 1

Commander
US Army Electronics Command
ATTN: AMSEL - VL
Ft. Monmouth, NJ 07703 — 2

Commander
US Army Electronics Command
ATTN: AMSEL - WL - N (R. Giordano)
Ft. Monmouth, NJ 07703 — 1

Optical Coating Laboratory Inc.
P.O. Box 1599
ATTN: Mr. George Lundgren
Santa Rosa, CA 95403 — 1

Optical Coating Laboratory Inc.
P.O. Box 1599
ATTN: Mr. John Walker
Santa Rosa, CA 95403 — 1

Commander US Army Aviation Systems Command ATTN: AMCPM - UA P.O. Box 209 St. Louis, MO 63166	1
Sikorsky Aircraft Division of United Aircraft Corp ATTN: Mr. Michael J. Salkind Stratford, CT 06602	1
Optical Science Consultants P.O. Box 388 ATTN: Dr. David L. Fried Yorba Linda, CA 92686	2
Commander US Army Combat Developments Experimentation Command ATTN: CDCEC - EX Fort Ord, CA 93941	2
Sierracin Corporation 12780 San Fernando Road ATTN: Mr. John A. Haynes Sylmar, CA 91324	1
Hughes Helicopters Div of Summa Corp ATTN: Mr. E. P. Phiesendorfer Culver City, CA 90230	1
Westinghouse Defense & Electronic Systems Center Systems Development Division ATTN: MS 434 (Daumit, Higby, Goodell, Kiesel) Baltimore, MD 21203	6